

TALLINN UNIVERSITY OF TECHNOLOGY  
DOCTORAL THESIS  
26/2019

# **Cyclohexanohemicurbit[ $n$ ]urils, their Synthesis, Formation Mechanism, and Complexation**

ELENA PRIGORCHENKO

**TAL  
TECH**  
PRESS

TALLINN UNIVERSITY OF TECHNOLOGY  
School of Science  
Department of Chemistry and Biotechnology

This dissertation was accepted for the defence of the PhD degree in chemistry 18/04/2019

**Supervisor:** Prof. Riina Aav  
Department of Chemistry and Biotechnology  
Tallinn University of Technology  
Tallinn, Estonia

**Opponents:** Prof. Vladimír Šindelář  
Department of Chemistry  
Masaryk University  
Brno, Czech Republic

Senior Researcher Uno Mäeorg  
Department of Chemistry  
University of Tartu  
Tartu, Estonia

**Defence of the thesis:** 28/05/2019, Tallinn

**Declaration:**

Hereby I declare that this doctoral thesis, my original investigation and achievement, submitted for the doctoral degree at Tallinn University of Technology, has not been previously submitted for doctoral or equivalent academic degree.

Elena Prigorchenko

-----  
signature



European Union  
European Regional  
Development Fund



Investing  
in your future

Copyright: Elena Prigorchenko, 2019  
ISSN 2585-6898 (publication)  
ISBN 978-9949-83-435-8 (publication)  
ISSN 2585-6901 (PDF)  
ISBN 978-9949-83-436-5 (PDF)

TALLINNA TEHNIKAÜLIKOO  
DOKTORITÖÖ  
26/2019

**Tsükloheksanohemikukurbit[ $n$ ]uriilid,  
nende süntees, tekkemehhanism ja  
komplekseerumine**

ELENA PRIGORCHENKO



# Contents

List of Publications .....	6
Author's Contribution to the Publications .....	7
Author's Other Publications and Conference Presentations .....	8
Introduction .....	9
Abbreviations .....	10
1 Literature overview .....	12
1.1 Stepwise synthesis and head-to-tail cyclisation .....	12
1.2 Dynamic combinatorial chemistry .....	14
1.2.1 Kinetic vs thermodynamic control during reaction .....	15
1.2.2 Reversible covalent bonds .....	16
1.3 Important features of the synthesis of macrocycles .....	18
1.3.1 Conformational vs configurational preorganisation .....	18
1.3.2 Intra- vs inter-molecular reactions .....	20
1.4 Cucurbit[ <i>n</i> ]urils .....	22
1.4.1 Synthesis and mechanism of formation .....	23
1.4.2 Chiral cucurbit[ <i>n</i> ]urils .....	25
1.4.3 Hemicucurbit[ <i>n</i> ]urils .....	26
2 Aims of the study .....	34
3 Results and discussion .....	35
3.1 <i>Trans</i> -cyclohexanohemicucurbit[6]uril .....	35
3.1.1 Synthesis and structure (Publication I and II) .....	35
3.1.2 Complexation properties .....	38
3.2 <i>Trans</i> -cyclohexanohemicucurbit[8]uril (Publications III and IV) .....	42
3.2.1 Structure and homologues .....	42
3.2.2 Synthesis of cyclohexanohemicucurbiturils .....	44
3.2.3 Structure and complexation of cyclohexanohemicucurbit[8]uril .....	53
3.3 <i>Inverted-cis</i> -cyclohexanohemicucurbit[6]uril (Publication V) .....	54
3.3.1 NMR identification of new stereoisomer, the <i>inverted-cis</i> - cyclohexanohemicucurbit[6]uril .....	54
3.3.2 Synthesis and mechanism .....	57
3.3.3 Complexation .....	58
4 Conclusions .....	60
References .....	61
Acknowledgements .....	66
Abstract .....	67
Lühikokkuvõte .....	68
Appendix .....	69
Curriculum vitae .....	107
Elulookirjeldus .....	108

## List of Publications

The current thesis has been prepared from the following publications:

- I R. Aav, **E. Shmatova**, I. Reile, M. Borissova, F. Topić, K. Rissanen "New Chiral Cyclohexylhemicucurbit[6]uril" *Organic Letters*, **2013**, *15*, 3786–3789.
- II M. Öeren, **E. Shmatova**, T. Tamm, R. Aav "Computational and ion mobility MS study of (*all-S*)-cyclohexylhemicucurbit[6]uril structure and complexes" *Physical Chemistry Chemical Physics*, **2014**, *16*, 19198–19205.
- III M. Fomitšenko, **E. Shmatova**, M. Öeren, I. Järving, R. Aav "New homologues of chiral cyclohexylhemicucurbit[*n*]urils" *Supramolecular Chemistry*, **2014**, *26*, 698–703.
- IV **E. Prigorchenko**, M. Öeren, S. Kaabel, M. Fomitšenko, I. Reile, I Järving, T. Tamm, F. Topić, K. Rissanen, R. Aav "Template-controlled synthesis of chiral cyclohexylhemicucurbit[8]uril" *Chemical Communications*, **2016**, *51*, 10921–10924.
- V **E. Prigorchenko**, S. Kaabel, T. Narva, A. Baškir, M. Fomitšenko, J. Adamson, I. Järving, K. Rissanen, T. Tamm, R. Aav "Formation and trapping of the thermodynamically unfavoured *inverted*-hemicucurbit[6]uril" 2019, *manuscript available from ChemRxiv doi: 10.26434/chemrxiv.7977566.v1*.

## Author's Contribution to the Publications

The author's contributions to the papers in this thesis are as follows:

- I The author planned and conducted all synthetic experiments, obtained single crystals, and prepared all samples. The author participated in the final manuscript preparation and was responsible for the experimental part of the article.
- II The author synthesised the objects of the study and participated in the final manuscript preparation.
- III The author supervised the synthetic part of the article, and contributed to the experimental and analytical parts. The author also participated in the final manuscript preparation.
- IV The author planned and conducted all synthetic experiments, prepared samples for the complexation study, and obtained single crystals of (*R,R*)-cycHC[8]. The author also wrote the manuscript and supporting information.
- V The author planned, supervised, partially conducted the synthetic part of the article, and wrote the manuscript.

## Author's Other Publications and Conference Presentations

### Other publications

1. M. Fomitšenko, A. Peterson, I. Reile, H. Cong, S. Kaabel, **E. Prigorchenko**, I. Järving, R. Aav 'A quantitative method for analysis of mixtures of homologues and stereoisomers of hemicucurbiturils that allows us to follow their formation and stability' *New Journal of Chemistry*, **2017**, *41*, 2490–2497.
2. S. Kaabel, J. Adamson, F. Topić, A. Kiesilä, E. Kalenius, M. Öeren, M. Reimund, **E. Prigorchenko**, A. Lõokene, H. J. Reich, K. Rissanen, R. Aav 'Chiral hemicucurbit[8]uril as an anion receptor: selectivity to size, shape and charge distribution' *Chem. Sci.* **2017**, *8*, 2184–2190.

### Oral presentations

1. 'Uue Kiraalse Tsükloheksüülpoolkukurbituriili Struktuur ja Komplekseerimine' XXXIII Eesti Keemiapäevad, Tallinn, Estonia, 2013.
2. 'New Chiral Cyclohexylhemicucurbituril Structure and Complexation' 3<sup>rd</sup> International Conference on Cucurbiturils, Canberra, Australia, 2013.

### Poster presentations

1. 'Uus Enantiomeerne Poolkukurbit[6]urii' XXXII Eesti Keemiapäevad, Tartu, Estonia, 2011.
2. 'New Chiral Hemicucurbit[6]uril - A Host for Ions' International Conference on Materials and Technologies for Green Chemistry, Tallinn, Estonia, 2011.
3. 'Chiral Cyclohexylhemicucurbit[*n*]uril Homologues' 9<sup>th</sup> International Symposium on Macrocyclic and Supramolecular Chemistry, Shanghai, China, 2014.
4. 'Synthesis of the Cyclohexylhemicucurbit[*n*]urils' 8<sup>th</sup> Balticum Organicum Syntheticum, Vilnius, Lithuania, 2014.
5. 'Cyclohexylhemicucurbiturils as supramolecular necklace for guest molecule' 10<sup>th</sup> International Symposium on Macrocyclic and Supramolecular Chemistry, Strasbourg, France, 2015.

## Introduction

Macrocycles are cyclic molecules with a skeleton containing 12 to over 100 atoms. Macrocyclic structures are widely found in natural products; roughly 20% of known terrestrial and marine sources contain cycles of different sizes.<sup>[1]</sup> Macrocycles can be carbo- or heterocycles (i.e. containing atoms other than carbon, for example, O, N, S). Macrocycles are interesting from both synthetic and structural points of view. Their synthesis is challenging; however, these complicated structures exhibit unique properties.

As a crucial part of more than 100 important drugs currently on the market, there is incessant interest in exploring macrocyclic structures for the discovery of new therapeutic agents.<sup>[2]</sup> Besides medicinal use, macrocycles are famous for hosting small organic or inorganic molecules and ions. This ability is used in the molecular recognition field, specifically chromatography<sup>[3,4]</sup> and separation of enantiomers,<sup>[5]</sup> as well as in chemical sensors,<sup>[6]</sup> catching hazardous substances<sup>[7]</sup>, and in new materials.<sup>[8]</sup>

The synthesis of macrocycles is particularly difficult due to the final macrocyclisation step. Preorganisation, complex and long synthetic strategies, and high dilution conditions are limitations to synthesis. However, it is the price to be paid in order to obtain specific properties often associated with a complicated structure, which can be used in many application areas. Conventional multistep building of macrocyclic molecules can be avoided if targets are oligomeric macrocycles, which are synthesised through dynamic combinatorial chemistry.

Cucurbiturils (CB[n]) are examples of very successful oligomeric host molecules. This family of pumpkin-shaped container molecules are famous for extremely strong binding with a guest molecule (binding constants of up to  $3 \times 10^{15} \text{ M}^{-1}$ ). Normal CBs bind mainly positively charged species, but there is also a sub-class of hemicucurbiturils that prefer anions. The cucurbituril family has shown potential for application to various fields, such as catalysis<sup>[9]</sup>, chromatography<sup>[10]</sup>, construction of ion channels<sup>[11]</sup>, and functional and supramolecular polymers<sup>[12]</sup>. Recent results in medicinal chemistry discovered applications as drug delivery vehicles<sup>[13]</sup>, fluorescent capsules,<sup>[14,15]</sup> and hydrogels for 3D cellular engineering.<sup>[16]</sup>

The current thesis focuses on the synthesis of hemicucurbiturils. High yields and very selective procedures were found. The formation of differently sized macrocycles and the proposed mechanism of chain growth and macrocyclisation were investigated. Several new hemicucurbituril molecules were synthesised and described. Host-guest complexation with different molecules (including chiral discrimination) was observed and documented.

## Abbreviations

1D, 2D, 3D	One, two or three dimensional
Alloc	Allyloxycarbonyl
AM1	Austin Model 1 (semi-empirical quantum chemistry method)
aq.	Aqueous
BioU[ <i>n</i> ]	Biotin[ <i>n</i> ]uril
Bn	Benzyl
BU[ <i>n</i> ]	Bambus[ <i>n</i> ]uril
Bu	Butyl
CB[ <i>n</i> ]	Cucurbit[ <i>n</i> ]uril
CCS	Collision cross-section
CPK	Corey, Pauling, Koltun molecular model
cycHC[ <i>n</i> ]	Cyclohexanohemicucurbit[ <i>n</i> ]uril
<i>d</i> -chloroform	Deuterated chloroform
DCC	Dynamic covalent chemistry
DCL	Dynamic combinatorial library
DCM	Dichloromethane
DFT	Density functional theory
DIPEA	<i>N,N,N</i> -Diisopropylethylamine
DMF	Dimethylformamide
DMSO	Dimethylsulfoxide
DNA	Deoxyribonucleic acid
eq.	Equivalent
ESI-MS	Electrospray ionisation mass spectrometry
Et	Ethyl
FA	Formic acid
HC[ <i>n</i> ]	Hemicucurbit[ <i>n</i> ]uril
HOMO	The highest occupied molecular orbital
HPLC	High-performance liquid chromatography
HRMS	High resolution mass spectrometry
I	Intermediate
IBX	2-iodoxybenzoic acid
<i>i</i> -CB	<i>Inverted</i> -cucurbit[ <i>n</i> ]uril
<i>i-cis</i> -cycHC[6]	<i>Inverted-cis</i> -cyclohexanohemicucurbit[6]uril
LUMO	The lowest unoccupied molecular orbital
MALDI-TOF	Matrix-assisted laser desorption ionisation – time of flight
Me	Methyl
MESP	The map of electrostatic potential
MPA	$\alpha$ -methoxyphenylacetic acid
MTPA	$\alpha$ -methoxy- $\alpha$ -trifluoromethylphenylacetic acid
MOMCl	Methoxymethyl chloride
NMR	Nuclear magnetic resonance (spectroscopy)
<i>ns</i> -CB	<i>Nor-seco</i> -cucurbit[ <i>n</i> ]uril

PET	Photoinduced electron transfer
PNA	Peptide nucleic acid
Py	Pyridine
RC	Reactant complex
RNA	Ribonucleic acid
RP	Reverse phase
RT	Room temperature
TBA	Tetrabutylammonium
TBS	<i>Tert</i> -Butyldimethylsilyl
TFA	Trifluoroacetic acid
TfOH	Trifluoromethanesulfonic acid (triflic acid)
THF	Tetrahydrofuran
TIPS	Triisopropylsilyl
ts	Transition state
TsOH	<i>p</i> -Toluenesulfonic acid (tosylic acid)
TWIM-MS	Traveling-Wave Ion Mobility Mass Spectrometry
UV	Ultraviolet
XRD	X-ray powder diffraction

# 1 Literature overview

Macrocycles have very diverse structures, from relatively simple, such as Muscone<sup>[17]</sup> (Figure 1), to very complex, such as antiparasitic agent Avermectin B<sub>1a</sub> containing many functional groups. These molecules can be natural substances, extracted or separated from plants or microbes, or artificial, synthesised by chemists. Regardless the origin, cyclic molecules have unique properties and have been used in many fields from functional new materials to medicinal chemistry. For example, cyclic peptide Gramicidin S was very useful in the treatment of gunshot wounds and saved many lives during World War II.<sup>[19]</sup> In addition, crown ethers are used as sensors, solid-state electrolytes in batteries, artificial ion channels, antibiotics, *etc.*<sup>[20]</sup>

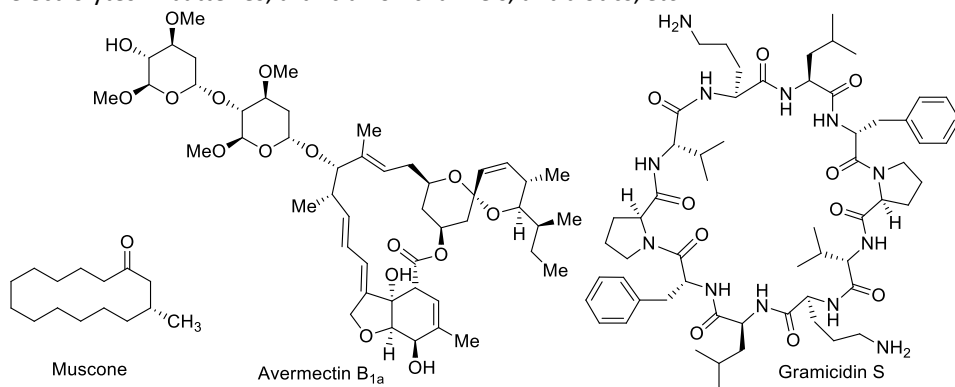


**Figure 1.** Structures of Muscone<sup>[17]</sup>, Avermectin B<sub>1a</sub>,<sup>[18]</sup> and Gramicidin S<sup>[21]</sup>.

From a synthetic point of view, there are two general methods of constructing macrocyclic structures. The first is stepwise synthesis using a conventional organic chemistry approach. Multistep procedures use an open-chain precursor and the final ring-closing step provides the target molecule. The second approach is via dynamic combinatorial chemistry, where composition of the resulting mixture of products is determined by the thermodynamic stabilities of each of the products.

## 1.1 Stepwise synthesis and head-to-tail cyclisation

Chemists may utilise for stepwise synthesis all possible reactions of organic chemistry. Depending on functionalities and the complicity of the final molecule, total synthesis may consist of an overwhelming number of steps. For example, the previously mentioned Avermectin B<sub>1a</sub> was synthesised in 46 steps.<sup>[18]</sup>

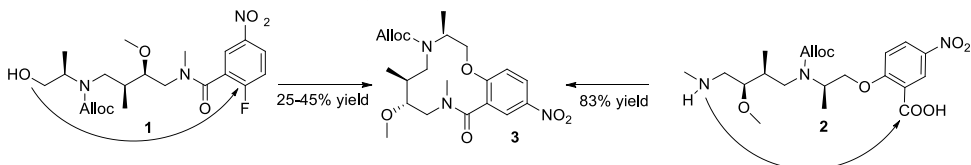


**Figure 2.** S<sub>N</sub>Ar reaction vs macrolactamisation for the synthesis of 3.<sup>[22]</sup>

The most challenging stage of the stepwise synthesis is the final head-to-tail cyclisation<sup>[21]</sup> of the corresponding open-chain precursor. Fitzgerald *et al.* showed how selection of the ring-closing strategy can increase yield drastically. The yield of

nucleophilic aromatic substitution ( $S_NAr$ ) of **1** was 25-45%. However, macrolactomisation of **2** gave an 83% yield of desired product **3** (Figure 2).<sup>[22]</sup>

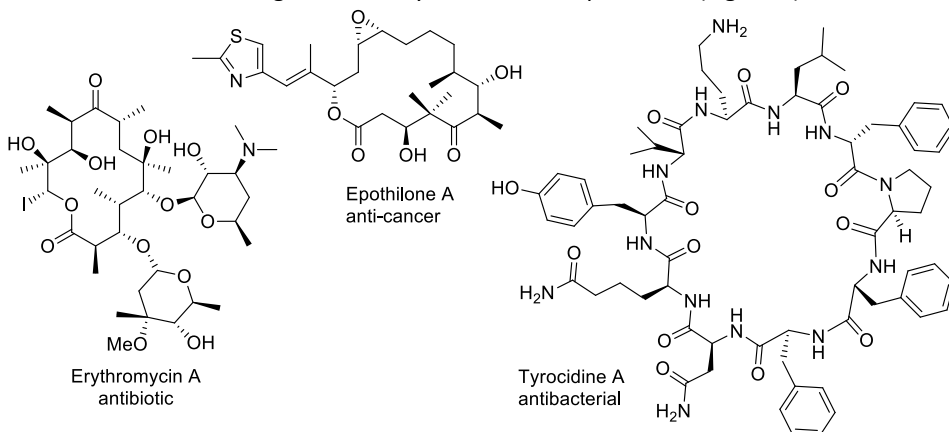


**Figure 3.** Examples of macrocyclic lactones and cyclic polypeptides used as pharmaceuticals.<sup>[23,24]</sup>

Important lactone and lactam groups very frequently occur in macrocyclic structures either in natural products or synthetic pharmaceuticals. As an example, in many antibiotics, such as Erythromycin A or anti-cancer agent Epothilone A (Figure 3). Therefore, lactonisation and lactamisation reactions are among the most popular for macrocyclisation. Several efficient powerful methodologies exist.<sup>[23]</sup> There are a number of examples, but here only the simple and efficient environmentally-friendly approach for the synthesis of macrocyclic lactones, lactams, and ketones will be described<sup>[25]</sup>. The method is based on photoinduced electron transfer (PET) reactions described by Yoshimi's group. The process consists of three steps (Figure 4). The first two steps are preparation of acrylate ester from the macrocyclic lactone and the final step is PET-promoted decarboxylation and cyclisation. Macrocyclisation yield depends on the concentration of the open-chain precursor and can vary from 29% to 84%. In more diluted conditions, yields are higher because of competing intermolecular reactions arising in more concentrated experiments (see chapter 1.2.3).<sup>[25]</sup>

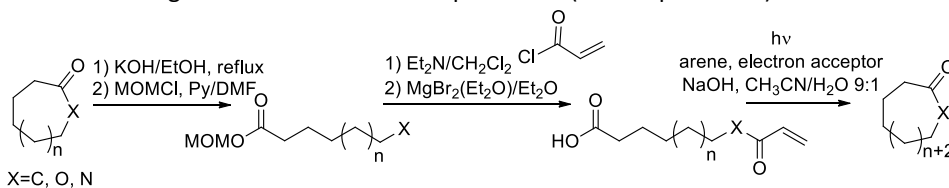


**Figure 4.** Macrocyclic lactone ring expansion and conversion to macrocyclic lactams and ketones through radical photocyclisation.<sup>[25]</sup>

Another valuable class of macrocycles worth mentioning here is cyclic polypeptides. These are polypeptide chains, which are able to form a cyclic structure. Over 40 cyclic peptide pharmaceuticals are already in medical use and one new drug appears every year. This class has antibacterial, antifungal, and anti-cancer activity, and can even be used for gastrointestinal disorder treatment.<sup>[26]</sup> The first examples of this class of compounds were separated from the extract of a soil bacillus. Tyrocidine A was discovered in 1939 by Dudos and Cattaneo<sup>[27,28]</sup> (Figure 3) and Gramicidin S was

discovered in 1941 by Gause and Brazhnikova (Figure 1)<sup>[19]</sup>. Interestingly, Tyrothricin (Tyrosur®), which is the mixture of Tyrocidine and Gramicidin, was the first commercial antibiotic and is still on market.<sup>[24]</sup> Different methods exist to obtain cyclic polypeptides, including solid-phase, enzymatic, and typical organic synthesis.<sup>[24]</sup> To obtain a C-C bond in the final macrocyclisation step, metal-mediated reactions are used; for example, Pd-catalysed reactions, including Stille, Heck, or Suzuki-Miyaura cross-couplings. These are powerful tools in the synthesis of the cyclic polypeptides. Mild conditions can be used and such reactions have good functional group tolerance.<sup>[29]</sup> As an example, synthesis of the 31-membered macrocycle of Rapamycin by Stille coupling is shown in Figure 5.<sup>[30]</sup>

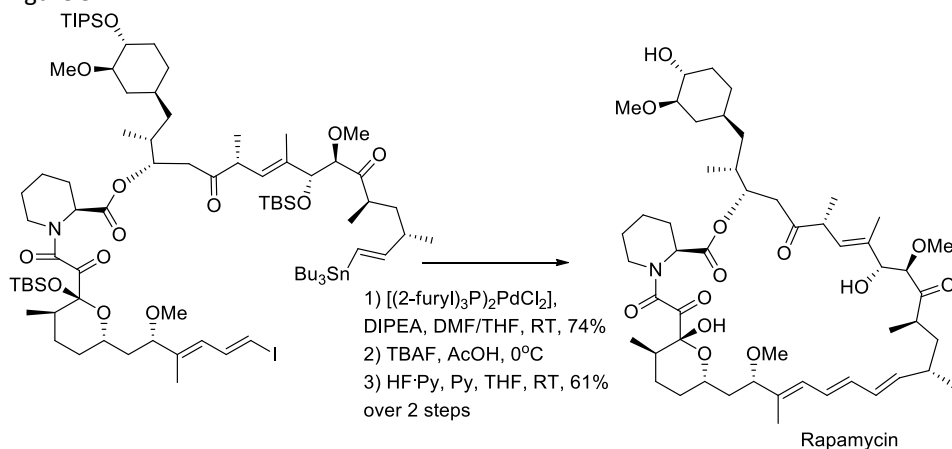


**Figure 5.** Stille macrocyclisation and completion of Rapamycin synthesis.<sup>[30]</sup>

Currently, organic chemists are well equipped to solve complicated tasks. Stepwise synthesis of the precursor can be quite challenging and time-consuming, but it is often the only method for constructing complicated architectures. Nevertheless, there are also macrocycles, which can be constructed in a single synthetic step. These approaches will be discussed in the next chapter.

## 1.2 Dynamic combinatorial chemistry

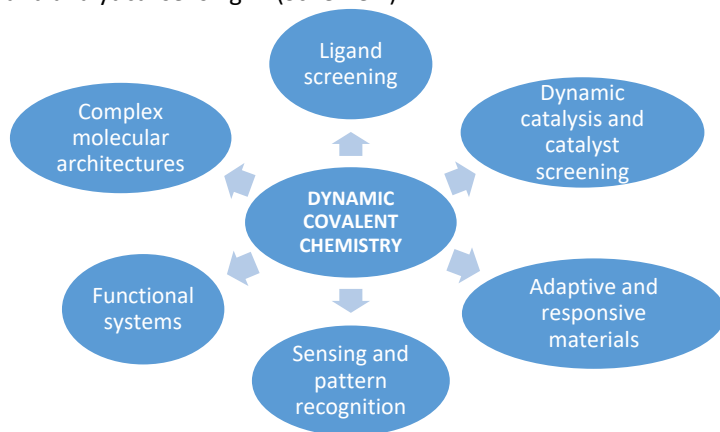
Dynamic combinatorial chemistry<sup>[31,32]</sup> (DCC, sometimes referred to in the literature by its alternative term – dynamic covalent chemistry<sup>[33]</sup>) is quintessence for covalent and supramolecular chemistry. It is an alternative approach to obtain complicated structures, including macrocyclic structures. All constituents of the reaction mixture in DCC are termed the dynamic combinatorial library (DCL). During the equilibration process, library members are interconverting into one another.<sup>[34]</sup>

Supramolecular chemistry<sup>[35]</sup> is the study of non-covalent interactions and complexes that operate under thermodynamic control. Fascinating superstructures are formed through non-covalent interactions, which are usually not very stable and exist only in solutions. This complicates their separation, investigation, and characterisation.

Dynamic covalent chemistry has much in common with supramolecular chemistry, including the dynamic and reversible nature of the bonds and so called 'error-checking', which ensures conversion of thermodynamically unstable products into the most stable ones. Despite the reversibility of both systems, DCC is much slower than supramolecular chemistry. Practically, DCC requires a catalyst in order to finish

equilibration in a reasonable amount of time. It is also important to mention that most dynamic covalent bonds are strong enough to not break or exchange without a catalyst. However, a number of external factors, such as temperature, concentration, and the presence of impurities can drastically influence the outcome of the reaction.<sup>[33]</sup>

The field of DCC is relatively new, but it has been applied widely to nanochemistry<sup>[36]</sup>, material science<sup>[37]</sup>, surface chemistry<sup>[38]</sup>, catalysis<sup>[39]</sup>, chemical biology<sup>[40]</sup>, and analytical sensing<sup>[41]</sup> (Scheme 1).



**Scheme 1.** Selected applications of DCC.<sup>[42]</sup>

### 1.2.1 Kinetic vs thermodynamic control during reaction

Traditionally, organic synthesis uses reactions under kinetic control (Figure 6) through irreversible chemical bonds and carefully chosen procedures. Such an approach is usual for the synthesis of natural or unnatural products and examples are presented in Chapter 1.1.<sup>[33]</sup>

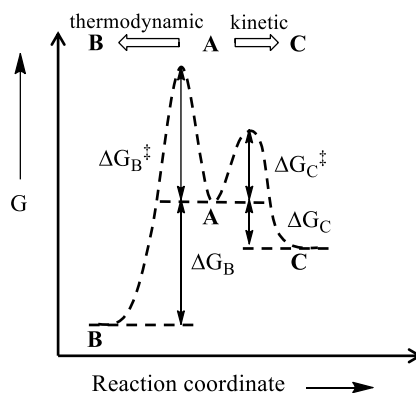


**Figure 6.** Free energy profile illustrating kinetic ( $A \rightarrow C$ ) versus thermodynamic ( $A \rightarrow B$ ) control of product distribution.<sup>[33]</sup>

A different approach concerns reversible covalent bonds under equilibrium conditions. When equilibration is reached fast enough and the reaction occurs under thermodynamic control (Figure 6), dynamic combinatorial chemistry is used.<sup>[31]</sup> In these reactions only relative stabilities ( $\Delta G_B$  and  $\Delta G_C$ ) of the products control the proportion in the resulting mixture. Consequently, the equilibrium and ratio of products forming can be influenced by: 1) modifying starting materials (steric or electronic effects) or

2) adding an excess of one of the starting compounds or removing desired product from the reaction mixture.<sup>[33]</sup>

### 1.2.2 Reversible covalent bonds

Compared to supramolecular interactions, dynamic covalent bonds are more slowly formed and, therefore, require catalysis to facilitate equilibration. This makes the system more complex; however, the presence of a catalyst allows equilibration to be obtained before further manipulations or analysis.<sup>[42]</sup>

One crucial aspect of reversible covalent bonds is the inherent symmetry. It determines the building block of the synthesised entity and the possible diversity of library formed (Figure 7).

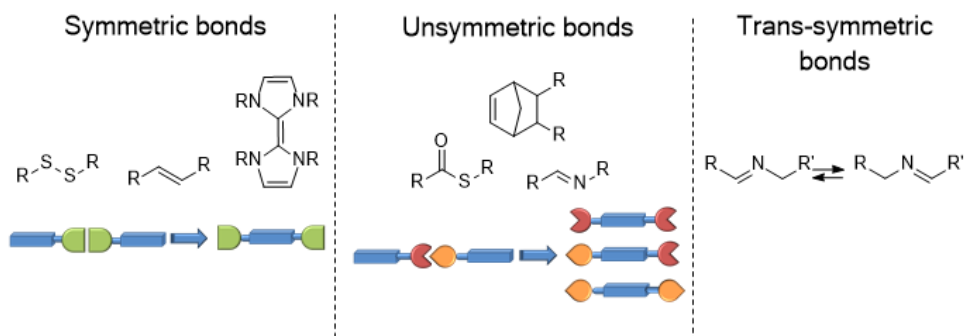


**Figure 7.** Examples of common dynamic covalent bonds within each symmetry class<sup>[42]</sup> and the design of building blocks and possible associations<sup>[34]</sup>.

Reversible bonds can be divided to main three categories. The first is symmetric, where both reacting partners have the same functional group and connection occurs through it; for example, disulphide exchange, alkene, or alkyne metathesis. The second is unsymmetrical, where partners with different functionality types form a covalent bond; for example, acyl transfer, C=N exchange, or acetal exchange. The third is trans-symmetric, where the reaction is unsymmetrical, but can be reversibly converted into one another. One disadvantage of symmetrical connections is that there is no information on the order of building blocks. No directionality is possible and self-exchange is inevitable. In the case of unsymmetrical bonds, due to complementarity of functional groups, it is easier to have different building blocks for screening. Substitutions on one reagent can be varied, while leaving the other unchanged.<sup>[42]</sup>

It is of central importance to control whether the dynamic system reaches equilibrium. There are two main methods to confirm the same. The first is the so called dual entry-point analysis. The final component distribution is controlled in two experiments, which were started with different compositions. It is very important to have equal concentrations of building blocks for both experiments. If the same distribution of components is observed in both cases, the system is operating under thermodynamic control. The second is the stationary phase perturbation method. Experiments under reaction conditions of interest are performed and equilibrate. When no change in composition is detected, another exchanging component is added. If after new equilibration, the distribution of initial components has changed, then the system before addition was in equilibrium. The influence on the physical properties of the system can be also used to test whether the system is at equilibrium.<sup>[42]</sup>

### 1.2.2.1 Dynamic imine bond

The unsymmetrical reversible dynamic bond formed during the C-N exchange reaction will be reviewed in detail. Imine-chemistry operates on key intermediates similar to the ones present during hemicucurbituril formation, which is the topic of the current thesis. In addition, imine-bond is one of the most used dynamic bonds in DCC.<sup>[43]</sup>

The reversible condensation reaction between aldehydes or ketones with amine derivatives under acidic catalysis results in imine bond formation (Figure 8). This reaction was discovered by German chemist Hugo Schiff in 1864<sup>[44]</sup> and compounds containing imine bonds are known as 'Schiff's bases' (Figure 8). Despite the fact that an imine bond has been known for such a long time, its dynamic nature was only discovered relatively recently.<sup>[45]</sup> Currently, imines are found in a variety of fields, including construction of self-sorting systems, synthesis of molecular walkers, molecular switches, different cages, and interlocked molecules.<sup>[43]</sup>

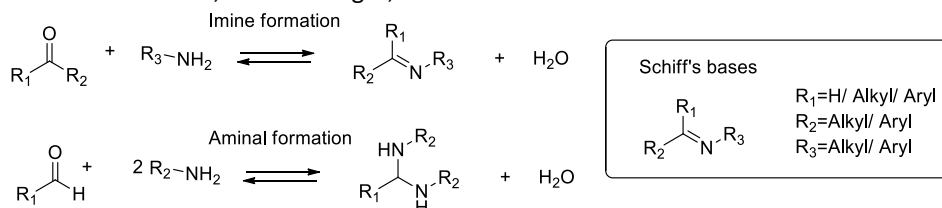


**Figure 8.** Imine and aminal formation reactions and Schiff's bases.<sup>[45]</sup>

There are many factors that can influence equilibrium during bond formation, such as pH, temperature, solvents, concentration, steric, and electronic factors.<sup>[43]</sup> Because imine formation is a reversible reaction, to direct the process towards product formation, it is common to remove water from the media. The imine formation and exchange mechanism and catalysis in water is well studied, but in organic media it is not well understood. On the basis of the recent studies, Di Stefano concluded that in an organic solvent it is a two-step concerted mechanism (Figure 9).<sup>[46]</sup>

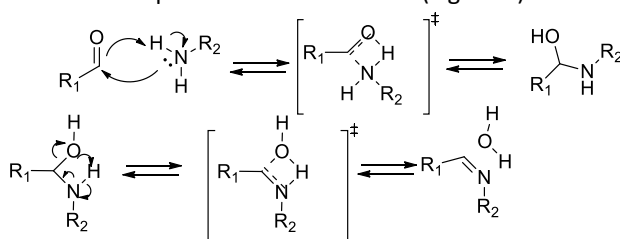


**Figure 9.** Formation and decomposition of hemiaminal in organic media via concerted mechanism.<sup>[46]</sup>

In addition to the starting compounds, the amine and aldehyde, during the imine exchange reaction there are several intermediates termed 'virtual constituents', which are unstable and nearly undetectable.<sup>[42]</sup> High-energy iminiums normally react very quickly with available nucleophiles.<sup>[47]</sup> Versute methodologies were invented to catch such labile intermediates as iminium<sup>[48]</sup> and hemiaminal<sup>[49]</sup> by synthetic cavitands.<sup>[42]</sup> Stabilisation by encapsulation of unstable species in the cavitand is a very elegant, inspiring solution and an example of a non-trivial application of macrocyclic host molecules.

Aromatic aldehydes in reaction with amines provide the most stable products compared to other carbonyl compounds. For this reason, aromatic aldehydes are

common in the generation of imine-based combinatorial libraries.<sup>[50]</sup> Lehn and co-workers reported ample research on imines formed from very different aldehydes and amines.<sup>[51]</sup> Possible complications faced during work with imine libraries are relatively low yields and lability during the chromatographic process in the presence of water. NMR analysis of complete crude reaction mixtures is usually used.

### 1.3 Important features of the synthesis of macrocycles

For both stepwise synthesis and dynamic combinatorial chemistry approaches towards macrocyclic structures, there are several important characteristic features. These will be discussed in the next sub-chapters.

#### 1.3.1 Conformational vs configurational preorganisation

While synthesising complex natural or synthetic structures, one of the main problems is preorganisation of the linear precursor before the ring-closure step.

Favourable preorganisation of the compound can be regarded as conformational and configurational. Conformational preorganisation means arrangement of precursor to the conformation in which the reacting ends of the open chain species exist in the closest distance possible. This promotes the cyclisation process and disfavors elongation of the chain. The template-effect can be considered a part of conformational preorganisation. Configurational preorganisation is considered a special case of conformational preorganisation, where stereochemistry of the formed intermediates plays a crucial role.<sup>[21]</sup>

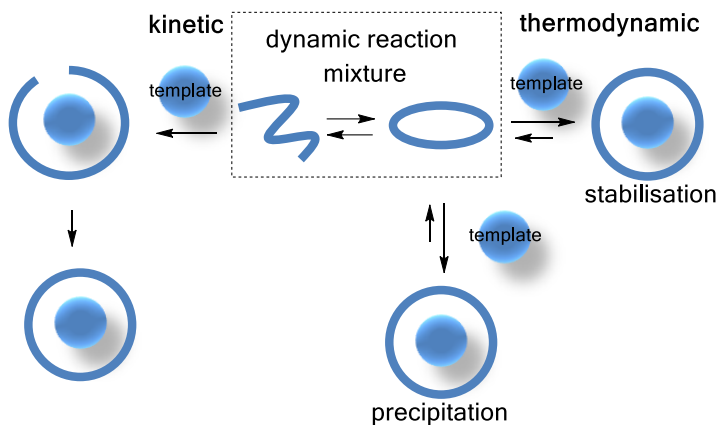
In addition, at the inception of supramolecular chemistry, Cram pointed out that *preorganisation is a central determinant of binding power*. “The more highly hosts and guests are organised for binding and low solvation prior to their complexation, the more stable will be their complexes.”<sup>[52]</sup> Therefore, complexation ability with the templating unit is one of the most important features of macrocyclic structures.

##### 1.3.1.1 Template effect

“A chemical template organises an assembly of atoms, with respect to one or more geometric loci, in order to achieve a particular linking of atoms.”<sup>[53]</sup> Thus, a template provides instructions via non-covalent bonds (such as hydrogen bonds, metal coordination, electrostatic, donor-acceptor, and  $\pi$ - $\pi$  interactions) for the formation of the only product from the reaction mixture.<sup>[54]</sup>

Busch divided templates into thermodynamic and kinetic types (Scheme 2).<sup>[55]</sup> Thermodynamic templating uses thermodynamic control in reversible reactions. In the reaction mixture, which is at equilibrium, the template binds to one of the products and shifts the equilibrium towards this product. The influence of the template in this case is only stabilisation of the product. For this reason, reaction yield is very high.<sup>[54]</sup>

Contrarily, kinetic templating works in irreversible reactions. The template must stabilise all the transition states during the formation of a desired product. A kinetic template may also bind the product more strongly than the starting material. As a result, product formation is favoured thermodynamically as well. Thus, it is difficult to determine which type of template operates in a specific reaction.<sup>[54]</sup>



**Scheme 2.** Schematic representation of kinetic and thermodynamic template effect.<sup>[47]</sup>

One of the oldest examples of the template effect was described almost a century ago by Seidel and Dick, which was the oligomerisation of *o*-aminobenzaldehyde (Figure 10). In the absence of a template, a linear trimer forms while in the presence of a metal ionic template (Ni(II), Zn(II), Co(II)), and tri- and tetradentate macrocycles are formed.<sup>[56]</sup>

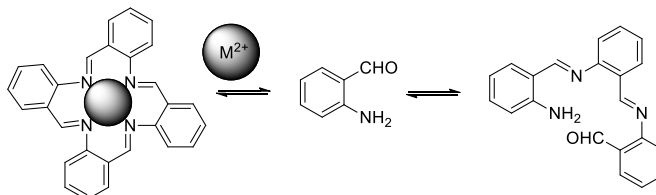


**Figure 10.** One of the earliest examples of thermodynamically templated imine synthesis.<sup>[56]</sup>

Another example of the template's importance in the synthesis of macrocycles are crown ethers.<sup>[57]</sup> The condensation reaction of the diphenol and dichloro compound (Figure 11) performed by Pedersen in 1967 was expected to produce polymeric product. Instead, it yielded up to 80% cyclic product indicating that additional factors influenced product formation. The presence of the potassium ion, originated from the base KOH, interacted with the ethyleneoxy units (-CH<sub>2</sub>CH<sub>2</sub>O-) of the open-chain or ring of the crown ether. These units are flexible and can adopt either *s-trans* or *s-cis* conformations. The latter provides perfect orientations for oxygen lone pairs in the centre. Oxygens of the diphenol units were already in the suitable orientation. Six oxygens from the open chain formed a coil around the template and made cyclisation highly favourable. Analogous template effects exist in the synthesis of nonaromatic crown ethers as well.<sup>[20]</sup>

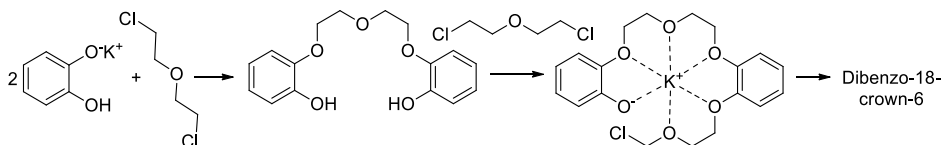


**Figure 11.** Template effect in the dibenzo-18-crown-6 synthesis.<sup>[20]</sup>

Templating properties of the neutral and cationic species have been well studied.<sup>[58,59]</sup> Anion-templated synthesis and binding was developed slowly partially due to the relatively diffuse nature of anions. In addition, anions have relatively high solvation free energy, pH sensitivity, large size, and variable shape / geometry.<sup>[60]</sup> Anions are important in various biological processes; for example, in protein folding<sup>[61]</sup>. 70-75% of enzyme substrates and co-factors are anions.<sup>[60]</sup>

The size and geometry of the templating anion are the main factors that play a role in the shape and connectivity of the final product.<sup>[62]</sup> The most common anionic templating agents are chlorides or halides in general, which are spherical, monoatomic, and vary in size (1.33 Å for F<sup>-</sup> to 2.20 Å for I<sup>-</sup>)<sup>[63]</sup>. In Figure 12 there are very elegant examples of chloride-mediated coordination assemblies. The first is Lehn's circular helicate **4**<sup>[64]</sup> formed from five tris(bipyridine) strands around a chloride ion, which shows the importance of anion size. In the presence of a chloride template, a pentanuclear species formed; however, in the presence of a sulphate anion, a selectively hexanuclear helicate structure formed.<sup>[64]</sup> The second is the beautiful structure of tetranuclear [12]mercuracarborand-4 (**5**) reported by Hawthorn<sup>[65,66]</sup>.

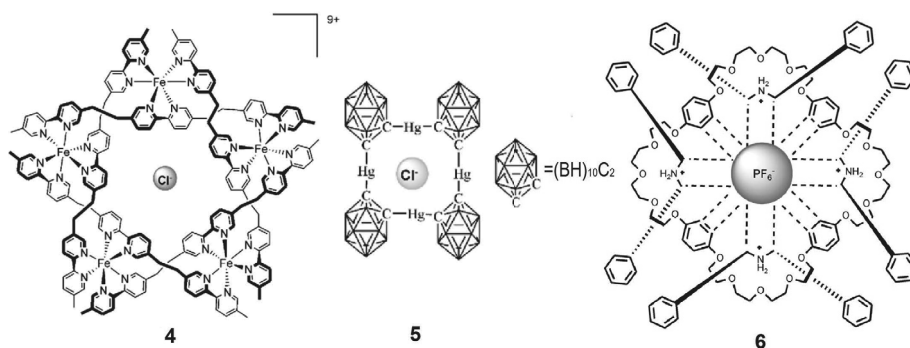


**Figure 12.** Templated structures of circular helicate **4**, tetranuclear [12]mercuracarborand-4 **5** and [5]-pseudorotaxane **6**. Figures are reprinted with permission from Elsevier, ref. <sup>[67]</sup>.

Increasing the size and structural complexity of the template due to a greater amount of "templating information" can result in more complex architectures.<sup>[68]</sup> The octahedral geometry of the hexafluorophosphate ion programmed through electrostatic interactions and hydrogen bonds formation of superstructure **6**, were made by Stoddart's group<sup>[69]</sup>.

### 1.3.2 Intra- vs inter-molecular reactions

Another important feature of the synthesis of macrocycles is the relation between intra- and inter-molecular reactions in the media. High-dilution conditions or pseudo-high-dilution conditions are a common inevitable parameter of most macrocyclisation synthetic procedures. High dilution favours intra-molecular processes over inter-molecular processes.<sup>[21,70]</sup> Intra-molecular reactions lead to elongation of oligomers and inter-molecular reactions cause macrocyclisation.<sup>[47]</sup> High-dilution conditions always complicate scaling of the process and do not favour 'greenness'.

Mandolini and co-workers described in great detail the synthesis of cyclophane formals (Figure 13).<sup>[71]</sup> Firstly, a complicated mixture of polymeric material and cyclic oligomers were obtained from dimer to hexamer as a result of an irreversible reaction

of bromochloromethane with benzene dimethanol. Yields of desired cyclic compounds were very low (1.2% to 3.7%). The same results were obtained in an acid-catalysed reversible oligomerisation process of a cyclic dimer in dilution conditions at 25°C. Authors varied starting cyclic oligomers, and no relation between the composition of the resulting mixture and the source of monomers was detected. However, only the concentration of the monomers in the reaction mixture had a direct influence on the proportion of the cycles formed. High dilution favoured formation of the smaller cycles. Use of the silver template and dichloromethane instead of chloroform allowed authors to increase the yield of the cyclic dimer up to 60%.

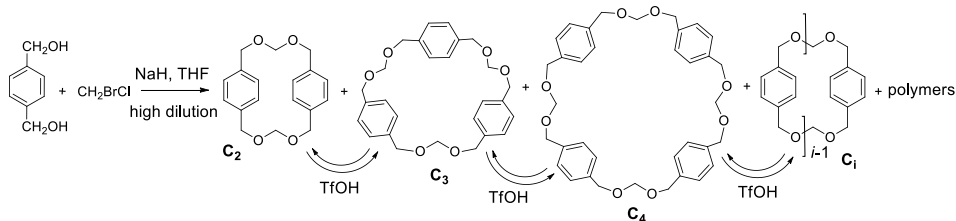


**Figure 13.** Irreversible reaction towards cyclophane formals and ring-ring equilibria triflic acid catalysis.<sup>[71]</sup>

In the same article, Mandolini also mentioned specific concentrations of monomers or effective molarity. The theoretical study of Jacobson and Stockmayer (JS theory)<sup>[72]</sup> predicted the existence of a concentration below which the equilibrium of the system consisted only of small cyclic compounds. At low concentrations, cyclisation occurred faster than chain growth. This difference in rates of the processes is expressed in effective molarity (EM<sub>i</sub>)<sup>[73]</sup>:

$$EM_i = \frac{K_{(intra)i}}{K_{inter}}$$

where  $K_{(inter)i}$  refers to the ring-chain equilibrium between the acyclic oligomer M<sub>i</sub> and the cyclic oligomer C<sub>i</sub> and  $K_{inter}$  is the equilibrium constant for the intermolecular reaction.

$$M_i \rightleftharpoons C_i$$

$$K_{(intra)i} = \frac{[C_i]}{[M_i]}$$

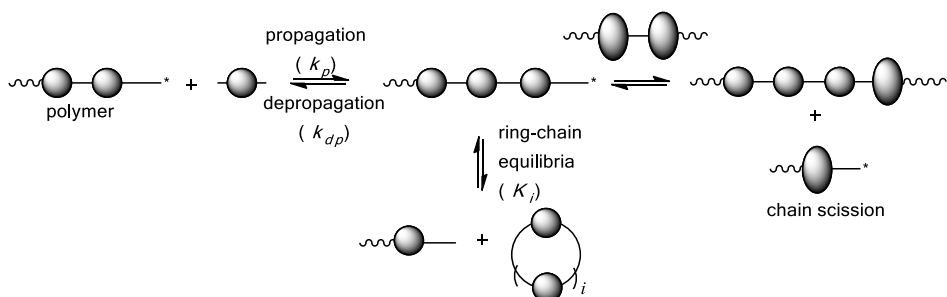
$$-A + B \rightleftharpoons -AB -$$

$$K_{inter} = \frac{[-AB -]}{[-A][B -]}$$

### 1.3.2.1 Dynamic polymerization

In the case of DCC intra- and intermolecular reactions acquire special terms and are of central importance. During dynamic polymerisation there are three types of processes occurring: a) elongation or propagation and reverse process depropagation, b) scission of the polymeric chain, and c) equilibration of cyclic and linear species (Scheme 3).<sup>[74]</sup>

The concentration of the monomers in the DCL plays a crucial role (JS theory) in the rates of the exchange reactions. Chain propagation is a second-order reaction, but cycle formation is first-order. As a result, at low concentrations, the cyclisation process occurs faster than propagation.<sup>[34]</sup>



**Scheme 3.** Three types of reversible processes occurring during dynamic polymerisation: a) propagation/depolymerization, b) chain scission, and c) ring-chain equilibria.<sup>[74]</sup>

If the system is truly reversible, it is responsive to direct stimuli. Changes in the environmental parameters, such as temperature, pressure, light, or the presence of a template can trigger a change in the system.<sup>[74]</sup>

## 1.4 Cucurbit[*n*]urils

More than a century ago, Behrend *et al.* synthesised the first cucurbit[*n*]uril (CB).<sup>[75]</sup> At that time the structure of the new macrocycle was not determined. Only in 1981, Mock and co-workers, with the help of X-ray diffraction, were able to reveal the structure of this pumpkin-shaped cyclic molecule.<sup>[76]</sup> From the beginning of 2000, Day<sup>[77]</sup>, Kim<sup>[78]</sup>, and Isaacs<sup>[79]</sup> contributed intensively to the cucurbituril family's "wealth and prosperity". Numerous cyclic, acyclic, normal and substituted homologues, analogues, derivatives, and congeners were synthesised and analysed (Figure 14).<sup>[80,81]</sup> Cucurbiturils are examples of the cooperation between template-assisted dynamic combinatorial chemistry and supramolecular chemistry.

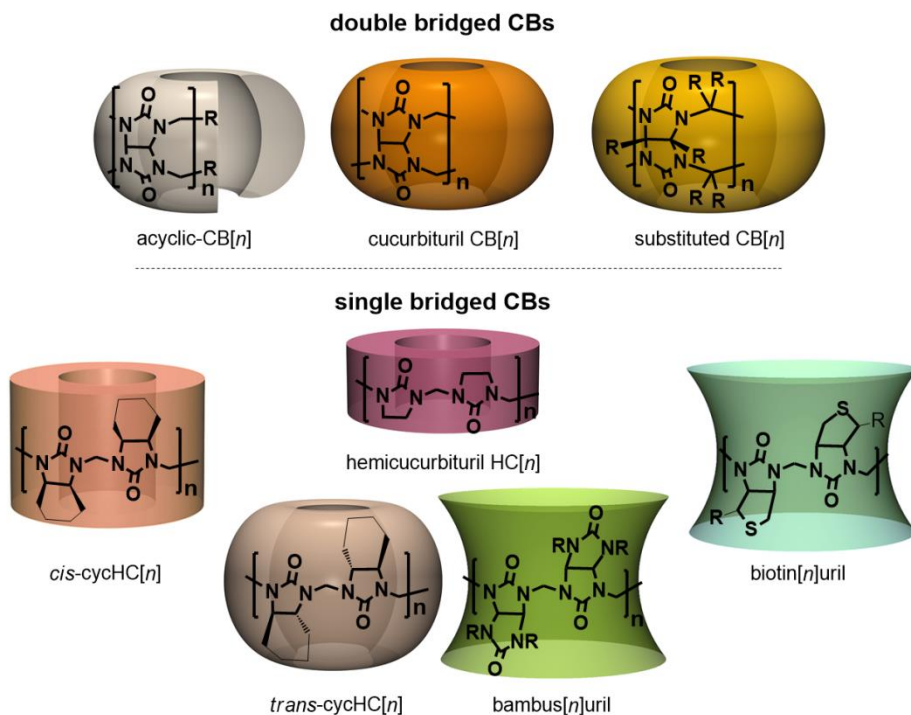


**Figure 14.** Cucurbit-type hosts.<sup>[82]</sup>

Cucurbiturils, with outstanding recognition ability, have been applied to a variety of fields, including medicinal<sup>[83]</sup> and material science.<sup>[84]</sup>

#### 1.4.1 Synthesis and mechanism of formation

For Mock and other early researchers working with CBs, their formation was "enigmatic spontaneous synthesis" (Figure 15).<sup>[76]</sup> Only in the first decade of the 21<sup>st</sup> century was the mechanism of formation determined.

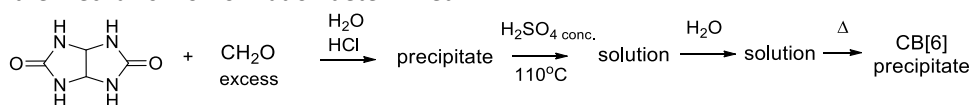


**Figure 15.** The first reaction scheme of CB[6] synthesis.<sup>[76]</sup>

Extensive work by the groups of Day<sup>[85,86]</sup> and Isaacs<sup>[79,87]</sup> revealed key mechanistic aspects. Isaacs studied the early stages of the reaction and Day described the final steps of the CB formation mechanism.

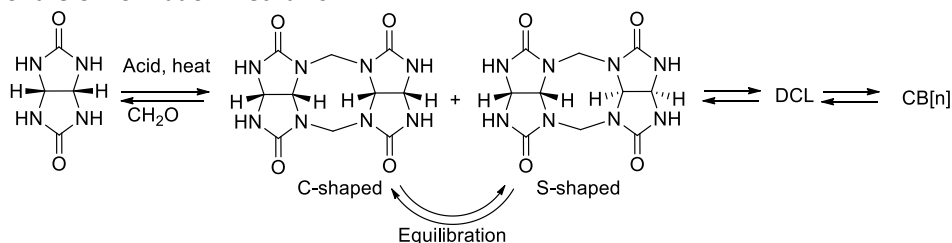


**Figure 16.** CB[n] formation mechanism.

The mechanism of CB[*n*] formation was named in analogy with step-growth polymerisation: step-growth cyclo-oligomerisation.<sup>[79]</sup> The first step (Figure 16) is acid catalysed condensation between two equivalents of formaldehyde and glycoluril, which results in the formation of S- and C-shaped dimers. A C-shaped dimer is at least 2 kcal/mol more stable than an S-shaped dimer, and these are in constant equilibration.<sup>[88]</sup> Further oligomerisation and back-biting reversible processes provided DCL of differently sized and shaped oligomers.

Isaacs *et al.* were able to separate reaction intermediates, such as oligomers (from dimers to hexamers), *ns*-CB[6] and ( $\pm$ )-*bis-ns*-CB[6], from the formaldehyde deficient reactions.<sup>[79]</sup> Isaacs *et al.* also obtained kinetic intermediates *i*-CB[6] and *i*-CB[7].<sup>[89]</sup> These inverted analogues could be converted to normal CB through heating in HCl, which confirmed the proposed mechanism as well as its kinetic nature.<sup>[87]</sup> Experiments with separate oligomers showed that fragmentation and recombination could occur before the final cyclisation step. When the chain grew long enough, an irreversible cyclisation occurred. Day<sup>[85]</sup> and Isaacs<sup>[79]</sup> both showed that CB[5]-CB[7] are thermodynamically stable, yet CB[8] could be converted to smaller rings.

The broad work of Day's group provided a complete overview of the influence of different parameters, such as acid nature and concentration, concentration of reactants and reaction temperature (Table 1) on product distribution.<sup>[85]</sup> There was no difference between the acids tested, as long as it was strong enough and in sufficient concentration. Temperature had a strong effect on reaction rate, but not on product distribution. However, the concentration of the starting compounds, in agreement with JS theory, played crucial role. A small glycoluril concentration induced cyclisation over oligomerization and small cycles prevailed. Higher concentrations resulted in the formation of larger rings.

**Table 1.** Effect of the acid type and concentration of the reactants on the distribution of the products.<sup>[85]</sup>

glycoluril mg/mL acid	acid	weight %			
		CB5	CB6	CB7	CB8
155-190	conc. H <sub>2</sub> SO <sub>4</sub>	12	88	<1	<1
155-190	9M H <sub>2</sub> SO <sub>4</sub>	23	44	23	8
155-190	conc. HCl	17	48	28	7
155-190	9M HCl	17	50	25	8
155-190	5M HCl	9	52	35	4
155-190	50% HBF <sub>4</sub>	28	43	24	5
155-190	melt TsOH	5	61	25	7
0.125	conc. HCl	58	42	-	-
1700	conc. HCl	3	44	33	12

The role of the template in the mechanism of cucurbituril formation is still up for debate. Day proposed, on the basis of AM1 calculations, that positive electrostatic potential in the inner cavity of the glycoluril moieties is attractive for the small anions to stabilise the open chain precursor.<sup>[85]</sup> On the other hand, potential positively charged templates had no pronounced effect on product distribution.<sup>[86]</sup>

#### 1.4.2 Chiral cucurbit[*n*]urils

The structure of normal-cucurbit[*n*]urils is symmetric.<sup>[82]</sup> This is one of the reasons why they form extremely strong binding with guest molecules. However, this restricts introduction of chirality into such symmetric molecules. There are only a few reported examples of chiral CB analogues (Figure 17).

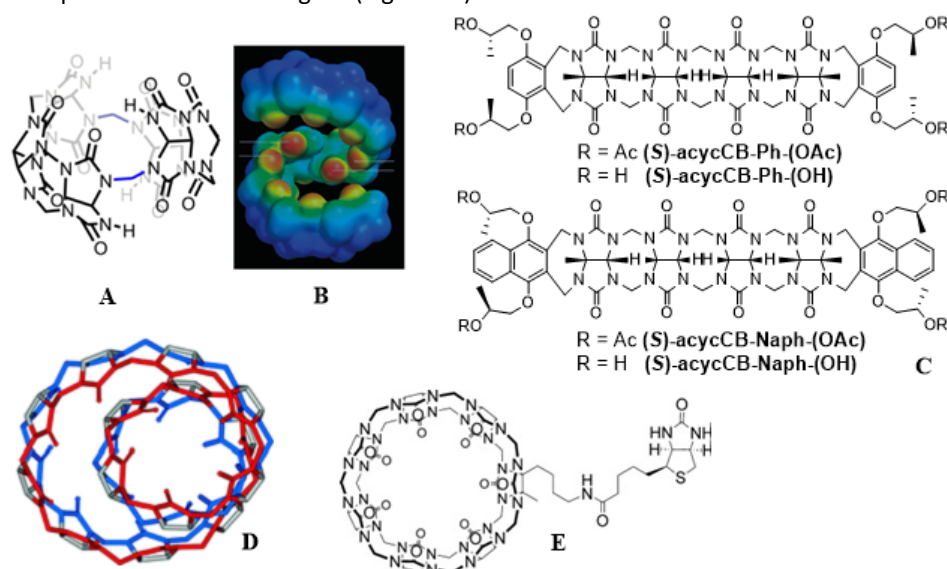


**Figure 17.** Chiral CBs: (A)  $(\pm)$ -bis-ns-CB[6]<sup>[82]</sup>, (B) acyclic 10-membered oligomer, (C) functionalised tetramers<sup>[82]</sup>, (D) twisted-CB[14], (E) mono-functionalised CB[7] connected with biotin. Figures B, D, and E are reprinted with permission from American Chemical Society and Wiley and Sons, ref. <sup>[90]</sup>, <sup>[91]</sup> and <sup>[13]</sup>, respectively.

Isaacs' research group was able to separate unusual members, including *ns*-CB[6], ( $\pm$ )-*bis-ns*-CB[6], and *bis-ns*-CB[10], from the paraformaldehyde deficient reactions (1 eq. glycoluril and 1.5 eq. paraformaldehyde).<sup>[79]</sup> The absence of one methylene bridge in the case of *ns*-CB[6] did not provide chiral properties, and only ( $\pm$ )-*bis-ns*-CB[6] with two bridges absent was entirely asymmetric (Figure 17A). Moderate formation of diastereoselective complexes with chiral amines was observed. Interpretation of complex formation with aliphatic amines was complicated by fast exchange, and that the host was available only as a racemic mixture.<sup>[92]</sup>

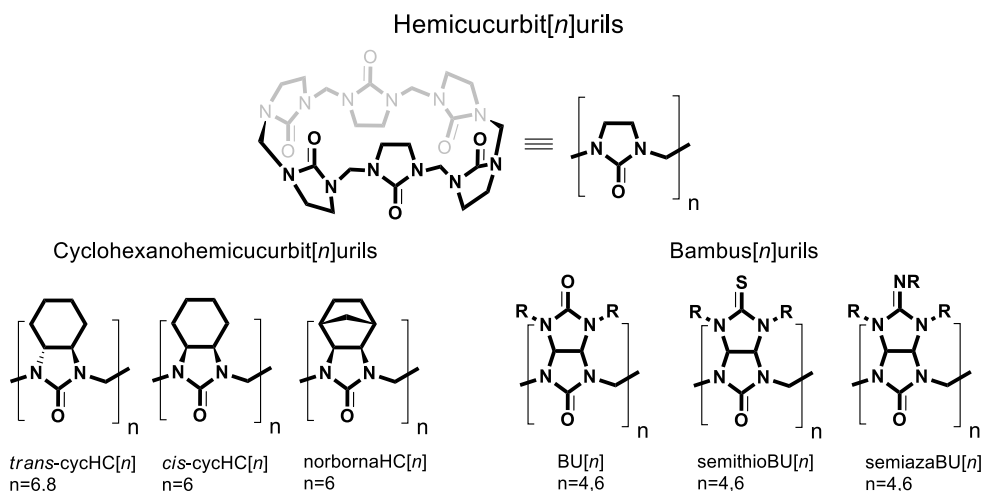
Acyclic CBs become chiral because of helical folding; for example, the reported 10-membered oligomer<sup>[90]</sup> (Figure 17B) or due to functionalisation by chiral terminal groups. Isaacs<sup>[93]</sup> (Figure 17C) reported an example of tetrameric oligomer functionalisation; however, the level of enantioselectivity was poor, likely due to the remote location of chiral centres from the complexation cavity of the tetramer.

In the case of large cucurbiturils, such as CB[13]-CB[15], axial chirality becomes possible, thus big cycles can form twisted structures (Figure 17D). The *twisted*-CB[14] cavity demonstrated adaptability. Complexation studies showed that binding with a small 1,4-butylammonium guest molecule with stoichiometry 1:2,  $K_o$   $1.9 \times 10^8$  M<sup>-1</sup> and  $2.9 \times 10^6$  M<sup>-1</sup> referred to two separate binding sites. However, binding with a larger 1,8-octyldiammonium guest occurred with stoichiometry 1:1 and  $K_o$   $7.9 \times 10^6$  M<sup>-1</sup>.<sup>[82,91]</sup>

Isaacs also introduced one functionalised monomer into the core of the CB[7], which was connected through a linker with biotin or another ligand (Figure 17E). Chirality of the resulting CB was achieved through chiral nature of the ligand. With the help of the new host the anti-cancer drug Oxaliplatin was efficiently transported towards cancer cells but no chiral interaction was studied.<sup>[13]</sup> Chirality in single-bridged CB (hemicucurbiturils) will be discussed further.

### 1.4.3 Hemicucurbit[*n*]urils

Inspired by cucurbituril chemistry, Miyahara and co-workers synthesised the first hemicucurbiturils<sup>[94]</sup> (HC), member of a new branch of the cucurbituril family, in 2004 (Figure 18). The monomer of the HC, ethylene urea, can be viewed as 'half' of the glycoluril (the monomer of CB); hence the name.<sup>[95]</sup> Hemicucurbiturils are not as numerous as cucurbiturils, but in recent years several interesting new members have appeared (Scheme 4). Generally, all HCs form guest-host complexes with anions through C-H...anion interactions and the chaotropic effect.<sup>[95,96]</sup>



**Scheme 4.** Hemicucurbit[*n*]uril representatives.

#### 1.4.3.1 Unsubstituted hemicucurbit[*n*]urils

The optimised procedure for a six-membered ring is an equimolar reaction of ethyleneurea and 37% formaline in 4 M HCl at room temperature. It yields in less than 30 minutes with 94% of the six-membered cyclic product as HCl adduct (Figure 18). The same mixture in 1M HCl at 55°C provides 93% of HC[12] in three hours.<sup>[94]</sup>

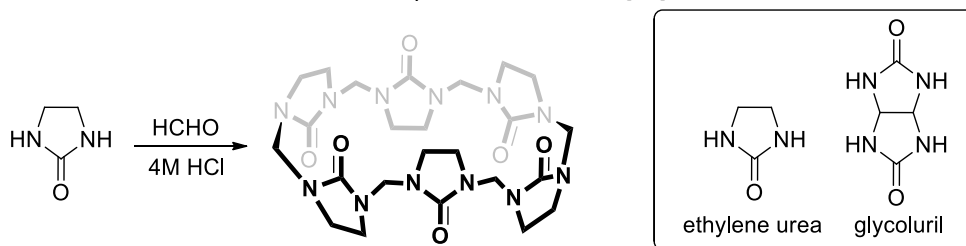


**Figure 18.** Synthesis of HC[6], ethylene urea, and glycoluril structures.<sup>[94]</sup>

HC[6], due to the alternate orientation of carbonyl groups, interacts most with anions, such as  $\text{Cl}^-$ <sup>[94]</sup>,  $\text{SCN}^-$ , and  $\text{I}^-$ <sup>[97]</sup>. Interestingly, it was reported by Buschmann that HC[6] interacts with ions of transition metals, including  $\text{Co}^{2+}$ ,  $\text{UO}^{2+}$ , and  $\text{Ni}^{2+}$ .<sup>[98]</sup> Some interactions of HC[6] with ferrocene and ferrocenium ions were recently reported.<sup>[99]</sup> In the case of HC[12], there is only one example of complexation. Two phenazine hydrochloride salt molecules were reported to be complexed into HC[12]; however, HC[6] forms a complex with the same guest at stoichiometry 1:1.<sup>[100]</sup> Unfortunately, HC[6] is poorly soluble in water and only some additives (e.g. thiocyanate) can improve it to some extent<sup>[97]</sup>. It can be easily dissolved in common organic solvents though, such as methanol and chloroform.<sup>[100]</sup>

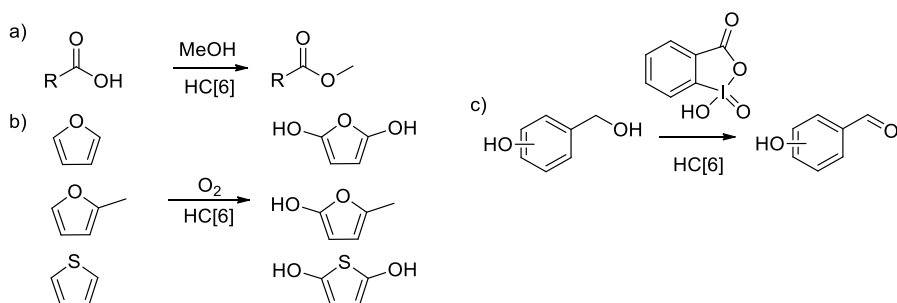


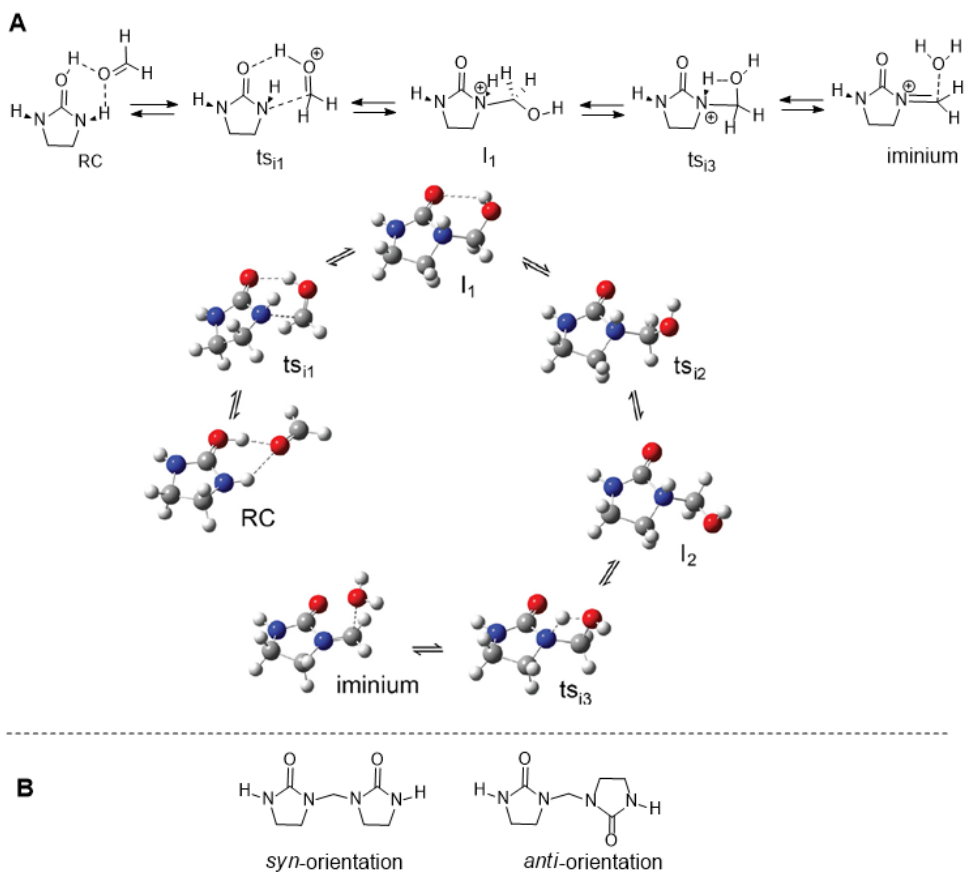
**Figure 19.** Catalysed by HC[6] reactions: a) esterification of conjugated carboxylic acids<sup>[101]</sup>, b) oxidation of furan, 2-methylfuran, and thiophene by oxygen in water,<sup>[102]</sup> c) oxidation of benzylic alcohols by IBX.<sup>[103]</sup>

HC[6] shows catalytic activity in some reactions (Figure 19). It was effective in the catalysis of the esterification reaction of small conjugated carboxylic acids<sup>[101]</sup>, oxidation of furan and 2-methylfuran and thiophene in water by oxygen naturally present in the mixture<sup>[102]</sup>. A hemicucurbituril-supported ionic liquid phase palladium catalyst was also recently prepared<sup>[104]</sup>. Tao's group described the ability of the HC[6] to perform chemoselective oxidation of hydrobenzoic alcohols by 2-iodoxybenzoic acid to aldehydes without over-oxidation.<sup>[103]</sup> Both HC[6] and HC[12] have been used by Buschmann *et al.* as carriers in water/chloroform extraction of cysteine, leucine, valine, phenylalanine, and serine.<sup>[105]</sup>

Due to the smaller number of atoms in the structure of hemicucurbiturils, as compared to double-bridged cucurbiturils, it is more convenient to investigate by means of computational chemistry. Yoo and Kang<sup>[106]</sup> recently published very detailed work concerning the mechanism of hemicucurbituril formation (Scheme 5A). The rate determining step of the first phase of cycle formation was the transformation of intermediate I<sub>2</sub> through ts<sub>3</sub> towards iminium. This statement is consistent with the experimental observations that high temperatures are often needed to generate enough iminium ions in the reaction mixture.

The mechanism of CB chain growth was step-growth cyclo-oligomerisation. In the case of hemicucurbiturils, the same mechanism was reported. In contrast with CBs, in HC monomers can be added in two ways: *syn*- and *anti*-pathways (Scheme 5B). The *anti*-pathway of the dimerisation was kinetically more favourable. Further oligomer growth transition states were similar to those calculated for the dimer. Moreover, 'alternate' conformation of the formed cycle was stabilised by greater flexibility compared to 'cone' conformation.

The conclusion of this study was that the rate-determining step for hemicucurbituril formation was formation of the iminium and barriers for oligomerisation and cyclisation were nearly half the iminium barrier. Formation of the HC[6], starting from ethyleneurea and formaldehyde in acidic conditions, was favoured kinetically as well as thermodynamically.<sup>[106]</sup>



**Scheme 5.** (A) Plausible mechanism for iminium formation and (B) acyclic methylene-bridged dimers. Figure A is reprinted with permission from Elsevier, ref. <sup>[106]</sup>.

All published hemicurbiturils to date will be reviewed and are divided into several sub-groups according to structural features. Due to the complex structure of this class of molecules, often trivial names are given to new members of this family by different synthetic chemists, which makes it difficult to classify in the CB family. This thesis focuses on the synthetic procedures, complexation properties, and possible applications published for the HCs.

#### 1.4.3.2 Cyclohexanohemicurbit[*n*]urils

The first *cis*-cycHC[6] was prepared by Wu and co-workers in 2009. Heating of a mixture of *cis*-octahydro-2H-benzimidazol-2-one with 1 eq. of paraformaldehyde in 4M HCl at 70°C for four hours provided, after purification, six-membered *cis*-cycHC in 78% yield (Figure 20). The crystal structure of this macrocycle showed ordinary for this class of molecules alternated orientation of the monomers. The solid state external complexes of CHCl<sub>3</sub> and CCl<sub>4</sub> with *cis*-cycHC[6] were described.<sup>[107]</sup>

Several names have been used for the *cis*-cycHC[6] compound. It was first named hemicyclohexylcurbit[6]uril<sup>[107]</sup>, then cyclohexylhemicurbituril<sup>[108]</sup>, but a preferable name would be cyclohexanohemicurbit[*n*]uril (cycHC). This is in agreement with IUPAC rules, where hemicurbituril is the parent compound and the prefix cyclohexano- defines the substituent on the parent macrocycle.

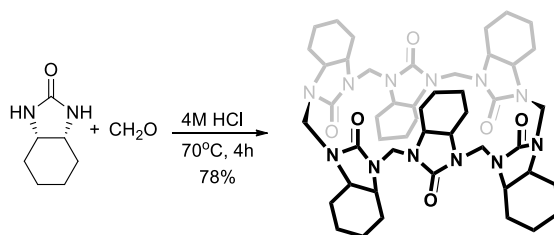


**Figure 20.** Synthesis of *cis-cycHC[6]*.<sup>[109]</sup>

In 2013 Šindelář reported one new macrocycle named norbornahemicucurbit[6]uril (norHC[6])<sup>[110]</sup>. It could also be viewed as cyclohexanohemicucurbit[6]uril with a methylene bridge substituent in the cyclohexane ring<sup>[95]</sup> (Figure 21). During MALDI-TOF MS analysis of the filtrate, after separation of the main product, 4-, 5-, 7-, and 8-membered homologues were detected.

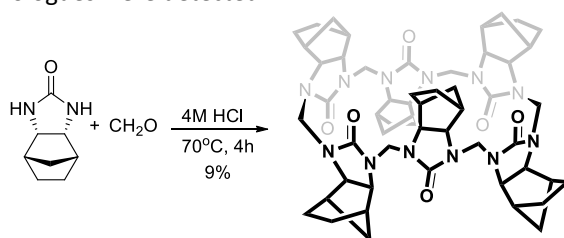


**Figure 21.** Synthesis of *norHC[6]*.<sup>[95]</sup>

This macrocycle was formed in relatively low yield, likely due to the bulkiness of the additional substituent on the cyclohexane ring. No complexation data were available for this macrocycle.

#### 1.4.3.3 *Bambus[n]uril*

Šindelář stated that bambusurils share properties of CBs and HCs, as the macrocycle is made from glycolurils, as CBs are, and the monomers are connected through single bridges as in HCs.<sup>[111]</sup> However, in reality, the alternate configuration of the monomers defined the chemical properties, similarly to all single-bridged hemicucurbit[*n*]urils. BU[*n*]s are the most studied among the single-bridged CB family members and currently many analogues have been synthesised (Figure 22).<sup>[112]</sup>

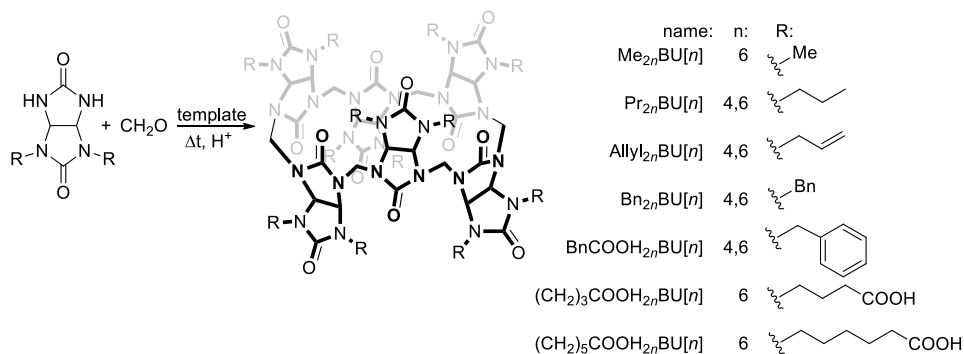


**Figure 22.** General scheme for the synthesis of BU[*n*].<sup>[112]</sup>

Bambus[*n*]urils are composed of *n* 2,4-substituted glycoluril monomers connected by one line of aminal bridges in the equatorial part of the molecule. This macrocycle was named for the resemblance of its structure to a bamboo stem.<sup>[111]</sup> BU synthesis is possible not only in aqueous conditions, but in organic media as well.<sup>[113]</sup> However, despite the large number of analogues synthesised, there have only been two homologues synthesised thus far: four- and six-membered BU[*n*]. In hemicucurbituril synthesis, the template has a more pronounced effect than in double-bridged cucurbiturils<sup>[86]</sup>. For bambusurils, in the absence of a template, four-membered cycles<sup>[112,114]</sup> are formed. An anionic template directs the formation of the six-membered cycle. For example, use of HCl afforded Me<sub>12</sub>BU[6]<sup>[111]</sup> in 30% yield, and the presence of BF<sub>4</sub><sup>-</sup> resulted in 80% yield of the six-membered macrocycle. When a variety of templates were tested for BU[6] synthesis, yields strongly depended on the affinity of the cycle formed towards the anionic template used.<sup>[115]</sup> Heck and co-workers showed that the use of a microwave reactor not only notably reduced reaction time, but it also increased yield, in some cases up to 90%.<sup>[116]</sup>

Generally, alkyl-substituted BU[*n*]s are not very soluble in water and organic solvents. However, the tetrameric cycle, which was always present in the reaction in an organic solvent as a by-product, has significantly better solubility and can be easily washed out from the solid hexameric product by chloroform.<sup>[113]</sup> Several water soluble macrocycles, such as BnCOOH<sub>12</sub>BU[6]<sup>[117]</sup>, (CH<sub>2</sub>)<sub>3</sub>COOH<sub>12</sub>BU[6], and (CH<sub>2</sub>)<sub>5</sub>COOH<sub>12</sub>BU[6]<sup>[118]</sup>, were recently synthesised.

From the reaction mixture, hemicucurbiturils are normally isolated as complexes with the corresponding template, typically halide ions. Šindelář's group was able to prepare anion-free BUs. Such molecules are much easier to use in further complexation studies. The first method consisted of replacement of the Cl<sup>-</sup> template, originated from the synthesis, by I<sup>-</sup> and its subsequent oxidation to I<sub>2</sub> by hydrogen peroxide or photochemistry methods. The resulting anion-free macrocycle precipitated.<sup>[119]</sup> Another method was to prepare BUs in organic media using HSO<sub>4</sub><sup>-</sup> template. The reaction media was then changed to water, templating ion became the cosmotropic highly hydrated SO<sub>4</sub><sup>2-</sup> and was washed out from the cavity of the macrocycle by water.<sup>[118]</sup>

Macrocyclic structures are able to form complexes with guest molecules. A four-membered BU is too small to accommodate any ion or molecule inside the cavity. However, it was reported that substituted BU[4]s, such as BnBU[4], due to deeper binding pockets formed by benzyl-substituents, were able to accommodate two acetonitrile molecules.<sup>[113]</sup>

Nevertheless, the main binding studies used hexameric BUs. BU[6] has a hydrophobic inner cavity, which is able to bind anions. Computational and X-ray studies showed that there are 12 weak C-H...anion hydrogen bonds that participate in host-guest interaction. The relatively flexible structure of the BUs allowed for the accommodation of various anions, from F<sup>-</sup> to PF<sub>6</sub><sup>-</sup>, and association constants varied from 1.0 × 10<sup>3</sup> to 1.0 × 10<sup>7</sup>.<sup>[112]</sup> Due to the synthesised water soluble analogues, complexation of BUs was possible in both organic and aqueous media and the strongest binding was observed for ClO<sub>4</sub><sup>-</sup> in water.<sup>[117]</sup> In solution, the stoichiometry of the BU binding and inorganic anions was 1:1 no matter which anion and solvent was used. Exceptionally strong binding of BU in water can be explained by numerous hydrogen bonds forming in the cavity and by enthalpy driven complexation based on expulsion of so-called high energy water by guests from the inner cavity of the host molecule<sup>[96,120]</sup>.

In solid state, complexes with stoichiometry 1:1 and 1:2 (BU:guest), were observed.<sup>[113,121,122]</sup>

Bambusurils can find application, due to the ability to bind anions. As BU[6] forms complexes with inorganic anions through slow exchange in a  $^1\text{H}$  NMR timescale, the complexes have unique chemical shifts and it is possible to visualize binding of anions. Thus, BU[6] can be used in the identification of different anions in the mixture. Šindelář and co-workers developed a method for quantification of up to five different anions in mixture within 5% error.<sup>[123]</sup>  $\text{Me}_{12}\text{BU}[6]$  was used as the reductant in the photochemical reaction with methylviologen.<sup>[121]</sup>  $\text{Bn}_{12}\text{BU}[6]$  and fluorinated BU[6] were used as carriers of anions in the liquid membrane during electromembrane extraction.<sup>[124,125]</sup>

Sulphur and nitrogen containing BU analogues were introduced by Keinan and Reany. Such compounds were termed hetero-bambusurils or semithio- and semiaza-BUs (Figure 23).

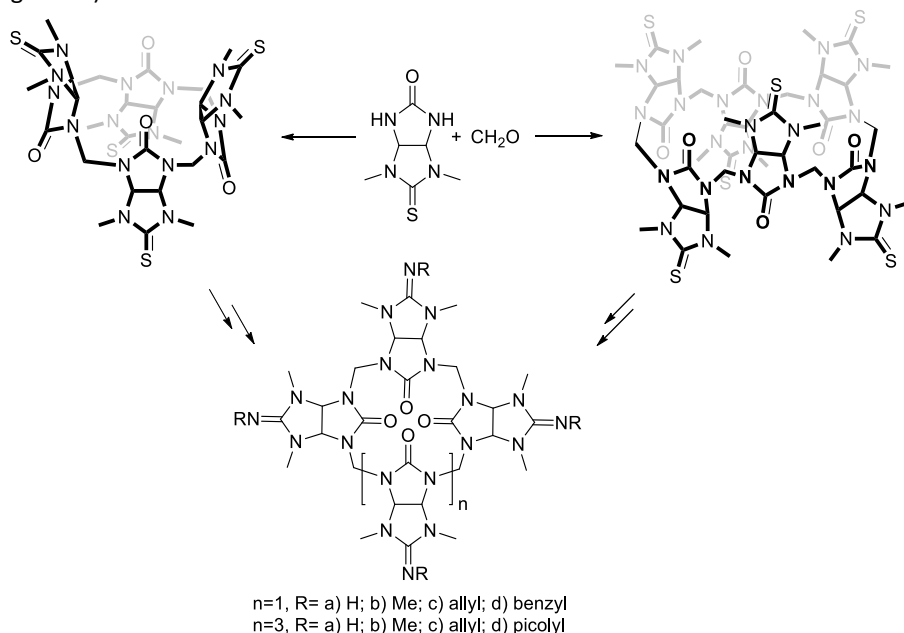


**Figure 23.** Synthesis of semithio- and semiaza-BUs.<sup>[126]</sup>

Despite the conclusions from the computational study of Pichierri<sup>[127,128]</sup>, which predicted the possibility of the existence of stable sulphur analogues of CBs, all recent attempts at the same were unsuccessful. Keinan and Reany's review provides an overview of the different approaches towards hetero-glycolurils, though many were not successful. The importance of the C=O functionality in bambusuril formation was observed experimentally. The condensation reaction of formaldehyde with thio-glycolurea did not result in thioacylaminal bridge formation. Semithio-bambusurils (semithio-BU) can be formed only if the bridge is built between the ethylene part of the monomer and sulphur is in the outer part of the molecule.<sup>[47,114]</sup> Using Heck's reaction conditions, four- and six-membered semithio-bambusurils were synthesised.<sup>[114]</sup> Semithio-bambusurils can be transformed into semiaza-bambusurils (semiaza-BU) by a two-step one-pot reaction (Figure 23).<sup>[129]</sup>

Semithio-BU[6] is insoluble in organic solvents and only the presence of certain anions can dissolve it in DMSO. Affinity towards halides of semithio-BU[6], in order, is  $\text{Br}^- > \text{I}^- > \text{Cl}^-$ , which is different than for normal BU[6]<sup>[117]</sup>. Semithio-BU[4] is too small to accommodate anions inside the cavity, but it showed interaction with cations  $\text{Hg}^{2+}$  and  $\text{Pd}^{2+}$  from outside the macrocycle.<sup>[114]</sup> Semiaza-BU[6] can uniquely form guest-host complexes with three anions simultaneously: two triflate anions and either bromide or iodide.<sup>[126]</sup> In addition, BU[6], semithio- and semiaza-BU[6] were compared as transmembrane transporters for  $\text{Cl}^-$ . All three were good anion binders, but semithio-BU[6] was the most efficient transporter.<sup>[111]</sup>

#### 1.4.3.4 Biotin[6]uril

In 2014 Pittelkow *et al.* published the synthesis of the first water soluble hemicucurbituril-type macrocycle – biotin[6]uril (BioU[6])<sup>[130]</sup>, which consisted of six D-biotin monomers (Figure 24). A mixture of D-biotin with paraformaldehyde in 3.5 M  $\text{H}_2\text{SO}_4$  with halide template (NaBr) heated at 60°C for two days provided BioU[6] in 63% yield.

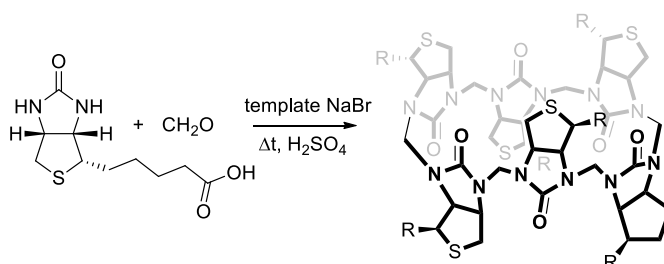


**Figure 24.** Synthesis of BioU[6].<sup>[109]</sup>

The six-membered macrocycle has an alternate orientation of monomers, hydrophobic cavity, and 12 C-H functions, which were potential hydrogen bond donors. Concerning the chirality of D-biotin and the possible number of stereo- and regio-isomers of the final molecule, only one isomer was isolated in relatively high yield.

The proposed mechanism of formation was trimerisation of quickly formed biotin-dimers.<sup>[109]</sup> BioU[6] showed complexation preferring softer anions over harder anions ( $\text{SCN}^- > \text{I}^- > \text{Br}^- > \text{Cl}^-$ ).<sup>[131]</sup>

In 2015 BioU[6] was modified to be soluble in organic solvents by esterification. Methylated (BioU[6]me<sub>6</sub>), ethylated (BioU[6]et<sub>6</sub>), and butylated (BioU[6]bu<sub>6</sub>) biotinurils were prepared. Hexaesters showed good complexation with  $\text{Cl}^-$  and moderate complexation with  $\text{NO}_3^-$  and  $\text{HCO}_3^-$ . No binding of  $\text{SO}_4^{2-}$  was detected. For all three BioU[6] esters, transmembrane transport of anions was investigated. BioU[6]bu<sub>6</sub> with a long lipophilic chain had the best transporting results; however, all three showed good anion transportation ability.

## 2 Aims of the study

Macrocyclic container-molecules exhibit unique properties, which can be used in industry, pharmacology, and other important fields. These molecules can encapsulate organic molecules and ions, fully modifying the environment for the guest molecule, similarly to enzymes.

Hemicucurbit[*n*]urils are a relatively new branch of the cucurbit[*n*]uril family. At the beginning of this PhD study, few four- and six-membered and single twelve-membered hemicucurbituril were reported. Moreover, important features, such as chirality, which is of central importance in nature, are only present in exceptional CB family examples. To determine new specific applications, a deep understanding of macrocycle structure and behaviour is required. A wider variety of the shapes and dimensions of the host molecules will open up new horizons for application and development.

The particular aims of this study are:

- to obtain new chiral hemicucurbiturils and characterise their structures;
- to optimise synthetic procedures for enantiomerically pure cycHC[6] and larger macrocycles;
- to study structure and properties of the new chiral macrocycles;
- to study the mechanism of cyclohexanohemicucurbiturils' formation;
- to investigate host-guest complexes of the new macrocycles.

### 3 Results and discussion

The following section of the thesis focuses on the synthesis of the new chiral cyclohexanohemicucurbit[*n*]urils ((*S,S*)-cycHC[6], (*R,R*)-cycHC[6], or *trans*-cycHC[6] in general), structural features, and complexation. In the current work, racemic mixtures of the *trans*-cycHC[6] and its monomer octahydro-2H-benzimidazol-2-one were not used, thus, the general name *trans*-cycHC will be used for enantiomerically pure macrocycles if the exact configuration is not particularly important. The first part of the following chapter covers synthesis of the enantiomerically pure *trans*-cycHC[6], its geometry, and electronic structure. In the second part, with the help of computational chemistry and analytical methods, interactions that play a role in complexation with organic molecules and ions will be described. The third part outlines the route towards larger homologues of *trans*-cycHC[*n*] and *trans*-cycHC[8] in particular. The focus is on optimisation of the synthetic procedure starting from monomers or via the reversible *trans*-macrocyclisation process from cycHC[6]. The formation mechanism of cycHCs are discussed in detail. The fourth part describes the structure, synthesis, and complexation of another new HC, the *inverted-cis*-cyclohexanohemicucurbit[6]uril (*i-cis*-cycHC).

#### 3.1 *Trans*-cyclohexanohemicucurbit[6]uril

Chirality is a very important structural feature in nature. RNA, DNA, enzymes, proteins, sugars, and hormones are all chiral. The fact that there are not many examples of chiral hosts in the cucurbituril family is a major drawback. The chiral complexation ability of CBs has not yet been well studied.<sup>[82]</sup> Introduction of chiral and enantiomerically pure hosts is of great importance.

##### 3.1.1 Synthesis and structure (Publication I and II)

On the basis of the first synthesis of cyclohexanohemicucurbit[6]uril, published by Li and co-workers,<sup>[107]</sup> we envisioned formulation of its chiral isomer. The approach was to start the synthesis from inexpensive and commercially available cyclohexane-1,2-diamine *cis*-/*trans*-mixture. The relatively simple two-step synthesis provided an enantiomerically pure urea derivative in good yield (Figure 25).<sup>[132,133]</sup> After careful purification, the obtained urea was used as a starting compound for the synthesis of the *trans*-macrocycle under the conditions reported by Li<sup>[107]</sup>. In the literature, heating of the *cis*-urea derivative with formaldehyde in 4 M aqueous hydrochloric acid at 70°C for four hours resulted in a good yield of *cis*-cycHC[6]. In the case of enantiomerically pure cyclohexa-1,2-diylurea, after four hours under the same conditions, a heterogeneous mixture with peculiar properties was formed. The obtained substance, which was viscous and insoluble in common organic solvents, was a mixture of oligomers of different lengths. Following a reaction mixture by NMR showed that one set of signals was steadily growing and after reaction prolongation to 24 hours, (*R,R*)- or (*S,S*)-cycHC[6] were obtained with up to 85% yield (Figure 26). The structure of isolated product was determined to be the six-membered macrocycle HCl complex, according to ESI-MS and quantitative NMR techniques. To obtain the desired *trans*-cycHC[6], it was also possible to use hydrobromic acid; however, the yield decreased to 75%. Other acids, such as trifluoroacetic, sulfuric, and hydroiodic in aqueous conditions were not suitable for the synthesis of cycHC[6]. In the case of sulfuric and hydroiodic acids, probable side reactions and decomposition of the starting compound occurred. During the oligomerisation process in aqueous media, competing

nucleophilic addition of water to the imine intermediate occurred and, therefore, strong acidic conditions were used to eliminate water from the hydroxyaminal intermediate. Trifluoroacetic acid with acid dissociation constant  $pK_a=0.23$ <sup>[134]</sup> in water was probably not acidic enough to secure fast equilibration between dynamic library members. Another possible reason was the weak complexation between the anionic template and the hexameric oligomer in water, which resulted in no cyclisation.

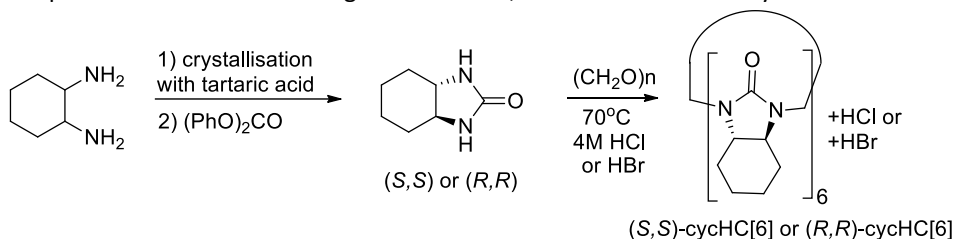


**Figure 25.** Synthesis of (S,S)- and (R,R)-cyclohexanohecticurbit[6]urils starting from cyclohexane-1,2-diamine.<sup>[132,133]</sup>

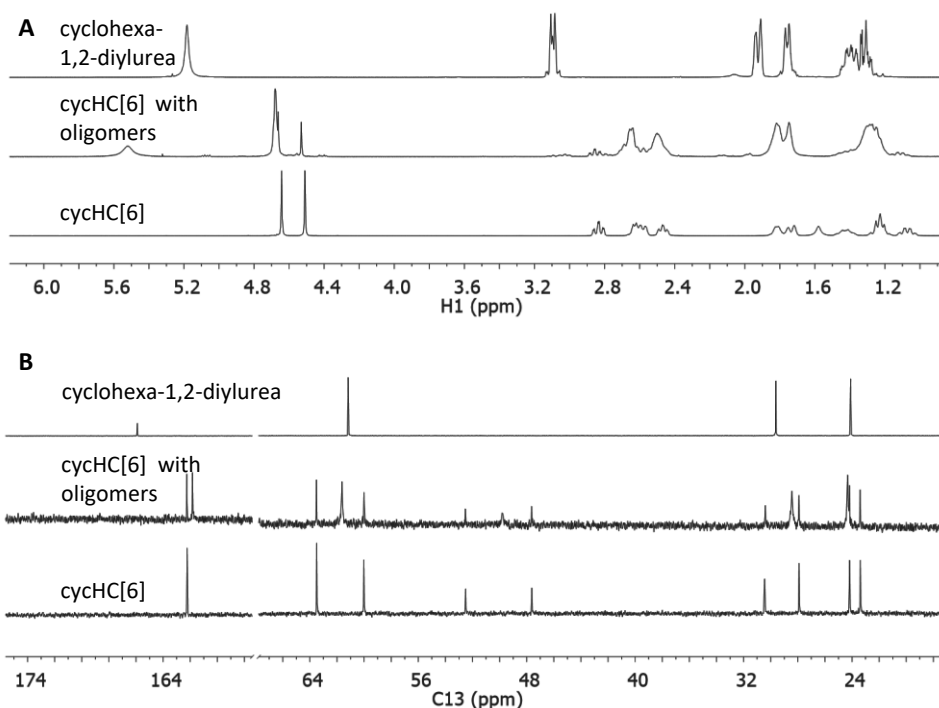


**Figure 26.** (A)  $^1\text{H}$ - and (B)  $^{13}\text{C}$ -NMR spectra of cyclohexane-1,2-diamine, mixture of cycHC[6] and oligomers (products of uncompleted reaction,) and cycHC[6].

After several attempts, mono-crystals of *trans*-cycHC[6] were obtained from the mixture of  $\text{CCl}_4$  and diisopropylethylamine. The crystal structure showed that six monomers adopted the 'alternate' orientation (Figure 27) characteristic of all single bridged HCs. No guest molecule was incorporated in the cavity of the macrocycle. Obviously, strongly basic diisopropylethylamine abstracted/neutralised the chloride ion during crystallization. The cyclohexyl rings leaned toward each other close the opening

of the macrocycle, such that the shape of this HC was similar to a cucurbiturils' pumpkin or ball shape. This was as opposed to the bambusuril<sup>[112]</sup> or *cis*-cycHC[6]<sup>[107]</sup>, where portals are wider than the central part of the molecule (Figure 14).

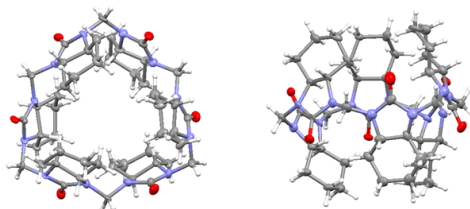


**Figure 27.** Crystal structure of *(S,S)*-cycHC[6].

If the dimensions of the non-collapsible empty void in *trans*-cycHC[6] are compared with those of other known macrocycles, *trans*-cycHC[6] is large enough to accommodate a guest molecule or ion. The opening of *trans*-cycHC[6] is 2.2 Å, which is comparable to the corresponding value of 2.4 Å in cucurbit[5]urils.<sup>[135]</sup> The cavity size of cycHC[6] is wider, and the distance between the two opposite carbonyl carbons is 5.3 Å, compar<sup>[135]</sup>

ble to the cavity size of 5.8 Å in cucurbit[6]uril<sup>[135]</sup> and 5.3 Å in  $\alpha$ -cyclodextrin<sup>[136]</sup>. The height of *trans*-cycHC[6] is 12.1 Å, taking into account the van der Waals radii of relevant atoms.

*Trans*-cycHC[6] has a polar belt bearing urea functionalities in the middle and nonpolar cyclohexyls around the openings. The monomers are linked to each other via one methylene bridge, thus, cyclohexyl rings are relatively flexible, and the size of the opening could possibly be increased (Publication II). This hypothesis was experimentally confirmed in later complexation studies of *trans*-cycHC[8].<sup>[137]</sup> Dimensions of the narrow portals of the macrocycle allow bulky guest ions into the cavity as a result of the conformational change of the host.

Computational studies on the structure of *trans*-cycHC[6] contributed to a deeper understanding and better prediction of structural and complexation properties, which were confirmed experimentally. The highest occupied molecular orbital (HOMO) of the *(S,S)*-cycHC[6] is located on the heteroatoms of the macrocycle (Figure 28A, for computational details see Publication II). The HOMO lobes on nitrogens are located on both inner and outer sides of the macrocycle. In addition, the HOMO is located on cyclohexyls. Therefore, the binding site for cationic species is spread around the molecule and partially inside the cavity. The lowest unoccupied molecular orbital (LUMO, Figure 28B) is concentrated in the centre of the cavity. Thus, it was assumed that electron rich compounds can be encapsulated into the cavity of the *(S,S)*-cycHC[6].

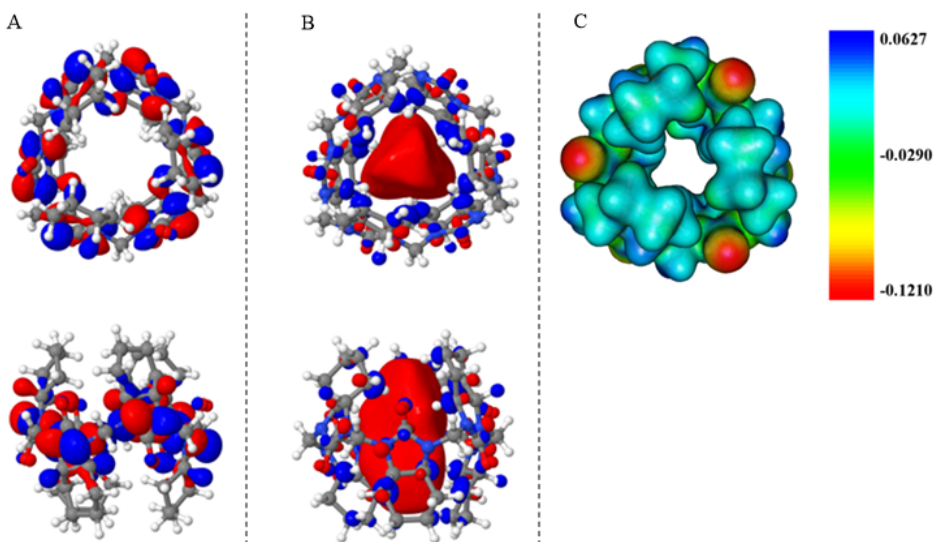


**Figure 28.** Electronic structure of *(S,S)*-cycHC[6]: (A) HOMO, (B) LUMO, (C) MESP.

The map of electrostatic potential (MESP) for *(S,S)*-cycHC[6] is shown in Figure 28C. The most electron-rich regions (red areas) were on the oxygen atoms, while the most electron-deficient areas (blue areas) were found on the methylene bridges and the centres of cyclohexyl groups. As a result, the openings of the macrocycle were rather electron-poor. Due to the chiral character of the urea monomers, one of the electron-rich nitrogens faced inside the cavity of the *trans*-cycHC[6] and another faced outside. The complexation of both an anion and a proton inside the cavity of the macrocycle is feasible; however, spatially larger electron-poor guests are expected to bind outside of the macrocycle (Publication II).

### 3.1.2 Complexation properties

Generally, different hosts are selective toward different types of guests. At the beginning of this PhD study, information about the complexation properties of hemicucurbiturils was controversial. Buschmann *et al.* reported HC[6] to form complexes with both anions<sup>[97]</sup> and cations<sup>[98]</sup>, which was intriguing. Thus, the first step of the complexation study of *(R,R)*-cyclohexanohemicucurbit[6]uril was screening the interaction with different classes of substances using NMR and MS analysis (Figure 29).

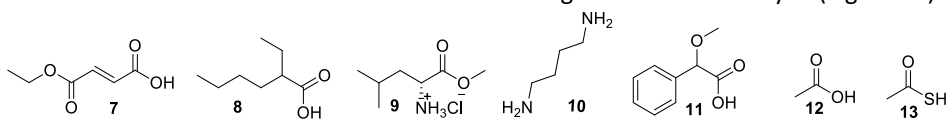


**Figure 29.** Structures of studied compounds **7-13** that formed complexes with *(R,R)*-cycHC[6].

The addition of one equivalent of *(R,R)*-cycHC[6] to the solution of compounds **7-11** in chloroform caused a <sup>13</sup>C-NMR chemical shift change in small molecules. However, no chemical shift change for the macrocycle was detected. During ESI-MS analysis, mixtures **7-10** with cycHC[6] were studied. The molecular ions of cycHC[6]+carboxylic acids **7** and **8** were detected in negative mode (as carboxylates) and cycHC[6]+amino

group containing compounds **9** and **10** were detected in positive mode (in protonated form). This confirmed the existence of 1:1 complexes. In addition, a 2:1 (2 cycHC[6]:**10**) complex with diammoniumbutane **10** was detected by ESI(+)-MS (for the complexation study details see Publication I).

Binding with chiral acid was studied to reveal the stereoselective behaviour of cycHC[6]. The formation of diastereomeric complexes between methoxyphenylacetic acid (MPA) **11** and (*R,R*)-cycHC[6] was detected by  $^{13}\text{C}$ -NMR. Mixtures of MPA and cycHC[6] in ratios of 5:1, 1:1, and 1:5 were analysed. The splitting of  $^{13}\text{C}$ -NMR signals of *rac*-MPA along with an accompanying chemical shift change was observed. Figure 30 shows representative  $^{13}\text{C}$ -NMR fragments of MPA signals at C3 carbon. In the case of enantiomerically pure samples of MPA (Figure 30A), the addition of (*R,R*)-cycHC[6] caused a shift and because the exchange process was fast on the NMR timescale, no splitting of the peak occurred. Chemical shift corresponded to the average signal between complexed and non-complexed acid. Owing to complexation with cycHC[6], the *R*-MPA C3 signal shifted more upfield compared to the C3 of complexed *S*-enantiomer. For mixtures with different ratios of MPA and cycHC[6] (Figure 30B), the higher the number of complexed MPA molecules, the greater shift observed.

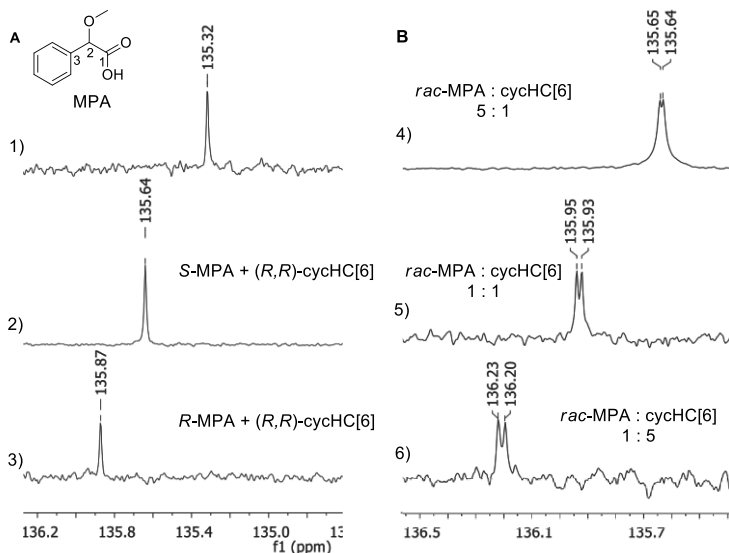


**Figure 30.** Structure of MPA **11** and fragments of  $^{13}\text{C}$ -NMR spectra of C3 signals: (A) 1) MPA, 2) *S*-MPA complex with (*R,R*)-cycHC[6], and 3) *R*-MPA complex with (*R,R*)-cycHC[6], (B) 4) *rac*-MPA and (*R,R*)-cycHC[6] in 5:1 ratio, 5) *rac*-MPA and (*R,R*)-cycHC[6] in 1:1 ratio, and 6) *rac*-MPA and (*R,R*)-cycHC[6] in 1:5 ratio.

Diffusion NMR measurements of (*R,R*)-cycHC[6] with guests **7-13** were performed to confirm that NMR chemical shift changes were a result of complexation and not caused by other factors. For example, a change of ion strength or acidity of the solution can induce a change in the dissociation of the carboxylic acid and, therefore, also influences the chemical shift. The diffusion NMR technique can be used to evaluate the mobility of different dissolved species in solution and has been exploited for studying intermolecular complexation and solution state aggregates. Moreover, diffusion methods allow for estimation of the binding constant  $K_a$  from a single measurement. It is an acceptable alternative to titration studies.<sup>[138–140]</sup>

**Table 2.** Diffusion coefficients  $D$  ( $10^{-10}$  m<sup>2</sup>/s) and association constants  $K_a$  (M<sup>-1</sup>) of guest molecules with (*R,R*)-cycHC[6] host in 1:1 mixtures in CDCl<sub>3</sub>.

guest	$D_{free}$	$D_{bound}$	$D_{cycHC[6]}$	$K_a$
none			5.26±0.01	
<b>7</b>	9.09±0.01	6.91±0.01	4.68±0.01	73.2±0.5
<b>8</b>	9.66±0.01	8.66±0.01	5.27±0.01	14.4±0.1
<b>9</b>	5.18±0.01	4.87±0.01	5.11±0.01	NA
<b>10</b>	13.94±0.01	12.17±0.01	5.16±0.01	11.9±0.5
<b>S-11</b>	10.34±0.01	8.94±0.01	5.29±0.01	20.1±0.2
<b>R-11</b>	$D_{free}$ of S-MPA was used	8.59±0.01	4.99±0.01	27.2±0.8
<b>12</b>	15.48±0.02	13.85±0.02	4.83±0.01	8.0±0.5
<b>13</b>	18.45±0.07	18.56±0.02	5.27±0.01	0±0.5

$D_{free}$  denotes uncomplexed guest;  $D_{bound}$  is a complexed guest and  $D_{cycHC[6]}$  is a complexed macrocycle; binding of **9** could not be reliably determined, as diffusion methods are not suitable for binding evaluation when the  $D$  of guests and macrocycles are very close.

As can be seen from the Table 2, the self-diffusion coefficients ( $D$ ) of small molecules, which reflect the rate of thermal translational motion of dissolved species, decreased in the presence of (*R,R*)-cycHC[6]. These measurements clearly indicated intermolecular interaction and support the earlier observations from ESI-MS and 1D NMR, compounds **7-12** indeed form complexes with (*R,R*)-cycHC[6]. Despite the fact that the association constants were relatively small (up to 73.2 M<sup>-1</sup> for monoethylfumaric acid **7**).

Based on literature<sup>[94,111]</sup>, chlorine and bromine anions from the reaction mixture should be incorporated into the hemicucurbituril's inner cavity. Unfortunately, attempts to obtain a crystal structure of the macrocycle's complexes failed. MS, <sup>13</sup>C-, and diffusion NMR analyses showed that compounds with very different complexation characteristics, such as carboxylic acids and amines, had an interaction with (*R,R*)-cycHC[6]. However, the nature of the interaction was unclear and whether inclusion complexes formed or were bound from the outside remained unknown at that time.

A systematic search for binding sites for guest molecules was performed by Mario Öeren using computational chemistry (Publication II). Based on these results, anionic guests strongly preferred binding inside the macrocycle (Figure 31). All spherical halogen anions induced symmetrical changes in the structure of the macrocycle and flexible cyclohexyls covered the anion (Figure 31A). In the case of halides, the interaction energies decreased with the growth of the halide. However, in the case of non-spherical guests, such as anions of formic acid, deformation of the macrocycle occurred (Figure 31B). From the computational study, formate had a high interaction energy with (*S,S*)-cycHC[6], but distortion of the macrocycle geometry by this ion partially cancelled the effect of the strong interaction.

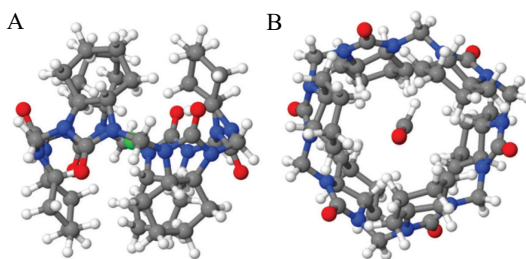


**Figure 31.** Calculated complexes of *trans*-cycHC[6] with anions (A) Cl<sup>-</sup> and (B) HCOO<sup>-</sup>.

The search for a proton binding site resulted in six possible locations. In the lowest-energy geometry, the proton was attached to the nitrogen atom inside of the macrocycle (Figure 32A). It is important to mention that the binding of larger cations through the inner cavity was much less probable, due to the size and position of the LUMO. For the non-dissociated species, binding from outside the macrocycle was favourable in all cases (Figure 32B).

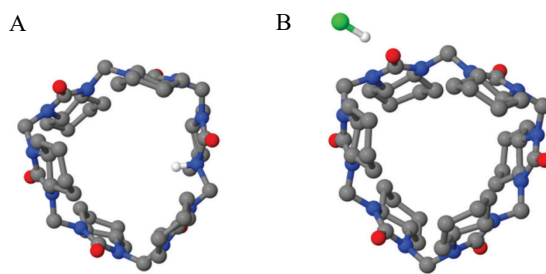


**Figure 32.** Structures of the lowest energy geometries of (A) protonated (*S,S*)-cycHC[6] and (B) (*S,S*)-cycHC[6] HCl complex. Hydrogen atoms, except the added proton, were omitted for clarity.

In *d*-chloroform, it was not possible to observe complexation of *trans*-cycHC[6] with different halides by means of NMR. Solubility of *trans*-cycHC[6] in other organic solvents was rather poor. Despite the fact that halide complexes were observed by mass-spectrometric analysis, all attempts to measure binding strength or rank the affinity for halogen ions by ESI-MS were unsuccessful. The results of experiments were not reproducible, because of system contamination with Cl<sup>-</sup>. From the reaction mixture, cycHC[6] was obtained as Cl<sup>-</sup> or Br<sup>-</sup> complexes; however, after chromatographic purification with CH<sub>2</sub>Cl<sub>2</sub>/methanol eluent, it tended to be anion free. This conclusion was made on the basis of NMR titration with TBABr or TBAI in *d*-chloroform, where no shift was observed for cycHC[6]. However, in a different solution system (5% acetic acid in methanol) used for ESI-MS, complexes with Br<sup>-</sup> and I<sup>-</sup> were detected.

To overcome previously mentioned problems concerning solubility and to experimentally confirm computational results, traveling-wave ion mobility mass spectrometry analysis (TWIM-MS) was used. The collision cross-section (CCS) values measured by ion-mobility MS and those calculated for Cl<sup>-</sup>, Br<sup>-</sup>, HCOO<sup>-</sup>, and H<sup>+</sup> were in good agreement. CCS of the complexes with anions were very similar (Figure 33), supporting the host-guest complexation model. The CCS of protonated cycHC[6] was slightly larger, possibly due to the opened portals. The CCS of the [cycHC[6]+Na<sup>+</sup>]

complex was significantly larger than the other CCS values, showing that sodium interacted with the macrocycle HOMO from the outside.

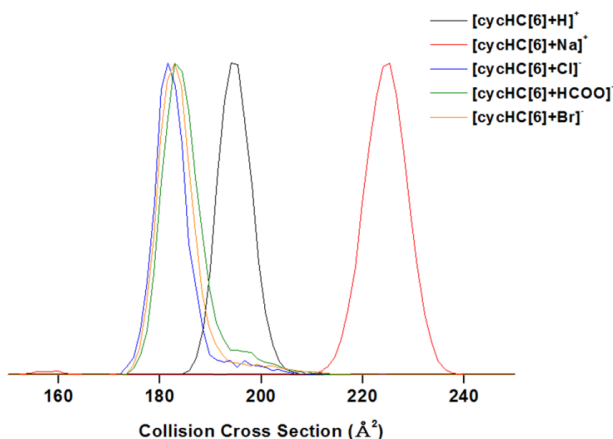


**Figure 33.** Ion-mobility mass-spectra of studied (*S,S*)-cycHC[6] complexes.

## 3.2 *Trans*-cyclohexanohemicucurbit[8]uril (Publications III and IV)

### 3.2.1 Structure and homologues

All CB family members are oligomeric macrocycles; therefore, differently sized normal CB[*n*]s can be synthesised as a mixture in one batch.<sup>[78,85,141]</sup> Analogously, in the case of hemicucurbiturils, different homologues of the favourable six-membered macrocycle can be formed (Publication III).

A crude reaction mixture of (*R,R*)-cycHC[6] in 0.1% formic acid in acetonitrile was carefully examined by RP-HPLC-MS analysis (Figure 34). 7-, 8-, 9-, and 10-membered homologues of (*R,R*)-cycHC[6] were observed. Unfortunately, the amounts were too small for separation. Studies on the influence of temperature on composition of the reaction mixture revealed no dependence in the range of 60–90°C. Purification of the crude product by RP flash chromatography produced (*R,R*)-cycHC[8] in 11% yield.

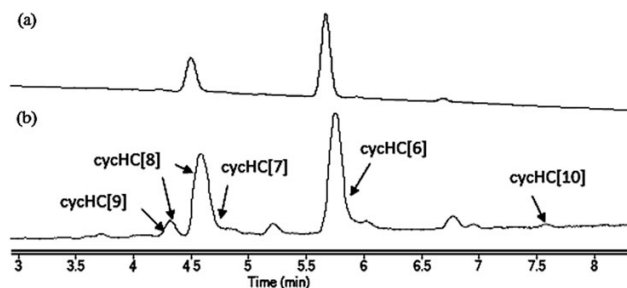


**Figure 34.** RP-HPLC–MS chromatograms of (*R,R*)-cycHC[9], (*R,R*)-cycHC[8], (*R,R*)-cycHC[7], (*R,R*)-cycHC[6], and (*R,R*)-cycHC[10]: (a) detected by UV at 210 nm and (b) detected by (+)ESI-MS.

NMR analysis of the cycHC[8] showed (Figure 35, c and d) that the macrocycle was highly symmetric, and all monomers were equal. Chirality of the starting compounds remained in the product as a pair of methylene bridges seen on the spectra. This was a specific feature of the chiral hemicucurbiturils, as two subsequent bridges had different

electronic surroundings (Figure 35, a and b). In the case of the first type of methylene bridge (C8), because of the alternate orientation of the monomers, both adjacent carbons were C1 and the protons were faced outside the macrocycle. The second type of bridge-carbons were C9, which were surrounded by C2 carbon protons pointing inside the cavity.

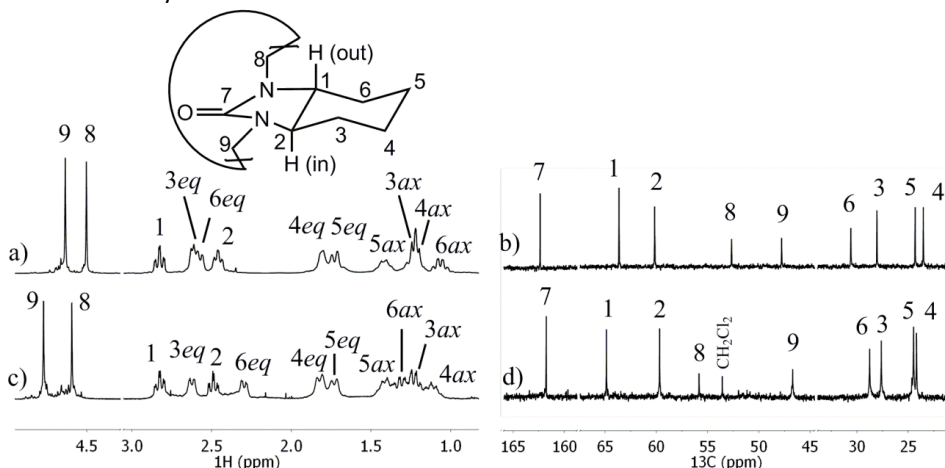


**Figure 35.** Assigned <sup>1</sup>H and <sup>13</sup>C NMR spectra of a), b) (*R,R*)-cycHC[6] and c), d) (*R,R*)-cycHC[8].

NMR data were in good agreement with the computationally obtained structure of (*R,R*)-cycHC[8] (Figure 36). The equatorial belt of the macrocycle adopted a square-like shape, having methylene bridges with carbons on the corners of the macrocycle. According to the computationally optimised structure, all cyclohexyl rings were in chair conformation, which was in good agreement with high value of <sup>3</sup>J(HH)-coupling constants (>11 Hz) between the cyclohexyl axial protons observed by <sup>1</sup>H-NMR. Modelling confirmed that monomers were in alternate orientations and cyclohexyl rings leaned slightly over the opening, as in the case of (*R,R*)-cycHC[6]. The diameter of (*R,R*)-cycHC[8]'s portal was 4.6 Å, which was within the corresponding values of normal cucurbiturils<sup>[135]</sup>; CB[6] was 3.9 Å and CB[7] was 5.4 Å. The cavity diameter at the equator of the (*R,R*)-cycHC[8] macrocycle was 8.5 Å, which was comparable to the 8.8 Å CB[8] cavity size. (*R,R*)-cycHC[8] had a barrel shape and cavity dimensions similar to normal cucurbiturils.

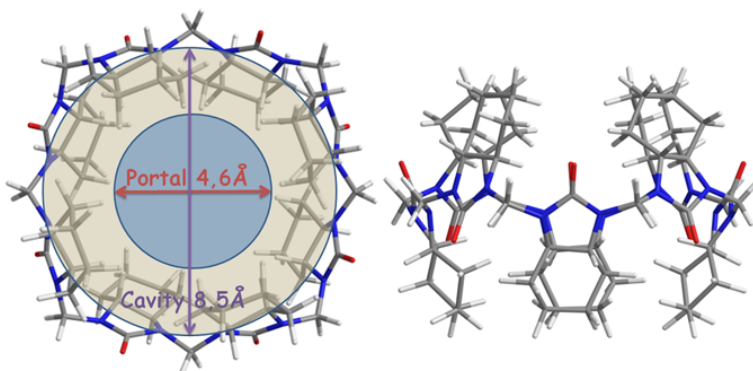


**Figure 36.** Calculated structure of (*R,R*)-cycHC[8]: top and side view.

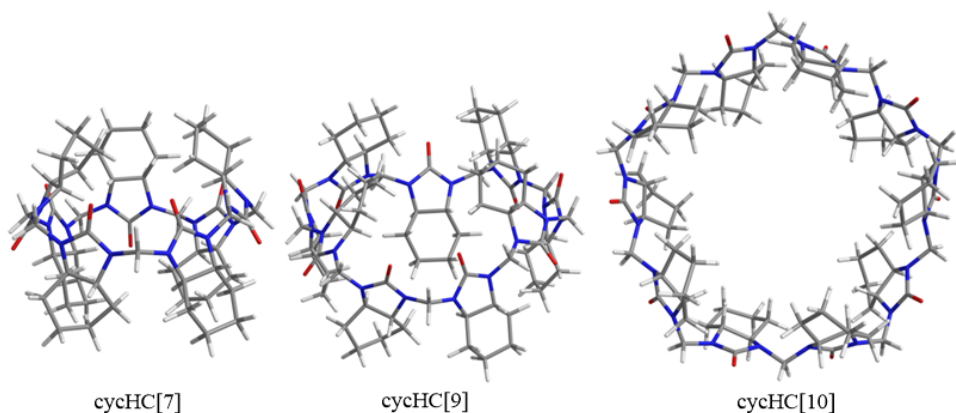


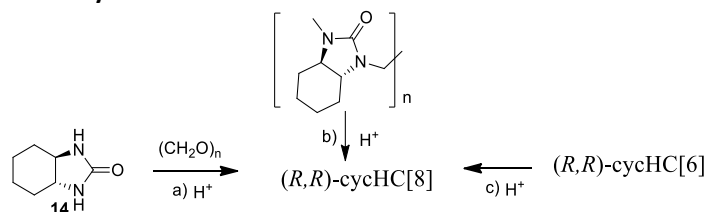
**Figure 37.** Calculated structures of *(R,R)*-cycHC[7], *(R,R)*-cycHC[9], and *(R,R)*-cycHC[10].

Geometries of 7-, 9-, and 10-membered homologues were also calculated (Figure 37). Macrocycles with an odd number of monomers were not as symmetrical. The two portals were not equal because of two aligned urea cycles, but the geometries were almost barrel-shaped. Unfortunately, only trace amounts of 7-, 9- and 10-membered cycHCs were formed under the studied conditions, such that the conformation could not be experimentally described.

In the negative ion mode of MS analysis, complexes of *(R,R)*-cycHC[8] with chloride and formate anions were detected, confirming that the newly substituted hemicucurbituril could bind anions similar to other alternate-oriented cucurbituril family members.

Further investigation and optimisation of the reaction conditions revealed that the previous hypothesis about the presence of an eight-membered homologue in the hydrochloric acid reaction mixture was not correct. The typical synthetic procedure, heating urea monomers and formaldehyde in hydrochloric acid only produced oligomers and the six-membered cycle: *(R,R)*-cycHC[6]. It was later noted during HPLC analysis that the amount of *(R,R)*-cycHC[8] was increasing over time. Thus, this transformation may occur as a result of the reaction catalysed by formic acid, which was one of the HPLC eluents, as well as one of the components in the HPLC sample.

### 3.2.2 Synthesis of cyclohexanohemicucurbiturils



**Scheme 6.** Synthetic scheme for obtaining *(R,R)*-cycHC[8] from a) *R,R*-cyclohexa-1,2-diylurea, b) a mixture of oligomers, and c) *(R,R)*-cycHC[6] under acidic catalysis and in the presence of an appropriate template.

In Scheme 6 there are three potential ways to produce *(R,R)*-cycHC[8] (Publication IV). The investigation began with the transformation of *(R,R)*-cycHC[6] to *(R,R)*-cycHC[8]

(Scheme 6 c), as this was previously noted in the HPLC sample. Examples of screened reaction conditions are shown in Table 3.

**Table 3.** Representative examples from screening the reaction conditions<sup>a</sup> for the transformation of compound (*R,R*)-cycHC[6] to (*R,R*)-cycHC[8], monitored by HPLC.

No.	Reaction conditions Acid (eq.)/Solvent	Ratio of ( <i>R,R</i> )-cycHC[8] to ( <i>R,R</i> )- cycHC[6]
1	HCOOH(10)/CH <sub>3</sub> CN	no reaction
2	HCOOH (10)/CHCl <sub>3</sub>	50:50
3	HCOOH (300)/H <sub>2</sub> O	no reaction
4 <sup>b</sup>	HCOOH (300)/-	oligomers
5	HCOOH (300)/-	83:17
6	HCOOH (300)/CHCl <sub>3</sub>	60:40
7	HCOOH (300)/CH <sub>3</sub> CN	90:10
8	CH <sub>3</sub> COOH (300)/CHCl <sub>3</sub> or CH <sub>3</sub> CN	0:100
9	CH <sub>3</sub> COOH(300)/H <sub>2</sub> SO <sub>4</sub> (50)/CH <sub>3</sub> CN	50:50
10	H <sub>2</sub> SO <sub>4</sub> (300)/CH <sub>3</sub> CN	decomposition
11 <sup>c</sup>	CF <sub>3</sub> COOH(300)/CH <sub>3</sub> CN	95:5

<sup>a</sup>Unless noted otherwise, (*R,R*)-cycHC[6] (0.04 M) was reacted in the listed media at RT for 24 hours; <sup>b</sup>Reaction temperature 100°C; <sup>c</sup>Reaction time was 2 hours.

The choice of solvents was dictated by the solubility of *trans*-cycHC[6], which was relatively poor in most organic solvents and water. CycHC[6] is soluble in chlorinated solvents, such as dichloromethane (DCM) and chloroform, or in carboxylic acids, such as formic and acetic acid. Generally, the macrocycle transformation from one homologue to another did not proceed under heterogeneous conditions. For example, the same concentration of formic acid in acetonitrile, which resulted in a heterogeneous reaction mixture, did not catalyse the *trans*-macrocyclisation reaction at all. In contrast, in chloroform for 24 hours, a 1:1 ratio of six- and eight-membered cycHC was observed (Table 3, entries 1 and 2). Because of the homogeneity issue, water was not a suitable media for the reaction (Table 3, entry 3). Heterogeneity caused by the insolubility of inorganic salts (NaPF<sub>6</sub>) had no pronounced effect on reaction progress (Table 4, entry 3).

Increasing the reaction temperature impeded the formation of (*R,R*)-cycHC[8] and mainly oligomers were detected. Reaction in pure formic acid at room temperature provided good conversion; however, at 100°C over 24 hours only oligomers were detected (Table 3, entry 4 and 5). In addition, acid concentration was determinative. Within 24 hours in a homogeneous reaction mixture in the presence of 10 eq. of formic acid in chloroform, half of the (*R,R*)-cycHC[6] was converted to (*R,R*)-cycHC[8] (Table 3, entry 2). The reaction rate was increased by a 300-fold excess of formic acid (Table 3, entries 5-7). The highest conversion of (*R,R*)-cycHC[6] to (*R,R*)-cycHC[8] was obtained in the case of formic acid catalysis in the presence of acetonitrile as the co-solvent (Table 3, entry 7). Likely, acetonitrile assisted proton transfer into the macrocycle. Under these conditions, (*R,R*)-cycHC[8] was isolated in the gram scale to produce 71% yield.

Acetic acid for 72 hours only partially decomposed (*R,R*)-cycHC[6] into oligomers (Table 3, entry 8); therefore, acetate ion was not a suitable template for

macrocyclisation. In the case of a mixture of acetic and sulphuric acids with acetonitrile as a co-solvent, the macrocycle enlargement reaction occurred favourably (Table 3, entry 9). However, even over long time periods, (*R,R*)-cycHC[8] did not become the major product. When 300 eq. of sulphuric acid were used in acetonitrile, very quick decomposition of starting compounds occurred. Subsequently, trifluoroacetic acid, a very strong organic acid, was used as the catalyst (Table 3, entry 11). This resulted in the transformation of (*R,R*)-cycHC[6] to (*R,R*)-cycHC[8] 10 times faster than under formic acid catalysis, and (*R,R*)-cycHC[8] was isolated in 71% yield (For further details, see SI Publication IV). The remarkable selectivity of the six-membered macrocycle (*R,R*)-cycHC[6] conversion to eight-membered (*R,R*)-cycHC[8] prompted a study into the mechanism of the transformation.

### 3.2.2.1 Kinetic study

With the goal of identifying the intermediates of the transformation of (*R,R*)-cycHC[6] to (*R,R*)-cycHC[8], the formic acid catalysed reaction was chosen as a model (Table 3, entry 7), due to its slower and experimentally more convenient reaction rate.

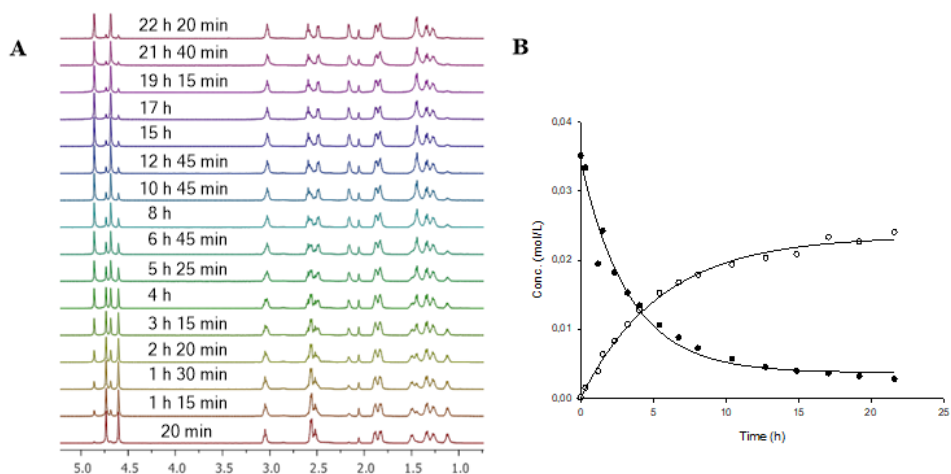


**Figure 38.** (A) Stacked  $^1\text{H-NMR}$  spectra recorded during (*R,R*)-cycHC[6] transformation to (*R,R*)-cycHC[8]. Bridge methylene peak (4.6 ppm for (*R,R*)-cycHC[6] and 4.8 ppm for (*R,R*)-cycHC[8]) integrals were used for the collection of kinetic data. (B) Kinetics plot of (*R,R*)-cycHC[6] (filled dots) and (*R,R*)-cycHC[8] (empty dots).

No intermediates were detected during the transformation of (*R,R*)-cycHC[6] to (*R,R*)-cycHC[8] in the NMR timescale (Figure 38A). The kinetic data (Figure 38B) revealed that the overall reaction was pseudo first-order, and reached a plateau. Significantly, the consumption rate of (*R,R*)-cycHC[6],  $k_{\text{obs}}=0.30 \pm 0.03 \text{ h}^{-1}$ , and the formation rate of (*R,R*)-cycHC[8],  $k_{\text{obs}}=0.18 \pm 0.01 \text{ h}^{-1}$ , were similar. In addition, the sum of the peak integrals of macrocycles, relative to an internal reference, decreased only 5% during the reaction, which indicated that the occurrence of side reactions was minimal. To test whether the plateau at the end of the reaction was caused by an equilibrium between the starting material and the product, isolated (*R,R*)-cycHC[8] was placed into a mixture of formic acid and acetonitrile. Indeed, a small amount of the six-membered homologue (*R,R*)-cycHC[6] was formed, confirming the reversible nature of interconversion of six- and eight-membered *trans*-cycHCs, with the equilibrium strongly shifted towards the formation of (*R,R*)-cycHC[8].

### 3.2.2.2 Identification of intermediates

Pittelkow *et al.* [130] stated that dimers were the main intermediates in the formation of biotin[6]uril. Two compounds (*R,R*)-cycHC[6] and (*R,R*)-cycHC[8], differ by a dimer unit. In order to check whether the fragmentation-recombination during the macrocycle ring enlargement proceeds via dimer addition, introduction of the  $^{13}\text{C}$  label to methylene bridges of (*R,R*)-cycHC[6] was performed.  $^{13}\text{C}$ -labelled and non-labelled (*R,R*)-cycHC[6] were used in a 1:1 mixture for the synthesis of (*R,R*)-cycHC[8]. If the transformation of (*R,R*)-cycHC[6] to (*R,R*)-cycHC[8] proceeds via dimer addition it should be reflected in the isotope-distribution pattern. In that case, even numbers of  $^{13}\text{C}$ - and  $^{12}\text{C}$ -isotopes would prevail in the resulting (*R,R*)-cycHC[8]. The experiment, however, proved that this was not the case. The number of  $^{13}\text{C}$ -isotopes in isolated (*R,R*)-cycHC[8] followed a normal distribution, including all species and complexes observed by ESI-MS (Figure 39). This fact demonstrates that the transformation of (*R,R*)-cycHC[6] to (*R,R*)-cycHC[8] does not proceed via dimer addition, and random differently sized oligomers and monomers are involved in the reaction.

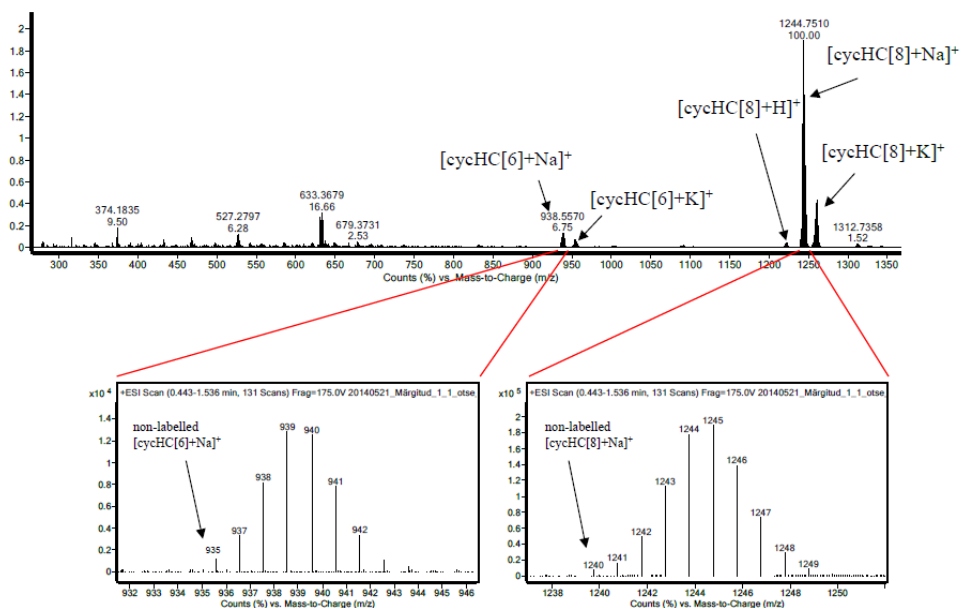


**Figure 39.** HRMS spectra of the reaction mixture of labelled and unlabelled (*R,R*)-cycHC[6] in 1:1 FA/ACN solution measured after 48 hours.

HRMS analysis of the crude reaction mixture showed the presence of cyclohexanohemicurbit[6-10]urils and linear oligomers (up to an octamer) (Figure 40). Open-chain oligomers were either capped by hydrogens on both ends (Figure 40, compounds **14b-14h**) or had one hydrogen at one of the terminal ureas substituted by a methyleneformate group (Figure 40, compounds **17b-17h**). This data allowed for the proposition of the reaction mechanism described in next sub-chapter.

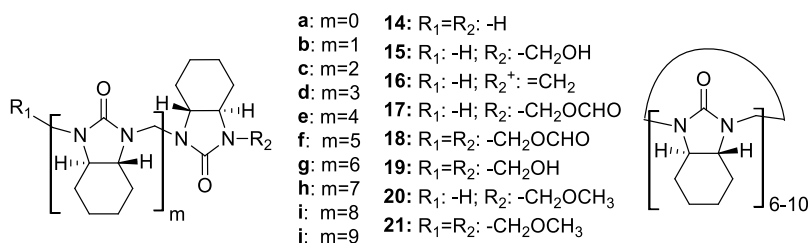


**Figure 40.** Structures of compounds detected by HRMS during the formation of (*R,R*)-cycHC[8]

### 3.2.2.3 Mechanism of cyclohexanohemicucurbituril formation

The large number of observed intermediates gives reason to suggest the presence of a dynamic combinatorial library (DCL), which is characteristic of dynamic covalent chemistry (DCC).<sup>[31,34,74,142–144]</sup> Thus, the equilibrium between *trans*-cycHC[6] and *trans*-cycHC[8] would be under thermodynamic control. CycHC[6] transformation to cycHC[8] can be considered consistent with several steps (Figure 41): (a) cycle opening, (b) chain growth, and (c) template-assisted cyclisation.

Two important experimental observations discussed in the previous chapter were: a) the existence of differently sized oligomers in the reaction mixture and b) the Gaussian distribution of <sup>13</sup>C labelled methylene bridges in the product. Both indicate that the chain growth step actually involves propagation, depropagation, and chain scission processes, which occur after cycHC[6] cycle opening.

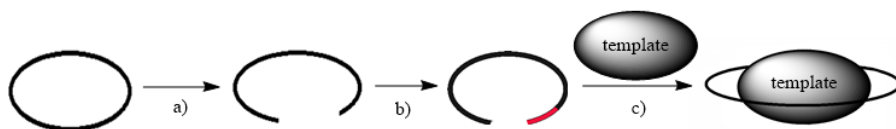
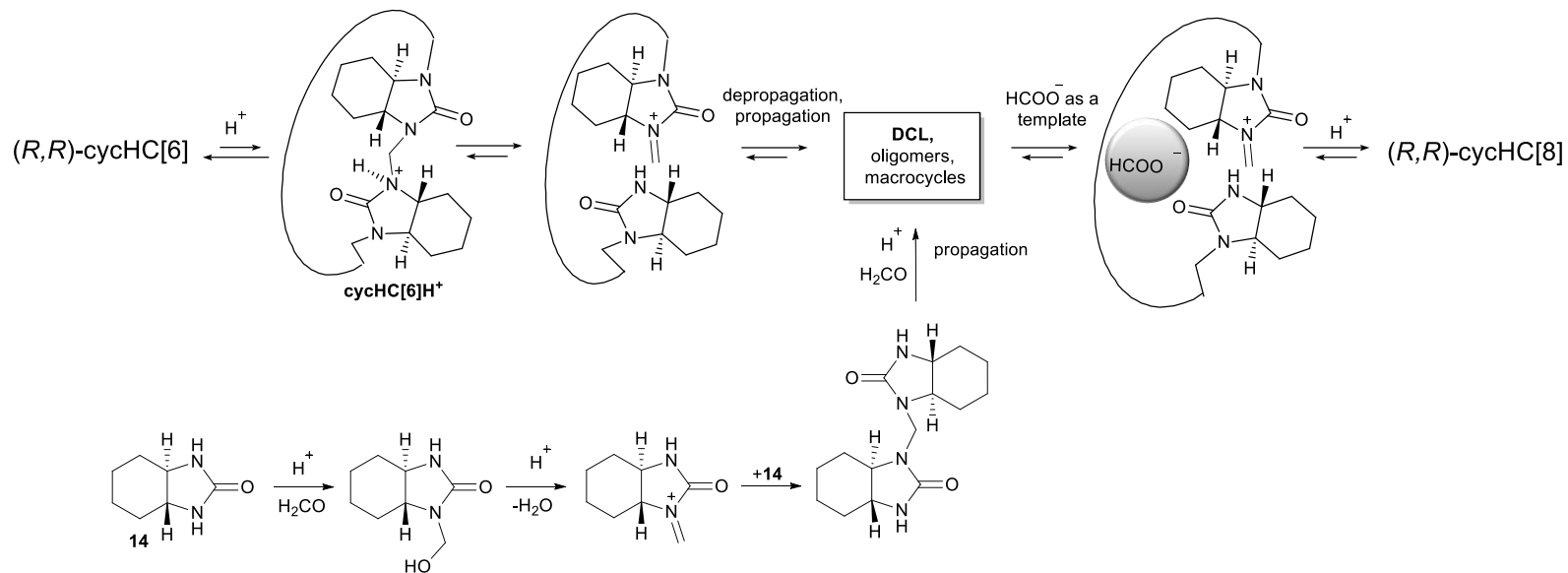


**Figure 41.** Schematic representation of the (*R,R*)-cycHC[6] transformation to (*R,R*)-cycHC[8]: a) cycle opening, b) chain growth, and c) template-assisted cyclisation.

As in all thermodynamically controlled reactions, cycHC[6] and cycHC[8] are equilibrating, and their equilibrium is influenced by both the ring-to-chain equilibrium and the equilibrium between the recombination (propagation) and fragmentation (depropagation) of the oligomeric chain (Chapter 1.3.2.1 and Scheme 2). The experimental value for the equilibrium constant  $K_{eq}$  of the overall reaction of *trans*-cycHC[6] transformation to *trans*-cycHC[8] is  $3.0 \times 10^5$ , which corresponds to a difference in Gibbs free energies ( $\Delta G$ ) of 31 kJ/mol in favour of (*R,R*)-cycHC[8]. The DFT-calculation of Gibbs free energy of differently sized (*R,R*)-cycHCs showed that the cycle strain was not a driving force in the formation of (*R,R*)-cycHC[8]. Instead, the templating effect of the formate anion amplified the formation of the eight-membered cycle by increasing the thermodynamic stability of the inclusion complex.

*Trans*-macrocyclisation was initiated by protonation. To open thermodynamically stable cycHC[6], acidic conditions were used. The acid did not have to be very strong, even relatively weak acetic acid was strong enough to catalyse the reaction in the presence of an appropriate template. Previous studies (Publication II) showed that *trans*-cycHC[6] can be protonated, and a favourable location for the proton is the nitrogen atom pointing inside the macrocycle.

On the basis of experimental data and calculated energies of the model system, a transformation mechanism of (*R,R*)-cycHC[6] to (*R,R*)-cycHC[8] was proposed. The key steps are outlined in Scheme 7. Protonation of (*R,R*)-cycHC[6] is a rate-limiting step and the reaction rate is dependent on the acid strength, as experimentally determined. The cycle opened as a result of the first methylene linkage breakage. A key intermediate iminium ion was formed. Therefore, the acylaminal bond between monomers was dynamic under acidic conditions. As a result of the formation of a dynamic combinatorial library through propagation/depropagation of oligomers, chain-scission, and self-association of oligomers occurred. The presence of a dynamic library, consisting of oligomeric, open-chain, and macrocyclic intermediates, was observed by HRMS.



**Scheme 7.** Proposed reaction mechanism of  $(R,R)\text{-cycHC}[8]$  formation catalysed by formic acid.

The template plays a central role in the cycle formation step (Figure 41c). Not all studied templates were equally effective. The shape and size of the anion were also crucial here. For example, an acetate template was shown not to be suitable for the formation of six- or eight-membered cycles (Table 3, entry 8). When  $\text{PF}_6^-$  was used, which was expected to be suitable for the cavity of the desired *trans*-cycHC[8] from both size and shape parameters, the reaction resulted in efficient conversion to the eight-membered macrocycle (Table 4, entry 3). Reaction in formic and trifluoroacetic acids led to eight-membered macrocycles as conjugate anions of corresponding carboxylic acids acted as templates (Table 4, entries 1 and 2). The solvent had a significant effect on the cycHC[8] formation rate. Polar aprotic solvents favoured stabilisation of the charged intermediates (protonated cycHC[6] and imines).<sup>[145]</sup>

Based on the proposed mechanism, the DCL could be generated from monomer **14** (Scheme 6, route a). Indeed, in formic and trifluoroacetic acids, or a  $\text{NaPF}_6$ /acetic acid mixture (*R,R*)-cycHC[8], it formed quite well (Table 4, entries 4–6). While comparing the formation of (*R,R*)-cycHC[8] from two different starting compounds, **14** and (*R,R*)-cycHC[6], the first reaction was much slower. The reason is the formation of the bond between the urea monomer and formaldehyde, which occurred through acid-promoted imine formation, which was a rate limiting step.<sup>[47,106]</sup> This step is absent in *trans*-macrocyclisation reactions, as all methylene bridges are already present in cycHC[6]. The best yield and selectivity were achieved with  $\text{CF}_3\text{COOH}$ , which provided (*R,R*)-cycHC[8] at a 73% yield on a gram scale. This route allowed for an enantiopure chiral macrocycle to be obtained very efficiently in two steps, starting from commercially available 1,2-cyclohexanediamine<sup>[132]</sup>.

Reversible reactions under thermodynamic control can be directed by external stimuli influencing the thermodynamic stability of the products. In case of the studied hemicucurbiturils, a template change to chloride resulted in directed equilibrium shift towards cycHC[6] (Figure 42). (*R,R*)-cycHC[8] was converted to (*R,R*)-cycHC[6] in the presence of a chloride anion under classical synthetic conditions<sup>[107]</sup> (Table 4, entry 8) or by using NaCl as a template in acetic acid at elevated temperature (Table 4, entry 9).

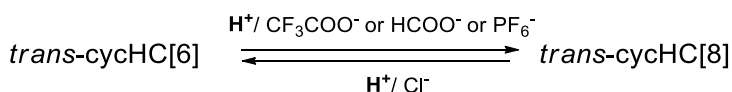


**Figure 42.** Template influence on the equilibrium between cycHC[6] and cycHC[8].

**Table 4.** Selected reaction conditions and the templates for (*R,R*)-cycHC synthesis.

No	Starting comp.	Additive/Acid/Solvent <sup>a</sup>	Template	Time (h), <i>T</i>	Ratio <sup>b</sup> of cycHC[8] to cycHC[6]	Product	Isolated yield of product
1	cycHC[6]	HCOOH/CH <sub>3</sub> CN	HCO <sub>2</sub> <sup>-</sup>	24, rt	92:8	cycHC[8]	71%
2	cycHC[6]	CF <sub>3</sub> COOH/CH <sub>3</sub> CN	CF <sub>3</sub> CO <sub>2</sub> <sup>-</sup>	1.5, rt	95:5	cycHC[8]	71%
3	cycHC[6]	NaPF <sub>6</sub> /CH <sub>3</sub> COOH/CH <sub>3</sub> CN	PF <sub>6</sub> <sup>-</sup>	24, rt	99:1	cycHC[8]	90%
4	<b>14</b>	HCOOH/CH <sub>3</sub> CN	HCO <sub>2</sub> <sup>-</sup>	24, rt	92:8	cycHC[8]	7%
5	<b>14</b>	NaPF <sub>6</sub> /CH <sub>3</sub> COOH/CH <sub>3</sub> CN	PF <sub>6</sub> <sup>-</sup>	24, rt	95:5	cycHC[8]	55%
6	<b>14</b>	CF <sub>3</sub> COOH/CH <sub>3</sub> CN	CF <sub>3</sub> CO <sub>2</sub> <sup>-</sup>	2, rt	96:4	cycHC[8]	73%
7 <sup>c</sup>	<b>14</b>	HCl/H <sub>2</sub> O	Cl <sup>-</sup>	24, 70°C	0:100	cycHC[6]	85%
8	cycHC[8]	HCl/H <sub>2</sub> O	Cl <sup>-</sup>	24, 70°C	5:95	cycHC[6]	71%
9	cycHC[8]	NaCl/CH <sub>3</sub> COOH	Cl <sup>-</sup>	24, 70°C	40:60	cycHC[6]	21%

<sup>a</sup>Generally 300 eq. of organic acid or 4 M HCl were used. <sup>b</sup>Determined by HPLC (See details in Pub. IV SI). <sup>c</sup>Described previously in Pub. I.

### 3.2.3 Structure and complexation of cyclohexanohemicucurbit[8]uril

The crystal structure confirmed the barrel-like shape of (*R,R*)-cycHC[8] (Figure 43). According to the crystal structure, the cavity of (*R,R*)-cycHC[8] was of sufficient size for the encapsulation of different guests.

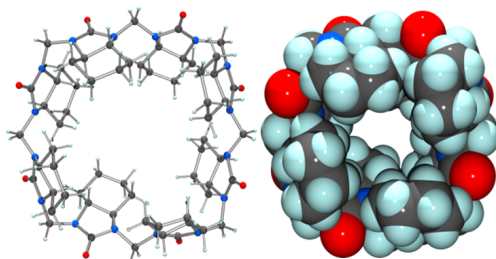


**Figure 43.** Top view of the crystal structure of cycHC[8] in ball and stick (left) and CPK (right) representations (colour code: C grey, N blue, O red, H turquoise).

Subsequent complexation studies performed by diffusion NMR in  $\text{CDCl}_3$  confirmed the ability of the (*R,R*)-cycHC[8] to form complexes with carboxylic acids. The comparative results of the complexation of (*R,R*)-cycHC[6] and (*R,R*)-cycHC[8] are presented in Table 5. The association constants of simple carboxylic acids (acetic, formic, and trifluoroacetic acids) followed the order of acidity (Table 5, entries 1-3) for both six- and eight-membered hosts. Analogously to small carboxylic acids, complexation with the more acidic  $\alpha$ -methoxy- $\alpha$ -trifluoromethylphenylacetic acid (MTPA) was stronger than with  $\alpha$ -methoxyphenylacetic acid (MPA) (Table 5, entries 4-7). *R*-handed (*R,R*)-cycHC[6] and (*R,R*)-cycHC[8] preferred different enantiomers of MPA (Table 5 entries 4 and 5). This may be due to the different geometries of complexes formed. *R*-handed cycHC[8] showed nearly double the affinity for *S*-MPA, as compared to the *R*-MPA confirming that (*R,R*)-cycHC[8] was able to form complexes enantioselectively. Further investigations showed that cycHC[8] was able to bind anions in methanol with good selectivity.<sup>[137]</sup>

**Table 5.** Association constants  $K_a$  ( $M^{-1}$ ) of carboxylic acids with (*R,R*)-cycHC[6] and (*R,R*)-cycHC[8] in 1:1 mixtures in  $\text{CDCl}_3$ .

No	Guest	CycHC[6] $K_a$	CycHC[8] $K_a$
1	$\text{CH}_3\text{COOH}$	$8.0 \pm 0.5^a$	$17 \pm 2$
2	$\text{HCOOH}$	$97 \pm 1$	$72.6 \pm 0.5$
3	$\text{CF}_3\text{COOH}$	$21 (\pm 3) \times 10^3$	$29(\pm 1) \times 10^3$
4	<i>R</i> -MPA	$27.2 \pm 0.8^a$	$27.0 \pm 0.5$
5	<i>S</i> -MPA	$20.1 \pm 0.2^a$	$53 \pm 3$
6	<i>R</i> -MTPA	n.d.	$3.3 (\pm 0.1) \times 10^2$
7	<i>S</i> -MTPA	n.d.	$3.0 (\pm 0.1) \times 10^2$

<sup>a</sup>Association constants from ref. <sup>[108]</sup>; n.d.- not determined.

### 3.3 Inverted-cis-cyclohexanohemicucurbit[6]uril (Publication V)

In order to compare properties of chiral cycHC[n]s with diastereomer *cis*-cycHC[6] **23**, published by Wu *et al.*<sup>[107]</sup>, **23** was synthesised starting from *cis*-urea **22** (Figure 18). Surprisingly, in addition to previously known *cis*-cycHC[6] **23**, another six-membered cycHC[n] diastereomer was obtained in almost equal amounts.

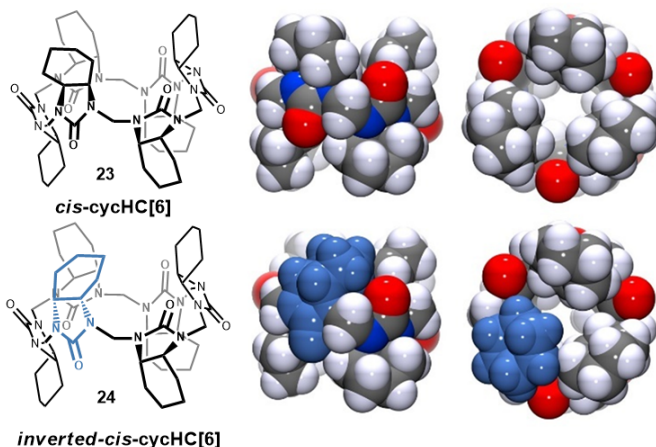


**Figure 44.** *Cis*- and *inverted-cis*-cycHC[6] **23**, **24** crystal structures (the *inverted* monomer of **24** is shown in blue).

#### 3.3.1 NMR identification of new stereoisomer, the *inverted-cis*-cyclohexanohemicucurbit[6]uril

Single crystal analysis of the new diastereomer of cycHC[6] showed that it had one monomer in an inverted configuration (Figure 44). Figures 44 and 45 show that *cis*-cycHC **23** is highly symmetric; however, the structure of **24** is quite different.

Careful analysis of 1D and 2D NMR spectra in tandem with XRD analysis allowed for the structure of the additive to be ascertained. As *inverted-cis*-cycHC[6] **24** had a plane of symmetry (Figure 45), cutting the number of atoms in half and simplifying the analysis of such a complicated structure. The two sides of the molecule were equal; therefore, there were four different monomers, which were labelled  $\alpha$ ,  $\beta$ ,  $\gamma$ , and  $\delta$ . All C-atoms were numbered and a Greek letter denoted the monomer each belonged to (Figure 45). Monomer  $\alpha$  is inverted (shown in blue in the Figure 44). Here, it is important to stress that monomers in the molecule were in an alternate orientation; therefore, numeration of the carbon atoms of the subsequent urea monomers were changing direction (Figure 45 structure **24**). All hydrogen and carbon atoms were assigned when analysing the COSY, HSQC, HMBC, and NOE spectra, as well as the chemical shifts and coupling constants (see Publication V).

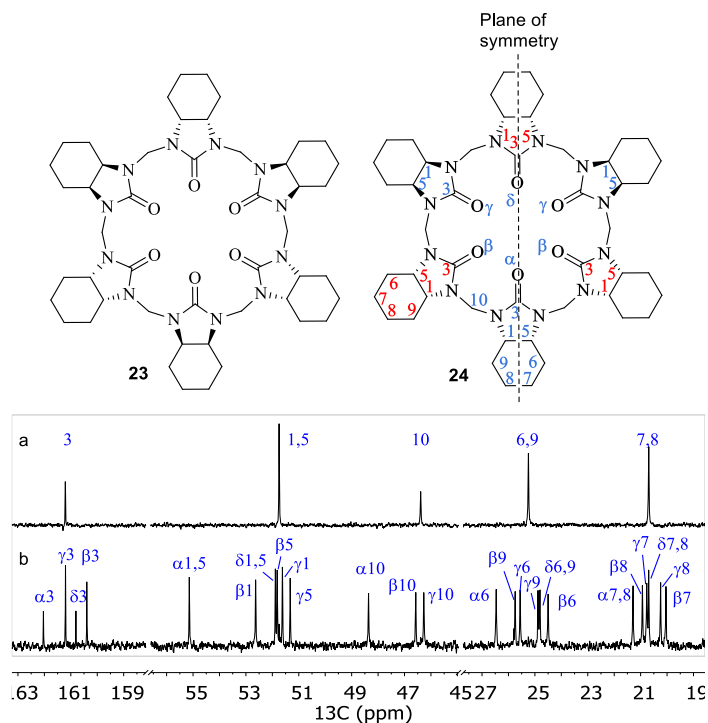


**Figure 45.** Schematic structures of **23** and **24** with numbered atoms and fragments of  $^{13}\text{C}$ -NMR spectra from (a) **23** and (b) **24**.

The COSY spectrum (Figure 46) shows a correlation cross peak for  $\beta_1$  and  $\beta_5$ , as well as for  $\gamma_1$  and  $\gamma_5$  hydrogens. Thus, these hydrogen atoms are of the same monomers and have different chemical shifts. In Figure 46, these pairs of hydrogens are shown with arrows of certain colours and the respective cross peaks are circled in the same colour.  $\alpha$  and  $\delta$  monomers are symmetrical; therefore, the  $\alpha_1$  and  $\delta_1$  hydrogen atoms give only a single peak in the  $^1\text{H}$  NMR spectrum and no cross peaks can be seen in the COSY spectrum. Thus, the symmetry plane crosses the molecule between the two.

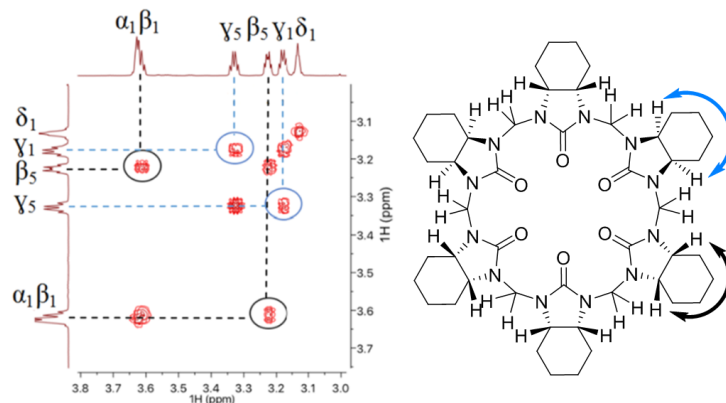


**Figure 46.** Part of a COSY spectrum, indicating neighbouring hydrogens, marked by arrows on the structure. The respective crosspeaks are indicated by circles in the figure.

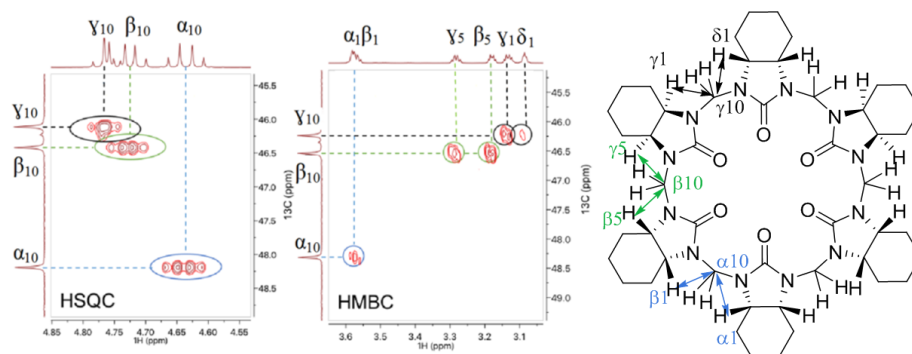


**Figure 47.** Parts of an HSQC and an HMBC spectra. The correlations in the spectrum are marked by arrows on the molecular structure.

The HSQC signals shown on Figure 46 clearly indicate correlation between  $\alpha_{10}$ ,  $\beta_{10}$ , and  $\gamma_{10}$  methylene bridge carbon atoms and the respective hydrogens. In addition, the HMBC spectrum (Figure 47) shows that  $\alpha_1$  and  $\beta_1$  hydrogen atoms both have an interaction with the  $\alpha_{10}$  bridge carbon atom and, therefore, are located next to the same bridge. From the previously mentioned COSY spectrum, the  $\alpha_1$  hydrogen atoms are from the symmetrical monomer. The fact that  $\alpha_1$  and  $\beta_1$  hydrogens both are correlated with  $\alpha_{10}$  carbon atoms is reflected by the blue arrows in Figure 47. By the same logic,  $\delta_1$  and  $\gamma_1$  hydrogen atoms are correlated with the  $\gamma_{10}$  bridge carbon atom, (marked with black arrows) and the  $\delta_1$  hydrogen atoms are from the symmetrical monomer. In addition, the  $\beta_5$  and  $\gamma_5$  hydrogen atoms are correlated in the HMBC spectrum with the  $\beta_{10}$  bridge carbon atoms (marked with green arrows).

The NOESY spectrum (Figure 48) shows cross peaks between  $\delta_1$  and  $\gamma_1$  hydrogen atoms and between  $\delta_1$  and  $\beta_5$  hydrogen atoms. Thus, all hydrogen atoms point towards the cavity of the *i-cis*-cycHC[6]. Moreover, there is a cross peak between  $\gamma_5$  and  $\beta_5$  hydrogen atoms, which supports the same conclusion. These correlations are outlined in the 3D figure obtained from the crystal structure of the *i-cis*-cycHC[6] (Figure 48). For  $\alpha_1$  hydrogen atoms, no cross peaks are detected, which confirms that these hydrogen atoms point away from the cavity of the macrocycle.

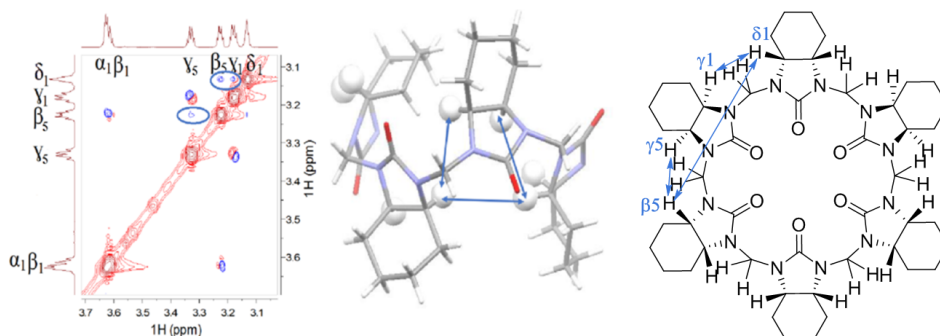


**Figure 48.** Part of a NOESY spectrum indicating hydrogen atoms, which are in close proximity. The crystal structure shows the same hydrogens in the solid state and demonstrates the close proximity (two monomer units were omitted in the crystal structure for clarity). The arrows indicate NOE correlations.

### 3.3.2 Synthesis and mechanism

Classical conditions for the synthesis of normal cucurbiturils and hemicucurbiturils, under which an equimolar mixture of *cis*-urea **22** and formaldehyde was heated in 4 M HCl were applied. Under these conditions, Wu *et al.* [107] isolated pure cycHC[6] at 78% yield; however, in this study, a mixture of **23** and **24** in nearly an equal ratio was instead obtained. The ratio of macrocycles varied batch-to-batch (Table 6 entry 1) and total yield of both macrocycles was in the range of 55-77%.

An example of *inverted*-CB[6] and *inverted*-CB[7]<sup>[89]</sup> gave reason to suspect that *inverted*-cycHC[6] was one of the thermodynamically less stable side products of the step-growth oligomerisation. After subjecting both six-membered macrocycles **23** and **24** to the same reaction conditions separately (Table 6, entries 5-6), only small amounts of **23** were transformed to **24**, yet nearly 2/3 of **24** was transformed into **23**. This led to the conclusion that **23** was thermodynamically more stable than **24**. Increasing the temperature to 80°C under microwave irradiation (MW) or 110°C in an oil-bath did not affect the ratio of the formed cycHCs (Table 6, entries 2 and 3). Moreover, reaction time prolongation from 4 to 17 hours had no significant influence on the result. However, when the concentration of HCl was doubled to 8 M, the amount of **23** increased significantly. The proposed explanation is that in 4 M HCl both products were stabilised by the template and, as a result of precipitation, both were out of the equilibration process. Chloride had a stronger stabilising effect on *cis*-cycHC[6] **23**, and in case of more concentrated HCl, where the template concentration was higher, a more stabilised product formed.

**Table 6.** Screened reaction conditions (see Publication V).

No	Starting compound	aq. HCl (M)	Temp., Time	Ratio of cycHC[6] <sup>a</sup> <b>23 : 24</b>	Yield <b>23+24</b> (%)
1	<b>22</b>	4	70°C, 4h	1.4 :1 to 1:1.4 <sup>b</sup>	55-77
2	<b>22</b>	4	MW (80°C), 2h	1.2:1	74
3	<b>22</b>	4	110°C, 4h	1.1:1	78
4	<b>22</b>	8	70°C, 4h	3.3:1	84
5	<b>23</b>	4	100°C, 3h	19.3:1	n.d.
6	<b>24</b>	4	100°C, 3h	1.3:1	n.d.

<sup>a</sup>Determined through UV-HPLC calibration curves, standard deviation varies 1-11%;

<sup>b</sup>Reaction was repeated five times, from 100 mg to 1 g scale of starting compound **22** (see Publication V for details).

The proposed mechanism of *i-cis*-cycHC[6] formation is as follows. During the step-growth oligomerisation, analogously to cucurbiturils' formation mechanism, monomers can be added in two ways: so-called C- and S-type oligomers, analogously to **25** and **26** dimers in Figure 49 (configurations *R,S,S,R* and *R,S,R,S*, respectively). Computational studies showed that one inverted monomer may be added with the same probability during entire oligomerisation process. Dimer **26** was lower in energy and only complexation with Cl<sup>-</sup> made **25** more thermodynamically stable. Template assisted precipitation of cyclic compounds out of the reaction media produced the kinetic product **24** and restricted its conversion to the thermodynamically more stable *cis*-cycHC[6] **23**.

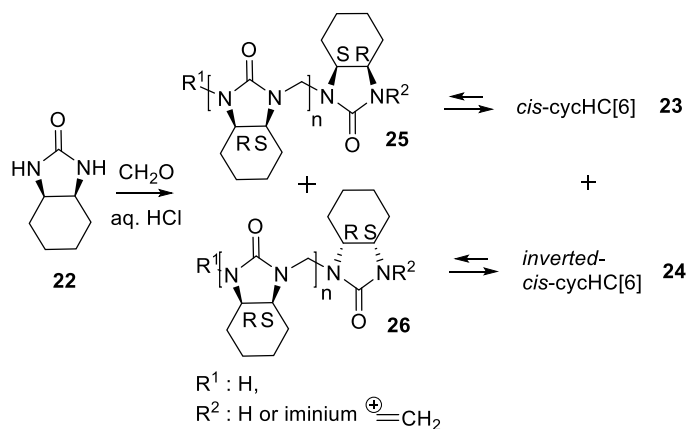


**Figure 49.** Diastereomeric dimers **25** and **26** as intermediates in *cis*- and *i-cis*-cycHC[6] formation.

### 3.3.3 Complexation

To determine the influence of shape on the complexation ability of cycHC[6]s, interaction with trifluoroacetic acid (TFA) for three macrocycles, (*R,R*)-cycHC[6], *cis*-cycHC[6] **23**, and *i-cis*-cycHC[6] **24**, was investigated. In addition, the methylated monomers (*R,S*)- and racemic (*R\*,R\**)-(N,N'-dimethyl)-cyclohexa-1,2-diyureas, **27** and **28**, were synthesised to compare properties and cyclic structures. A series of <sup>19</sup>F-NMR titration experiments were conducted (Table 7). Surprisingly, Job's method revealed 1:2 stoichiometry in the case of cycHC[6]s' complexes with TFA. For cyclohexadiylurea derivatives, stoichiometry of 1:1 was established. The positive cooperativity for the binding of a second TFA molecule with all cycHC[6] was witnessed. Better complexation of *cis*-monomeric urea **27** with TFA was observed, as compared to chiral monourea **28**, complexation may have been induced by the difference in shape (Figure 50). The same trend was preserved in the case of macrocyclic entities. The best binder for the TFA was *cis*-cycHC[6] **23**. Asymmetric (*R,R*)- and *i-cis*-cycHC[6] **24** showed good complexation ability, with association constants  $1.8 \cdot 10^5$  and  $6.7 \cdot 10^5$ , respectively (Table 7, entries 1 and 3).

**Table 7.** Association constants *K* of cycHC[6]s and mono-ureas **27** and **28** with TFA, determined by <sup>19</sup>F-NMR titration in CDCl<sub>3</sub>.

No	Urea derivative	$K_{11}(M^{-1}) \cdot 10^2$	$K_{12}(M^{-1}) \cdot 10^2$	$K_{tot}(M^{-2}) \cdot 10^5$
1	( <i>R,R</i> )-cycHC[6]	$2.8 \pm 0.1$	$6.3 \pm 0.2$	$1.8 \pm 0.1$
2	<b>23</b>	$7.3 \pm 0.7$	$16 \pm 1$	$12 \pm 2$
3	<b>24</b>	$8.8 \pm 0.7$	$7.6 \pm 0.9$	$6.7 \pm 0.9$
4	<b>27</b>	$43 \pm 5$	-	
5	<b>28</b>	$21 \pm 2$	-	

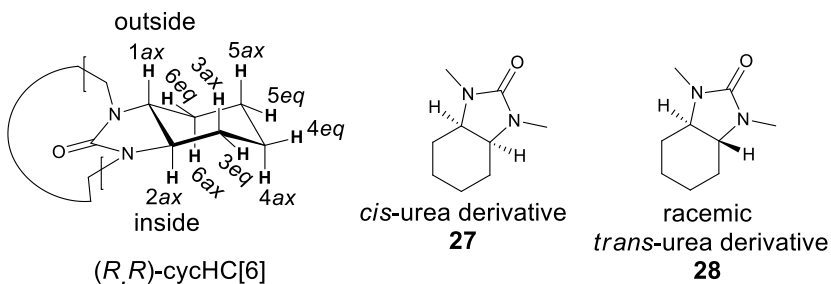


**Figure 50.** Structures of (R,R)-cycHC[6] and urea derivatives **27** and **28** (protons shown are participating in complexation with TFA).

To understand whether binding of TFA occurred inside or outside the cavity, an analysis of the following (R,R)-cycHC[6] protons was conducted (Figure 50). Proton 1ax at 2.77 ppm shifted upon addition of 16 eq. of TFA to 2.86 ppm. However, proton 2ax at 2.40 ppm, which is positioned inside the cavity, did not change upon addition of TFA (see Publication V for supporting information). Thus, external complexation with fast exchange on the NMR time scale was proposed.

## 4 Conclusions

The first enantiomerically pure cucurbit[n]uril family member – cyclohexanohemicucurbit[6]uril – was synthesised at a yield up to 85%. Its reaction conditions and crystal structure were reported. Complexation studies of cyclohexanocucurbit[6]uril revealed interaction with organic and inorganic acids, halides, and amines. The chiral nature of the new macrocycle resulted in the formation of diastereomeric complexes with methoxyphenylacetic acid, which were detected by NMR. Using the diffusion NMR technique, association constants for small organic compounds, such as monoethylfumaric acid or butanediamine with cycHC[6], were obtained.

Modes of complexation were analysed to determine that anionic species interacted with LUMO inside the cavity, and protons interacted with HOMO inside the macrocycle. However, larger cations and non-dissociated acids could only bind outside of the host molecule. Experimental results from ion-mobility MS studies supported computational conclusions.

Eight-membered enantiomerically pure cyclohexanohemicucurbituril was detected and separated by RP flash chromatography. Its structure was determined by NMR and MS methods. The existence of 7-, 9-, and 10-membered homologues was reported.

A highly efficient synthetic method providing enantiomerically pure cycHC[8] was developed. The crystal structure of the first eight-membered single-bridged cucurbituril and its complexation with carboxylic acids were reported. Studies of reaction kinetics, intermediates, and the influence of acid type, solvents, and templates on the reaction rate were performed and resulted in a proposed reaction mechanism. It started from either a urea derivative, an oligomeric mixture, or cycHC[6]. Formation of a dynamic combinatorial library of intermediates was followed by the final template-assisted cyclisation step, which resulted in the formation of cycHC[8].

The thermodynamically unfavoured *inverted-cis*-cyclohexanohemicucurbit[6]uril was detected and the structure of the first inverted single-bridged cucurbituril was described by NMR, MS, and X-ray diffraction techniques. Its formation mechanism was proposed. Parameters influencing formation of the thermodynamically unfavoured diastereomeric macrocycles were investigated and optimised. Complex formation of the *i-cis*-cyclohexanohemicucurbit[6]uril and trifluoroacetic acid with 1:2 stoichiometry was observed and a binding mode from outside the macrocycle was proposed on the basis of NMR titration analysis.

Through this work, the family of cucurbiturils was significantly enlarged by the introduction of new enantiomerically pure, variably sized, stereoisomeric single-bridged cucurbiturils. Efficient synthetic approaches for the generation of new host molecules can be applied to host-guest chemistry, which is a tool for designing molecular machines, new sensors, and materials useful in the pharmaceutical, agricultural, and chemical industries.

## References

- [1] A. T. Frank, N. S. Farina, N. Sawwan, O. R. Wauchope, M. Qi, E. M. Brzostowska, W. Chan, F. W. Grasso, P. Haberfield, A. Greer, *Mol. Divers.* **2007**, *11*, 115–118.
- [2] A. K. Oyelere, *Curr. Top. Med. Chem.* **2010**, *10*, 1359–1360.
- [3] Y. Li, Z. Sheng, C. Zhu, W. Yin, C. Chu, *Talanta* **2018**, *178*, 195–201.
- [4] M. H. Hyun, *J. Sep. Sci.* **2003**, *26*, 242–250.
- [5] L. Szente, J. Szemán, *Anal. Chem.* **2013**, *85*, 8024–8030.
- [6] C. Zhu, L. Fang, *Curr. Org. Chem.* **2014**, *18*, 1957–1964.
- [7] S. Erdemir, M. Bahadir, M. Yilmaz, *J. Hazard. Mater.* **2009**, *168*, 1170–1176.
- [8] K. Baek, G. Yun, Y. Kim, D. Kim, R. Hota, I. Hwang, D. Xu, Y. H. Ko, G. H. Gu, J. H. Suh, et al., *J. Am. Chem. Soc.* **2013**, *135*, 6523–6528.
- [9] L. Scorsin, J. A. Roehrs, R. R. Campedelli, G. F. Caramori, A. O. Ortolan, R. L. T. Parreira, H. D. Fiedler, A. Acuña, L. García-Río, F. Nome, *ACS Catal.* **2018**, 12067–12079.
- [10] E. R. Nagarajan, D. H. Oh, N. Selvapalam, Y. H. Ko, K. M. Park, K. Kim, *Tetrahedron Lett.* **2006**, *47*, 2073–2075.
- [11] Y. J. Jeon, H. Kim, S. Jon, N. Selvapalam, D. H. Oh, I. Seo, C.-S. Park, S. R. Jung, D.-S. Koh, K. Kim, *J. Am. Chem. Soc.* **2004**, *126*, 15944–15945.
- [12] D. Kim, E. Kim, J. Kim, K. M. Park, K. Baek, M. Jung, Y. H. Ko, W. Sung, H. S. Kim, J. H. Suh, et al., *Angew. Chem. Int. Ed.* **2007**, *46*, 3471–3474.
- [13] L. Cao, G. Hettiarachchi, V. Briken, L. Isaacs, *Angew. Chem. Int. Ed.* **2013**, *52*, 12033–12037.
- [14] M. Li, M. B. Zaman, D. Bardelang, X. Wu, D. Wang, J. C. Margeson, D. M. Leek, J. A. Ripmeester, C. I. Ratcliffe, Q. Lin, et al., *Chem. Commun.* **2009**, 6807–6809.
- [15] E. Kim, J. Lee, D. Kim, K. E. Lee, S. S. Han, N. Lim, J. Kang, C. G. Park, K. Kim, *Chem. Commun.* **2009**, 1472–1474.
- [16] K. M. Park, J.-A. Yang, H. Jung, J. Yeom, J. S. Park, K.-H. Park, A. S. Hoffman, S. K. Hahn, K. Kim, *ACS Nano* **2012**, *6*, 2960–2968.
- [17] L. Ruzicka, *Helv. Chim. Acta* **1926**, *9*, 230–248.
- [18] S. Yamashita, D. Hayashi, A. Nakano, Y. Hayashi, M. Hirama, *J. Antibiot. (Tokyo)* **2016**, *69*, 31–50.
- [19] G. F. Gause, M. G. Brazhnikova, *Nature* **1944**, *154*, 703.
- [20] F. Davis, S. Higson, *Macrocycles: Construction, Chemistry and Nanotechnology Applications*, John Wiley & Sons, **2011**.
- [21] V. Martí-Centelles, M. D. Pandey, M. I. Burguete, S. V. Luis, *Chem. Rev.* **2015**, *115*, 8736–8834.
- [22] M. E. Fitzgerald, C. A. Mulrooney, J. R. Duvall, J. Wei, B.-C. Suh, L. B. Akella, A. Vrcic, L. A. Marcaurelle, *ACS Comb. Sci.* **2012**, *14*, 89–96.
- [23] A. Parenty, X. Moreau, G. Niel, J.-M. Campagne, *Chem. Rev.* **2013**, *113*, PR1–PR40.
- [24] S. H. Joo, *Biomol. Ther.* **2012**, *20*, 19–26.
- [25] K. Nishikawa, Y. Yoshimi, K. Maeda, T. Morita, I. Takahashi, T. Itou, S. Inagaki, M. Hatanaka, *J. Org. Chem.* **2013**, *78*, 582–589.
- [26] A. Zorzi, K. Deyle, C. Heinis, *Curr. Opin. Chem. Biol.* **2017**, *38*, 24–29.
- [27] R. J. Dubos, C. Cattaneo, *J. Exp. Med.* **1939**, *70*, 249–256.
- [28] R. D. Hotchkiss, R. J. Dubos, *J. Biol. Chem.* **1941**, *141*, 155–162.
- [29] E. A. Crane, K. A. Scheidt, *Angew. Chem. Int. Ed.* **2010**, *49*, 8316–8326.

- [30] A. B. Smith, S. M. Condon, J. A. McCauley, J. L. Leazer, J. W. Leahy, R. E. Maleczka, *J. Am. Chem. Soc.* **1995**, *117*, 5407–5408.
- [31] J.-M. Lehn, *Chem. – Eur. J.* **1999**, *5*, 2455–2463.
- [32] P. A. Brady, J. K. M. Sanders, *J. Chem. Soc. Perkin 1* **1997**, 3237–3254.
- [33] S. J. Rowan, S. J. Cantrill, G. R. L. Cousins, J. K. M. Sanders, J. F. Stoddart, *Angew. Chem. Int. Ed.* **2002**, *41*, 898–952.
- [34] P. T. Corbett, J. Leclair, L. Vial, K. R. West, J.-L. Wietor, J. K. M. Sanders, S. Otto, *Chem. Rev.* **2006**, *106*, 3652–3711.
- [35] J.-M. Lehn, *J. Incl. Phenom.* **1988**, *6*, 351–396.
- [36] P. Nowak, V. Saggiomo, F. Salehian, M. Colomb-Delsuc, Y. Han, S. Otto, *Angew. Chem. Int. Ed.* **2015**, *54*, 4192–4197.
- [37] R. J. Wojtecki, M. A. Meador, S. J. Rowan, *Nat. Mater.* **2011**, *10*, 14–27.
- [38] L. Tauk, A. P. Schröder, G. Decher, N. Giuseppone, *Nat. Chem.* **2009**, *1*, 649–656.
- [39] P. Dydio, P.-A. R. Breuil, J. N. H. Reek, *Isr. J. Chem.* **2013**, *53*, 61–74.
- [40] I. M. Serafimova, M. A. Pufall, S. Krishnan, K. Duda, M. S. Cohen, R. L. Maglathlin, J. M. McFarland, R. M. Miller, M. Frödin, J. Taunton, *Nat. Chem. Biol.* **2012**, *8*, 471–476.
- [41] K. Severin, in *Dyn. Comb. Chem.*, Wiley-Blackwell, **2010**.
- [42] W. Zhang, Y. Jin, *Dynamic Covalent Chemistry: Principles, Reactions, and Applications*, Wiley, **2017**.
- [43] M. E. Belowich, J. F. Stoddart, *Chem. Soc. Rev.* **2012**, *41*, 2003–2024.
- [44] H. Schiff, *Justus Liebigs Ann. Chem.* **1864**, *131*, 118–119.
- [45] C. D. Meyer, C. S. Joiner, J. F. Stoddart, *Chem. Soc. Rev.* **2007**, *36*, 1705–1723.
- [46] M. Ciaccia, S. D. Stefano, *Org. Biomol. Chem.* **2015**, *13*, 646–654.
- [47] S. Kaabel, R. Aav, *Isr. J. Chem.* **2018**, *58*, 296–313.
- [48] V. M. Dong, D. Fiedler, B. Carl, R. G. Bergman, K. N. Raymond, *J. Am. Chem. Soc.* **2006**, *128*, 14464–14465.
- [49] T. Iwasawa, R. J. Hooley, J. Rebek, *Science* **2007**, *317*, 493–496.
- [50] S. Patai, Ed., *The Chemistry of Carbon Nitrogen Double Bonds*, Wiley, London, New York, **1970**.
- [51] C. Godoy-Alcántar, A. K. Yatsimirsky, J.-M. Lehn, *J. Phys. Org. Chem.* **2005**, *18*, 979–985.
- [52] B. G. Malmström, *Nobel Lectures*, World Scientific Publishing Co., Singapore, **1992**.
- [53] D. H. Busch, *J. Incl. Phenom. Mol. Recognit. Chem.* **1992**, *12*, 389–395.
- [54] S. Anderson, H. L. Anderson, J. K. M. Sanders, *Acc. Chem. Res.* **1993**, *26*, 469–475.
- [55] M. C. Thompson, D. H. Busch, *J. Am. Chem. Soc.* **1964**, *86*, 5.
- [56] F. Seidel, W. Dick, *Berichte Dtsch. Chem. Ges. B Ser.* **1927**, *60*, 2018–2023.
- [57] C. J. Pedersen, *J. Am. Chem. Soc.* **1967**, *89*, 7017–7036.
- [58] F. Diederich, P. J. Stang, *Templated Organic Synthesis*, Wiley-VCH, Weinheim, **2000**.
- [59] R. Hoss, F. Vögtle, *Angew. Chem. Int. Ed. Engl.* **1994**, *33*, 375–384.
- [60] J. W. Steed, J. L. Atwood, *Supramolecular Chemistry, 2nd Edition*, Wiley, **2009**.
- [61] C. H. Henkels, J. C. Kurz, C. A. Fierke, T. G. Oas, *Biochemistry* **2001**, *40*, 2777–2789.
- [62] R. Sekiya, M. Fukuda, R. Kuroda, *J. Am. Chem. Soc.* **2012**, *134*, 10987–10997.
- [63] R. D. Shannon, *Acta Crystallogr. Sect. A* **1976**, *32*, 751–767.

- [64] B. Hasenknopf, J.-M. Lehn, B. O. Kneisel, G. Baum, D. Fenske, *Angew. Chem. Int. Ed. Engl.* **1996**, *35*, 1838–1840.
- [65] X. Yang, C. B. Knobler, M. F. Hawthorne, *Angew. Chem. Int. Ed. Engl.* **1991**, *30*, 1507–1508.
- [66] Z. Zheng, C. B. Knobler, M. F. Hawthorne, *J. Am. Chem. Soc.* **1995**, *117*, 5105–5113.
- [67] M. D. Lankshear, P. D. Beer, *Coord. Chem. Rev.* **2006**, *250*, 3142–3160.
- [68] R. Vilar, *Angew. Chem. Int. Ed.* **2003**, *42*, 1460–1477.
- [69] M. C. T. Fyfe, P. T. Glink, S. Menzer, J. F. Stoddart, A. J. P. White, D. J. Williams, *Angew. Chem. Int. Ed. Engl.* **1997**, *36*, 2068–2070.
- [70] P. Ruggli, *Justus Liebigs Ann. Chem.* **1912**, *392*, 92–100.
- [71] R. Cacciapaglia, S. Di Stefano, L. Mandolini, *J. Am. Chem. Soc.* **2005**, *127*, 13666–13671.
- [72] H. Jacobson, W. H. Stockmayer, *J. Chem. Phys.* **1950**, *18*, 1600–1606.
- [73] G. Ercolani, L. Mandolini, P. Mencarelli, S. Roelens, *J. Am. Chem. Soc.* **1993**, *115*, 3901–3908.
- [74] S. J. Rowan, S. J. Cantrill, G. R. L. Cousins, J. K. M. Sanders, J. F. Stoddart, *Angew. Chem. Int. Ed.* **2002**, *41*, 898–952.
- [75] R. Behrend, E. Meyer, F. Rusche, *Justus Liebigs Ann. Chem.* **1905**, *339*, 1–37.
- [76] W. A. Freeman, W. L. Mock, N. Y. Shih, *J. Am. Chem. Soc.* **1981**, *103*, 7367–7368.
- [77] A. I. Day, A. P. Arnold, R. J. Blanch, *Cucurbiturils and Method for Synthesis*, **2000**, WO2000068232A1.
- [78] J. Kim, I.-S. Jung, S.-Y. Kim, E. Lee, J.-K. Kang, S. Sakamoto, K. Yamaguchi, K. Kim, *J. Am. Chem. Soc.* **2000**, *122*, 540–541.
- [79] W.-H. Huang, P. Y. Zavalij, L. Isaacs, *J. Am. Chem. Soc.* **2008**, *130*, 8446–8454.
- [80] H. Cong, X. L. Ni, X. Xiao, Y. Huang, Q.-J. Zhu, S.-F. Xue, Z. Tao, L. F. Lindoy, G. Wei, *Org. Biomol. Chem.* **2016**, *14*, 4335–4364.
- [81] J. Lagona, P. Mukhopadhyay, S. Chakrabarti, L. Isaacs, *Angew. Chem. Int. Ed.* **2005**, *44*, 4844–4870.
- [82] R. Aav, K. A. Mishra, *Symmetry* **2018**, *10*, 98.
- [83] J. Chen, Y. Liu, D. Mao, D. Ma, *Chem. Commun.* **2017**, *53*, 8739–8742.
- [84] E. Masson, X. Ling, R. Joseph, L. Kyeremeh-Mensah, X. Lu, *RSC Adv.* **2012**, *2*, 1213–1247.
- [85] A. Day, A. P. Arnold, R. J. Blanch, B. Snushall, *J. Org. Chem.* **2001**, *66*, 8094–8100.
- [86] A. I. Day, R. J. Blanch, A. Coe, A. P. Arnold, *J. Incl. Phenom. Macrocycl. Chem.* **2002**, *43*, 247–250.
- [87] S. Liu, K. Kim, L. Isaacs, *J. Org. Chem.* **2007**, *72*, 6840–6847.
- [88] A. Chakraborty, A. Wu, D. Witt, J. Lagona, J. C. Fettinger, L. Isaacs, *J. Am. Chem. Soc.* **2002**, *124*, 8297–8306.
- [89] L. Isaacs, S.-K. Park, S. Liu, Y. H. Ko, N. Selvapalam, Y. Kim, H. Kim, P. Y. Zavalij, G.-H. Kim, H.-S. Lee, et al., *J. Am. Chem. Soc.* **2005**, *127*, 18000–18001.
- [90] W.-H. Huang, P. Y. Zavalij, L. Isaacs, *Org. Lett.* **2009**, *11*, 3918–3921.
- [91] Q. Li, S.-C. Qiu, K. Chen, Y. Zhang, R. Wang, Y. Huang, Z. Tao, Q.-J. Zhu, J.-X. Liu, *Chem. Commun.* **2016**, *52*, 2589–2592.
- [92] W.-H. Huang, P. Y. Zavalij, L. Isaacs, *Angew. Chem. Int. Ed.* **2007**, *46*, 7425–7427.
- [93] X. Lu, L. Isaacs, *Org. Lett.* **2015**, *17*, 4038–4041.
- [94] Y. Miyahara, K. Goto, M. Oka, T. Inazu, *Angew. Chem. Int. Ed.* **2004**, *43*, 5019–5022.

- [95] N. N. Andersen, M. Lisbjerg, K. Eriksen, M. Pittelkow, *Isr. J. Chem.* **2018**, *58*, 435–448.
- [96] K. I. Assaf, W. M. Nau, *Angew. Chem. Int. Ed.* **2018**, *57*, 13968–13981.
- [97] H.-J. Buschmann, E. Cleve, E. Schollmeyer, *Inorg. Chem. Commun.* **2005**, *8*, 125–127.
- [98] H.-J. Buschmann, A. Zielesny, E. Schollmeyer, *J. Incl. Phenom. Macrocycl. Chem.* **2006**, *54*, 181–185.
- [99] X.-Y. Jin, J.-L. Zhao, F. Wang, H. Cong, Z. Tao, *J. Organomet. Chem.* **2017**, *846*, 1–5.
- [100] D.-D. Xiang, Q.-X. Geng, H. Cong, Z. Tao, T. Yamato, *Supramol. Chem.* **2015**, *27*, 37–43.
- [101] H. Cong, T. Yamato, X. Feng, Z. Tao, *J. Mol. Catal. Chem.* **2012**, *365*, 181–185.
- [102] H. Cong, T. Yamato, Z. Tao, *J. Mol. Catal. Chem.* **2013**, *379*, 287–293.
- [103] H. Cong, T. Yamato, Z. Tao, *New J. Chem.* **2013**, *37*, 3778–3783.
- [104] R. Kurane, P. Bansode, S. Khanapure, D. Kale, R. Salunkhe, G. Rashinkar, *Catal. Lett.* **2016**, *146*, 2485–2494.
- [105] E. I. Cucolea, H.-J. Buschmann, L. Mutihac, *Supramol. Chem.* **2016**, *28*, 727–732.
- [106] I. K. Yoo, Y. K. Kang, *Chem. Phys. Lett.* **2017**, *669*, 92–98.
- [107] Y. Li, L. Li, Y. Zhu, X. Meng, A. Wu, *Cryst. Growth Des.* **2009**, *9*, 4255–4257.
- [108] R. Aav, E. Shmatova, I. Reile, M. Kuitinskaja, F. Topic, K. Rissanen, *Org. Lett.* **2013**, *15*, 3786–3789.
- [109] J. L. Atwood, *Comprehensive Supramolecular Chemistry II*, Elsevier, **2017**.
- [110] T. Fiala, V. Sindelar, *Synlett* **2013**, *24*, 2443–2445.
- [111] J. Svec, M. Necas, V. Sindelar, *Angew. Chem. Int. Ed.* **2010**, *49*, 2378–2381.
- [112] T. Lizal, V. Sindelar, *Isr. J. Chem.* **2018**, *58*, 326–333.
- [113] V. Havel, J. Svec, M. Wimmerova, M. Dusek, M. Pojarova, V. Sindelar, *Org. Lett.* **2011**, *13*, 4000–4003.
- [114] M. Singh, E. Solel, E. Keinan, O. Reany, *Chem. – Eur. J.* **2015**, *21*, 536–540.
- [115] T. Fiala, Bambusurils and Their Supramolecular Interactions with Organic Phosphates, Thesis, **2015**.
- [116] J. Rivollier, P. Thuéry, M.-P. Heck, *Org. Lett.* **2013**, *15*, 480–483.
- [117] M. A. Yawer, V. Havel, V. Sindelar, *Angew. Chem. Int. Ed.* **2015**, *54*, 276–279.
- [118] V. Havel, M. Babiak, V. Sindelar, *Chem. – Eur. J.* **2017**, *23*, 8963–8968.
- [119] J. Svec, M. Dusek, K. Fejfarova, P. Stacko, P. Klán, A. E. Kaifer, W. Li, E. Hudeckova, V. Sindelar, *Chemistry – A European Journal* **2011**, *17*, 5605–5612.
- [120] F. Biedermann, W. M. Nau, H.-J. Schneider, *Angew. Chem. Int. Ed.* **2014**, *53*, 11158–11171.
- [121] T. Fiala, L. Ludvíková, D. Heger, J. Švec, T. Slanina, L. Vetráková, M. Babiak, M. Nečas, P. Kulhánek, P. Klán, et al., *J. Am. Chem. Soc.* **2017**, *139*, 2597–2603.
- [122] V. Havel, V. Sindelar, M. Necas, A. E. Kaifer, *Chem. Commun.* **2014**, *50*, 1372–1374.
- [123] V. Havel, M. A. Yawer, V. Sindelar, *Chem. Commun.* **2015**, *51*, 4666–4669.
- [124] A. Šlampová, V. Šindelář, P. Kubáň, *Anal. Chim. Acta* **2017**, *950*, 49–56.
- [125] H. Valkenier, O. Akrawi, P. Jurček, K. Sleziaková, T. Lizal, K. Bartik, V. Šindelář, *Chem* **2019**, *5*, 429–444.
- [126] O. Reany, A. Mohite, E. Keinan, *Isr. J. Chem.* **2018**, *58*, 449–460.
- [127] F. Pichierri, *Chem. Phys. Lett.* **2004**, *390*, 214–219.

- [128] F. Pichierri, *Chem. Phys. Lett.* **2005**, *403*, 252–256.
- [129] M. Singh, E. Solel, E. Keinan, O. Reany, *Chem. – Eur. J.* **2016**, *22*, 8848–8854.
- [130] M. Lisbjerg, B. M. Jessen, B. Rasmussen, B. E. Nielsen, A. Ø. Madsen, M. Pittelkow, *Chem Sci* **2014**, *5*, 2647–2650.
- [131] M. Lisbjerg, B. E. Nielsen, B. O. Milhøj, S. P. A. Sauer, M. Pittelkow, *Org. Biomol. Chem.* **2015**, *13*, 369–373.
- [132] J. F. Larrow, E. N. Jacobsen, Y. Gao, Y. Hong, X. Nie, C. M. Zepp, *J. Org. Chem.* **1994**, *59*, 1939–1942.
- [133] Á. L. Fuentes de Arriba, D. G. Seisdedos, L. Simón, V. Alcázar, C. Raposo, J. R. Morán, *J. Org. Chem.* **2010**, *75*, 8303–8306.
- [134] J. B. Milne, T. J. Parker, *J. Solut. Chem.* **1981**, *10*, 479–487.
- [135] J. W. Lee, S. Samal, N. Selvapalam, H.-J. Kim, K. Kim, *Acc. Chem. Res.* **2003**, *36*, 621–630.
- [136] J. Szejtli, *Chem. Rev.* **1998**, *98*, 1743–1754.
- [137] S. Kaabel, J. Adamson, F. Topić, A. Kiesilä, E. Kalenius, M. Öeren, M. Reimund, E. Prigorchenko, A. Löökene, H. J. Reich, et al., *Chem. Sci.* **2017**, *8*, 2184–2190.
- [138] Y. Cohen, L. Avram, L. Frish, *Angew. Chem. Int. Ed.* **2005**, *44*, 520–554.
- [139] Y. Cohen, L. Avram, T. Evan-Salem, S. Slovak, N. Shemesh, L. Frish, in *Anal. Methods Supramol. Chem.*, Wiley-Blackwell, **2012**.
- [140] C. S. Johnson, *Prog. Nucl. Magn. Reson. Spectrosc.* **1999**, *34*, 203–256.
- [141] A. I. Day, R. J. Blanch, A. P. Arnold, S. Lorenzo, G. R. Lewis, I. Dance, *Angew. Chem. Int. Ed.* **2002**, *41*, 275–277.
- [142] Y. Jin, C. Yu, R. J. Denman, W. Zhang, *Chem. Soc. Rev.* **2013**, *42*, 6634–6654.
- [143] Y. Jin, Q. Wang, P. Taynton, W. Zhang, *Acc. Chem. Res.* **2014**, *47*, 1575–1586.
- [144] A. Herrmann, *Chem Soc Rev* **2014**, *43*, 1899–1933.
- [145] C. Reichardt, *Solvents and Solvent Effects in Organic Chemistry.*, Wiley-VCH, Weinheim/Germany, **2003**.

## Acknowledgements

The work presented in this thesis was conducted within the Department of Chemistry and Biotechnology of Tallinn University of Technology and was financially supported by the Estonian Ministry of Education and Research (PUT692 and CoE in Molecular Cell Engineering 2014-2020.4.01.15-0013), the ASTRA "TUT Institutional Development Programme for 2016-2022", "Graduate School of Functional Materials and Technologies" (2014-2020.4.01.16-0032), and Dora Programs.

I am most grateful to my supervisor, Prof. Riina Aav, for sharing her knowledge with me, for her outstanding motivation, and support of my everyday work. Thank you for introducing to me the fascinating world of chemistry and science. You showed me that sometimes a mistake can be a starting point to discovering something new and exciting.

This thesis would not be possible without members of our hemicucurbituril research group, past and present: Mario, Maria, Madli, Sandra, Anna, and Nastja. Thank you for the joy of working in the team, and your dedication to the common cause.

Current results were obtained with the help of Marina Kudrjašova, Maria Kuhtinskaja, Jasper Adamson, and Indrek Reile in the fields of NMR and MS. Many thanks for sharing your professional experience and kind assistance.

I would also like to express my gratitude to all collaborators and colleagues from the fourth floor for your help with the working process and the great time we have spent together during these years.

I would like to thank my chemistry teacher Lidia Rõbnikova, who instilled in me an interest in chemistry. I would also like to express my heartfelt gratitude to my first supervisor Konstantin Kislitsõn for a joyful time in the laboratory and his patience.

I am grateful to my parents Margarita and Yury, my brother Ilya and sister Olga, and my grandparents, relatives, and friends for all the support and encouragement.

Above all, I would like to thank my husband Ivan and son Stepan for inspiration and backing. You are the people who are always on my side.

## Abstract

### Cyclohexanohemicucurbit[*n*]urils: synthesis, formation mechanism, and complexation

This thesis provides an overview of macrocyclic properties and structure, and the synthesis of hemicucurbit[*n*]uril-type molecules. The literature review starts with an introduction of two possible synthetic approaches towards diverse and structurally complicated macrocycles. Conventional stepwise synthesis with subsequent head-to-tail cyclisation is a widely used method to obtain many drugs and materials. Another method towards macrocyclic entities is based on the reversibility of the chemical bonds and manipulation of equilibrium by external stimuli. Dynamic combinatorial chemistry is a relatively new branch of modern chemistry, which provides another dimension to chemical synthesis. The current work focuses on reversible covalent bonds, and imine in particular, as this bond plays a crucial role in the key intermediates formed during hemicucurbituril synthesis. Moreover, such important features as template effect, inter- and intra-molecular reactions, and equilibrium are discussed.

Hemicucurbiturils are a relatively new part of the cucurbituril (CB) family, which are barrel-shaped container molecules famous for extremely strong binding of cationic guest molecules. A brief overview of the literature concerning the synthesis and formation mechanism of cucurbiturils is supplemented by examples of chiral members of this family. Several structurally diverse HC analogues have already been synthesised, characterised, and applied. Careful study of all currently published hemicucurbituril-type macrocyclic hosts closes this chapter of the thesis.

The results and discussion chapter focuses on synthesis, characterisation, and complexation of the cyclohexanohemicucurbiturils (cycHC[*n*]). The chiral six-membered cycHC[6] is described, which is the first enantiomerically pure member of the CBs. The versatile investigation of structure, properties, and synthesis is presented. The distinctive feature of this enantiomeric host is its ability to form diastereomeric complexes with a chiral anionic guest. The larger cycHC eight-membered macrocycle was discovered, which was the first example of an octameric hemicucurbituril. Previously, only 6-membered and 12-membered HCs had been obtained. A deep and multilateral investigation of the cyclohexanohemicucurbituril's formation mechanism, identification of intermediates, and screening of synthetic conditions resulted in good reaction yields and a valuable contribution to the field of HCs. The synthesis and properties of the inverted analogue of *cis*-cycHC[6] were described based on screening reaction conditions and identifying the structure. Detailed interpretation of complicated NMR spectra is presented. The formation mechanism of the kinetic product, *i-cis*-cycHC[6], is proposed. Finally, the uncommon HC complexation stoichiometry of 1:2 for carboxylic acid was determined, and the binding of all three currently known cycHC[6] diastereomers are described.

As a result of the current work, several new macrocycles were added to the cucurbit[*n*]uril family. The first enantiomeric examples of this type of hosts and their diastereomeric complexes with guest molecules were reported and fully characterised. Comprehensive studies of formation mechanisms and structures of cycHCs allowed for an important contribution to be made to the field.

## Lühikokkuvõte

### Tsükloheksaanhemikukurbit[*n*]uriilid, nende süntees, tekkemehhanism ja komplekseerumine

Käesolev doktoritöö annab ülevaate hemikukurbituriil-tüüpi ainete supramolekulaarsetest omadustest, struktuurist ja sünteesist. Kirjanduse ülevaade kirjeldab kahte lähenemisviisi mitmekesiste ja struktuuriliselt keeruliste makrotsükliite saamiseks. Esimene on traditsiooniline viis, mis põhineb mitmeetapilisel avatud ahelaga vaheühendi sünteesil ja sellele järgneval terminaalsete rühmade tsükliseerimisel. See on laialdaselt kasutatav meetod ravimite ja erinevate materjalide saamiseks. Teine lähenemine põhineb dünaamiliselt tekkivate ja katkevate keemiliste sidemete ehk pöörduvate sidemete tekkel. Supramolekulaarsete interaktsioonide poolt juhitud dünaamiline kombinatoorne keemia, mis on suhteliselt uus suund kaasaegses keemias, võimaldab saavutada väga suurt efektiivsust keeruliste keemiste ühendite sünteesil. Antud töö keskendub pöörduvatel sidemetel ja täpsemalt aminaal-sideme tekkel, kuna neil on keskne roll hemikukurbituriilide sünteesil. Lisaks näidatakse mallide mõju inter- ja intramolekulaarsete reaktsioonide omavahelisele tasakaalule. Hemikukurbituriilid on suhteliselt uus haru kukurbituriilide arvukast perekonnast. Kukurbituriilid on tünnikujulised mahutid, mis on tuntud oma ülitugeva sidumisega katioonsete külaliskemikulaarsete molekulidega. Hemikukurbituriilid toimivad samuti molekulaarsete mahutitena, kuid seovad endasse pigem anioonide külaliskemikulaarsete molekulide, nad on leidnud kasutust katalüsaatoritena, anioonide transporteritena läbi raku-membraani, tahkes faasis elektroniülekandjatena ning anioonide sensoritena.

Käesolevas töös uuriti tsükloheksaanhemikukurbituriilide (cycHC[*n*]) sünteesi, iseloomustati nende struktuure ja komplekseerumist. Nimelt töötati välja esimeste enantiomeerselt puhaste kukurbituriilide perekonna liikmete (*S,S*)- ja (*R,R*)-cycHC[6] süntees. Kirjeldati kiraalse kuueühikulise hemikukurbituriili struktuuri ja omadusi kvantkeemiliste arvutuste, NMR, XRD ja MS meetoditega. Nende enantiomeersete „mahutite“ üheks eristatavaks omaduseks on võime moodustada diastereomeerseid komplekse kiraalsete külalisanioonidega. Järgnevalt uuriti, kuidas sünteesida suurema mahtuvusega cycHC homolooge ning avaldati esimese kaheksaühikulise hemikukurbituriili saamismeetod ning detekteeriti 7- kuni 10-ühikulised cycHC-d. Tänu põhjalikule tsükloheksaanhemikukurbituriili tekkemehhanismi uurimisele ja vaheühendite identifitseerimisele töötati välja väga efektiivne, happekatalüütiline malli poolt suunatud sünteesitee kiraalse 8-ühikulise cycHC[8] saamiseks. Lisaks töötati välja meetod esimese ühe pööratud monomeeriga hemikukurbituriili, *inverted-cis*-cycHC[6], sünteesiks ning pakuti välja selle termodünaamilistelt ebasoodsa ühendi tekkemehhanism.

Kokkuvõtteks, selle töö tulemusena rikastati kukurbituriilide perekonda mitme uue stereoisomeerse ja homoloogilise makrotsükliga. Mitmekülgsed ja põhjalikud ainete struktuuri ja tekkemehhanismi uuringud võimaldasid anda olulise panuse supramolekulaarse keemia valdkonda. Väljatöötatud meetodeid uute molekulaarsete mahutite sünteesiks saab rakendada molekulaarsete masinate, uute sensorite ja materjalide saamiseks. Need omakorda on vajalikud keemia-, farmaatsia- ja toiduainetööstuses ning põllumajanduses.

## Appendix

### Publication I

R. Aav, E. **Shmatova**, I. Reile, M. Borissova, F. Topić, K. Rissanen "New Chiral Cyclohexylhemicucurbit[6]uril" *Organic Letters*, **2013**, *15*, 3786–3789.

Reprinted with permission from American Chemical Society.



## New Chiral Cyclohexylhemicucurbit[6]uril

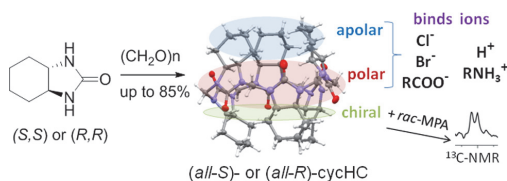
Riina Aav,<sup>\*†</sup> Elena Shmatova,<sup>†</sup> Indrek Reile,<sup>‡</sup> Maria Borissova,<sup>†</sup> Filip Topić,<sup>§</sup> and Kari Rissanen<sup>§</sup>

Department of Chemistry, Tallinn University of Technology, Akadeemia tee 15, 12618 Tallinn, Estonia, National Institute of Chemical Physics and Biophysics, Akadeemia tee 23, 12618 Tallinn, Estonia, and Department of Chemistry, Nanoscience Center, University of Jyväskylä, P.O. Box 35, 40014 Jyväskylä, Finland

riina@chemnet.ee

Received June 22, 2013

## ABSTRACT



The first enantiomerically pure members of the cucurbituril family, (*all-S*)- and (*all-R*)-cyclohexylhemicucurbit[6]urils (cycHC), were synthesized in good yield (up to 85%). The crystal structure of this new macrocycle clearly shows its ball-like shape. CycHC monomers adopt a “zigzag” conformation, having apolar cyclohexyls around the openings and polar ureas in the middle. Cyclohexylhemicucurbit[6]urils formed complexes with halides, carboxylic acids and amines and diastereomeric complexes with methoxyphenylacetic acid in organic media. The association constants of cycHC with small organic compounds were evaluated by diffusion NMR in chloroform.

The first synthesis of macrocyclic ureas was reported by Behrend et al. in 1905; later they were named cucurbiturils<sup>1</sup> by Mock et al. in 1981.<sup>2</sup> The pioneering work on the characterization of the first cucurbituril, CB[6], and its complexation studies performed by Mock were taken further by Kim and co-workers, who isolated new members of the cucurbituril family, CB[5], CB[7] and CB[8],<sup>3</sup> in 2000. Less than two years later, Day et al. isolated the host–guest pair CB[5]@CB[10].<sup>4</sup> Since then studies of cucurbiturils have dramatically grown in number, especially

with respect to their host–guest chemistry. Cucurbiturils form complexes with inorganic species (metallic cations and their counteranions) and with various organic guests, binding especially well with diammonium compounds.<sup>5</sup>

Not only has the family of cucurbiturils grown in the ring size of homologues, which differ in the number of monomers in the macrocycle, but also there has been progress in the synthesis of new relatives of cucurbiturils: inverted cucurbiturils (*i*CB[*n*]),<sup>6</sup> *ns*-cucurbit[*n*]urils,<sup>7</sup> and various cyclic<sup>8</sup> and acyclic congeners.<sup>9</sup> Soon after the discovery of the usefulness of the cucurbituril family, Miyahara et al.

<sup>†</sup>Tallinn University of Technology<sup>‡</sup>National Institute of Chemical Physics and Biophysics<sup>§</sup>University of Jyväskylä(1) Behrend, R.; Meyer, E.; Rusche, F. *Justus Liebigs Ann. Chem.* **1905**, 339, 1–37.(2) Freeman, W. A.; Mock, W. L.; Shih, N.-Y. *J. Am. Chem. Soc.* **1981**, 103, 7367.(3) Kim, J.; Jung, I.-S.; Kim, S.-Y.; Lee, E.; Kang, J.-K.; Sakamoto, S.; Yamaguchi, K.; Kim, K. *J. Am. Chem. Soc.* **2000**, 122, 540.(4) (a) Day, A.; Arnold, A. P.; Blanch, R. J.; Snushall, B. *J. Org. Chem.* **2001**, 66, 8094. (b) Day, A. I.; Blanch, R. J.; Arnold, A. P.; Lorenzo, S.; Lewis, G. R.; Dance, I. *Angew. Chem., Int. Ed.* **2002**, 41, 275.(5) For reviews, see: (a) Masson, E.; Ling, X.; Joseph, R.; Kyeremeh-Mensah, L.; Lu, X. *R. Soc. Chem. Adv.* **2012**, 2, 1213. (b) Isaacs, L. *Chem. Commun.* **2009**, 619. (c) Kim, K.; Selvapalam, N.; Ko, Y. H.; Park, K. M.; Kim, D.; Kim, J. *Chem. Soc. Rev.* **2007**, 36, 267. (d) Lagona, J.; Mukhopadhyay, P.; Chakrabarti, S.; Isaacs, L. *Angew. Chem., Int. Ed.* **2005**, 44, 4844.(6) (a) Isaacs, L.; Park, S.-K.; Liu, S.; Ko, Y. H.; Selvapalam, N.; Kim, Y.; Kim, H.; Zavalij, P. Y.; Kim, G.-H.; Lee, H.-S.; Kim, K. *J. Am. Chem. Soc.* **2005**, 127, 18000.(7) (a) Huang, W.-H.; Liu, S.; Zavalij, P. Y.; Isaacs, L. *J. Am. Chem. Soc.* **2006**, 128, 14744. (b) Huang, W.-H.; Zavalij, P. Y.; Isaacs, L. *Angew. Chem., Int. Ed.* **2007**, 46, 7425. (c) Huang, W.-H.; Zavalij, P. Y.; Isaacs, L. *Org. Lett.* **2008**, 10, 2577.(8) (a) Lagona, J.; Fettingner, J. C.; Isaacs, L. *J. Org. Chem.* **2005**, 70, 10381. (b) Zhao, J.; Kim, H.-J.; Oh, J.; Kim, S.-Y.; Lee, J. W.; Sakamoto, S.; Yamaguchi, K.; Kim, K. *Angew. Chem., Int. Ed.* **2001**, 40, 4233. (c) Isobe, H.; Sato, S.; Nakamura, E. *Org. Lett.* **2002**, 4, 1287. (d) Day, A. I.; Arnold, A. P.; Blanch, R. J. *Molecules* **2003**, 8, 74.(9) (a) Burnett, C. A.; Witt, D.; Fettingner, J. C.; Isaacs, L. *J. Org. Chem.* **2003**, 68, 6184. (b) Ma, D.; Zavalij, P. Y.; Isaacs, L. *J. Org. Chem.* **2010**, 75, 4786. (c) Lucas, D.; Isaacs, L. *Org. Lett.* **2011**, 13, 4112. (d) Ma, D.; Zhang, B.; Hoffmann, U.; Sundrup, M. G.; Eikermann, M.; Isaacs, L. *Angew. Chem., Int. Ed.* **2012**, 51, 11358.

synthesized hemicucurbiturils, HC[6] and HC[12], which can be viewed as cucurbiturils that are cut in half along the equator.<sup>10</sup> Li et al. synthesized and reported the crystal structure of a substituted hemicucurbituril *meso*-cyclohexylhemicucurbit[6]juril.<sup>11</sup> Hemicucurbiturils have, because of their “zigzag” conformation, a significantly different complexation ability from cucurbiturils. Hemicucurbit[6]jurils form complexes with selected anions, cations, and small molecules (water and formamide).<sup>10,12</sup>

In the most recent development in the member list of the cucurbituril family, the research group of Sindelar<sup>13</sup> introduced bambus[*n*]jurils, which combine the structural properties of cucurbiturils (glycouril monomers) and hemicucurbiturils (zigzag conformation). The list of bambus[*n*]jurils was increased by Rivollier et al.<sup>14</sup> this year. Compared to cucurbiturils, bambusurils have enhanced structural flexibility and good solubility in organic solvents.

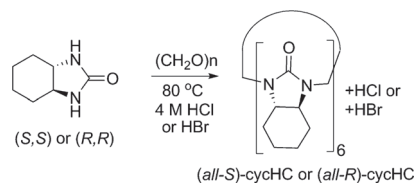
These given examples complete the list of known cucurbituril congeners, of which only one has been shown to exhibit chiral recognition toward an enantiomerically pure guest, the *nor-seco*-cucurbituril ( $\pm$ )-*bis-ns*-CB[6], which was synthesized from achiral monomers in racemic form.<sup>7b</sup>

In this paper, we describe the synthesis, structure, and complex formation of the new chiral (*all-R*)- and (*all-S*)-cyclohexylhemicucurbit[6]jurils.

Enantiomerically pure hemicucurbit[6]jurils ((*all-S*)- and (*all-R*)-cycHC, Scheme 1) can be synthesized from (*S,S*)- and (*R,R*)-cyclohexane ureas. Both enantiomers of starting ureas can be easily derived from 1,2-cyclohexanediamine by stereoselective crystallization with *L*- or *D*-tartaric acid<sup>15</sup> and subsequent carbonylation with diphenylcarbonate.<sup>16</sup> The enantiomeric purity of derived hemicucurbiturils is inherited from the *trans*-1,2-cyclohexanediamines.

Cyclohexylhemicucurbit[6]jurils (cycHC) are formed by heating the starting urea and formaldehyde in 4 M aqueous hydrochloric or hydrobromic acid. CycHC is the main product formed in thermodynamically controlled conditions and precipitates from the reaction mixture as HCl or HBr complex in good yield (85% of cycHC+HCl and 64% of cycHC+HBr) (Scheme 1). The existence of such reaction products as 1:1 halogenide complexes was determined by ESI-MS and quantitative NMR analysis. So far our attempts to isolate macrocyclic products from the reactions catalyzed by other acids, namely, sulfuric, trifluoroacetic, and hydroiodic acids, have failed.

**Scheme 1.** Synthesis of Cyclohexylhemicucurbit[6]jurils



CycHC formed carbon tetrachloride solvate monocystals from a mixture of CCl<sub>4</sub> and diisopropylethylamine. The crystal structure showed that 6 monomers incorporated into cycHC adopted zigzag conformations, as with all single-bridged members of the cucurbituril family (Figure 1). Strongly basic diisopropylethylamine abstracted/neutralized the hydrogen chloride during crystallization; therefore, halogenide was not incorporated in the crystal structure of cycHC. The cyclohexyl rings leaned toward each other, closing the opening of the macrocycle, so the shape of this macrocycle was more similar to cucurbiturils’ pumpkin or ball shape than to the bambusurils, with cavity shrinkage in the middle of the macrocycle.

The size of the opening of cycHC was found to be 2.2 Å, which is comparable to the corresponding value of 2.4 Å for cucurbit[5]juril.<sup>17</sup> The cavity size of cycHC was wider, and the distance between the two opposite carbonyl carbons was 5.3 Å, comparable to the cucurbit[6]juril cavity size of 5.8<sup>17</sup> and 5.3 Å in  $\alpha$ -cyclodextrin.<sup>18</sup> The height of cycHC was 12.1 Å. The given distances take into account the van der Waals radii of relevant atoms. In spite of the resemblance of the general shapes of cucurbituril and cyclohexylhemicucurbit[6]juril, their polar and lipophilic regions were arranged in opposite formations. CycHC had a polar belt bearing urea functionalities in the middle and nonpolar cyclohexyls around the openings. The monomers were linked to each other in cycHC via one methylene bridge; thus, cyclohexyl rings that were further apart from this bridge were flexible, and the size of the opening could increase. Therefore, cycHC could serve as a chiral host molecule that has unique complexation ability.

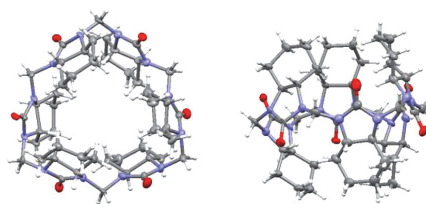


**Figure 1.** Crystal structure of (*all-S*)-cyclohexylhemicucurbit[6]juril.

(17) Lee, J. W.; Samal, S.; Selvapalam, N.; Kim, H.-J.; Kim, K. *Acc. Chem. Res.* **2003**, *36*, 621.

(18) Szejtli, J. *Chem. Rev.* **1998**, *98*, 1743.

(10) Miyahara, Y.; Goto, K.; Oka, M.; Inazu, T. *Angew. Chem., Int. Ed.* **2004**, *43*, 5019.

(11) Li, Y.; Lin, L.; Zhu, Y.; Meng, X.; Wu, A. *Cryst. Growth Des.* **2009**, *9*, 4255.

(12) Buschmann, H.-J.; Zielesny, A.; Schollmeyer, E. *J. Inclusion Phenom. Macrocyclic Chem.* **2006**, *54*, 181.

(13) (a) Svec, J.; Necas, M.; Sindelar, V. *Angew. Chem., Int. Ed.* **2010**, *49*, 2378. (b) Svec, J.; Dusek, M.; Fejfarova, K.; Stacko, P.; Klan, P.; Kaißer, A. E.; Li, W.; Hudeckova, E.; Sindelar, V. *Chem.—Eur. J.* **2011**, *17*, 5605. (c) Havel, V.; Svec, J.; Wimmerova, M.; Dusek, M.; Pojarova, M.; Sindelar, V. *Org. Lett.* **2011**, *13*, 4000.

(14) Rivollier, J.; Thuery, P.; Heck, M.-P. *Org. Lett.* **2013**, *15*, 480.

(15) (a) Larrow, J. F.; Jacobsen, E. N.; Gao, Y.; Hong, Y.; Nie, X.; Zepp, C. M. *J. Org. Chem.* **1994**, *59*, 1939. (b) Larrow, J. F.; Jacobsen, E. N. *Org. Syn., Coll.* **2004**, *10*, 96.

(16) Fuentes de Arriba, A.; Seidedos, D.; Simón, L.; Alcázar, V.; Raposo, C.; Morán, J. *J. Org. Chem.* **2010**, *75*, 8303.

The interaction of cycHC with small organic compounds was studied by NMR and MS analysis. Mixing cycHC and the compounds **1–5** as shown in Figure 2 in chloroform in equimolar ratios caused a  $^{13}\text{C}$  NMR chemical shift change of small molecules. As a representative example, the  $^{13}\text{C}$  NMR spectra of monoethylfumarate **1** with and without cycHC are shown in Figure 2. The nonequal direction of the  $^{13}\text{C}$  NMR chemical shift change of different monoethylfumarate **1** carbons supports the postulate of the existence of a host–guest complex between cycHC and acid **1**. In ESI-MS analysis of mixtures of **1–4** and cycHC, the molecular ions of complexes cycHC+carboxylic acids **1** and **2** were detected in negative mode (as carboxylates) and complexes cycHC+amino compounds **3** and **4** in positive mode (in protonated form), confirming the existence of 1:1 complexes. Also a 2:1 (cycHC:**4**) complex with diamine **4** was detected by MS.

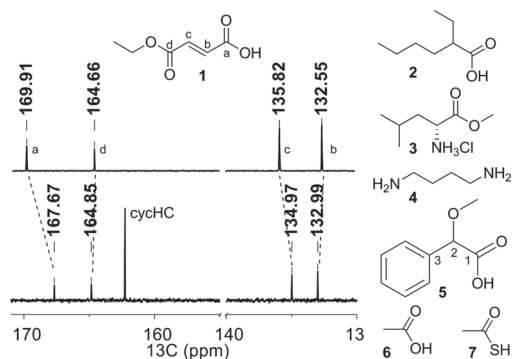


**Figure 2.**  $^{13}\text{C}$  NMR spectra of carboxylic acid **1** without (upper) and with (lower) (*all-R*)-cycHC and structures of **1–7**, whose complexes with cycHC were studied in this work.

The formation of diastereomeric complexes with methoxyphenylacetic acid (MPA) **5** and (*all-R*)-cycHC was detected in  $^{13}\text{C}$  NMR spectra. Mixtures of MPA and cycHC in ratios of 5:1, 1:1, and 1:5 were analyzed, and the splitting of *rac*-MPA  $^{13}\text{C}$  NMR signals along with an accompanying chemical shift change was observed. Figure 3 shows representative  $^{13}\text{C}$  NMR fragments with MPA signals at C3.

The complexed MPA signal of C3 was shifted downfield compared to the uncomplexed MPA C3 signal (Figure 3 spectrum d). Complexed and uncomplexed MPA did not give isolated signal pairs in spectra of MPA and cycHC mixtures, because of an exchange within the NMR time span. Nevertheless, diastereomeric complexes of (*R*)-MPA+(*all-R*)-cycHC and (*S*)-MPA+(*all-R*)-cycHC were distinguishable in all analyzed *rac*-MPA and (*all-R*)-cycHC mixture ratios. The mixtures of (*all-R*)-cycHC with enantiomerically pure MPA gave single peaks resonating at different frequencies, confirming the formation of diastereomeric complexes.

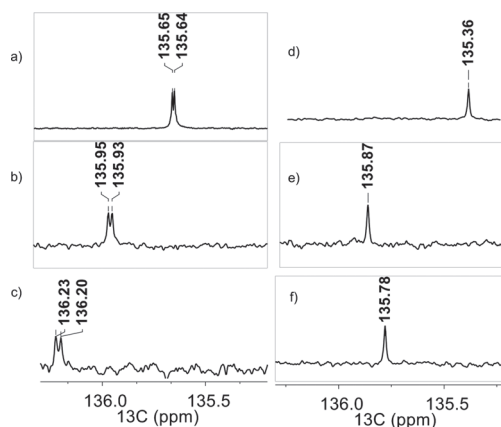


**Figure 3.** Fragments of  $^{13}\text{C}$  NMR spectra of MPA: C3 signals measured with and without (*all-R*)-cycHC: (a) *rac*-MPA and (*all-R*)-cycHC in 5:1 ratio; (b) *rac*-MPA and (*all-R*)-cycHC in 1:1 ratio; (c) *rac*-MPA and (*all-R*)-cycHC in 1:5 ratio; (d) MPA without cycHC; (e) (*S*)-MPA and (*all-R*)-cycHC in 1:1 ratio; (f) (*R*)-MPA and (*all-R*)-cycHC in 1:1 ratio.

Diffusion NMR measurements of cycHC with guests **1–5** and additionally with acetic acid **6** and thioacetic acid **7** were performed to confirm that NMR chemical shift changes are caused by complexation. Diffusion NMR can be used to evaluate the mobility of different dissolved species in solution and has been exploited for studying intermolecular complexation and solution state aggregates. Moreover, diffusion methods allow to get an estimate for the binding constant  $K_a$  from a single measurement, and it is an acceptable alternative to titration studies.<sup>20</sup>

As seen in Table 1, the self-diffusion coefficients ( $D$ ) of small molecules, which reflect the rate of thermal translational motion of dissolved species, decrease in the presence of cycHC. Although these preliminary measurements need further elaboration, they clearly indicate intermolecular interaction and support the earlier observations from ESI-MS and 1D NMR that compounds **1–6** form complexes with cycHC.

In the case of 1:1 host–guest complex formation and full inclusion of the guest, the host  $D$  value should not change upon complexation. The relation between molecular size and diffusion coefficient predicts that the self-diffusion coefficient of the host dimer should decrease at least 26% compared to the monomeric host  $D$  value.<sup>20c</sup> However, the small decrease of the complexed host's  $D$  (for example 11%

(19) Rymden, R.; Carlfors, J.; Stilbs, P. *J. Inclusion Phenom.* **1983**, *1*, 159.

(20) (a) Johnson, C. S. *Prog. Nucl. Magn. Reson. Spectrosc.* **1999**, *34*, 203. (b) Cohen, Y.; Avram, L.; Frish, L. *Angew. Chem., Int. Ed.* **2005**, *44*, 520. (c) Cohen, Y.; Avram, L.; Evan-Salem, T.; Slovak, S. Diffusion NMR in supramolecular chemistry and complexed systems. In *Analytical Methods in Supramolecular Chemistry*, 2nd ed.; Schalley, C. A. Ed.; Wiley: Weinheim, 2012; pp 197–285.

**Table 1.** Diffusion Coefficients  $D$  ( $10^{-10}$  m<sup>2</sup>/s) and Association Constants  $K_a$  ( $M^{-1}$ ) of Guests with (*all-R*)-cycHC Host in 1:1 Mixtures in CDCl<sub>3</sub>

guest	$D_{\text{free}}$	$D_{\text{bound}}$	$D_{\text{cycHC}}$	$K_a$
none			$5.26 \pm 0.01$	
<b>1</b>	$9.09 \pm 0.01$	$6.91 \pm 0.01$	$4.68 \pm 0.01$	$73.2 \pm 0.5$
<b>2</b>	$9.66 \pm 0.01$	$8.66 \pm 0.01$	$5.27 \pm 0.01$	$14.4 \pm 0.1$
<b>3</b>	$5.18 \pm 0.01$	$4.87 \pm 0.01$	$5.11 \pm 0.01$	NA
<b>4</b>	$13.94 \pm 0.01$	$12.17 \pm 0.01$	$5.16 \pm 0.01$	$11.9 \pm 0.5$
<b>S-5</b>	$10.34 \pm 0.01$	$8.94 \pm 0.01$	$5.29 \pm 0.01$	$20.1 \pm 0.2$
<b>R-5</b>	<sup>a</sup>	$8.59 \pm 0.01$	$4.99 \pm 0.01$	$27.2 \pm 0.8$
<b>6</b>	$15.48 \pm 0.02$	$13.85 \pm 0.02$	$4.83 \pm 0.01$	$8.0 \pm 0.5$
<b>7</b>	$18.45 \pm 0.07$	$18.56 \pm 0.02$	$5.27 \pm 0.01$	$0.0 \pm 0.5$

<sup>a</sup>  $D_{\text{free}}$  of *S*-MPA was used.

$D_{\text{free}}$  denotes uncomplexed guest,  $D_{\text{bound}}$  complexed guest, and  $D_{\text{cycHC}}$  complexed macrocycle. All samples were prepared in CDCl<sub>3</sub> at 26.5 mM concentration of each component and measured at 288 K in neat solutions or in 1:1 mixtures of guest and cycHC. Association constants  $K_a$  were calculated according to Rymden et al.<sup>19</sup> Binding of **3** could not be reliably determined, as diffusion methods are not suitable for binding evaluation when the  $D$  of guests and macrocycles are very close.

in case of guest **1**) can also be caused by simultaneous existence of complexes with different host–guest ratios, in addition to 1:1 ratio or by partial inclusion of the guest molecule.

It is important to note that association constants between organic molecules were measured in an organic solvent (CDCl<sub>3</sub>), and therefore lower affinities compared to the organic molecule complexes in aqueous solutions can be expected. Nevertheless, the determined  $K_a$  values reflect organic molecules' relative affinities toward cycHC. The nature of complexation with amino-substituted guests needs further elaboration, but preliminary conclusions on carboxylic acids can be drawn. The highest binding is observed with the most planar carboxylic acid **1**, and introduction of branching to the  $\alpha$  position of carboxylic acids **2** and **5** decreases  $K_a$ . There is a small difference in the association constants of (*all-R*)-cycHC with *S*- and *R*-MPA, indicating minor chiral recognition. The  $K_a$  for acetic acid **6**

is an order of magnitude lower than for the guest **1**, suggesting that polar and apolar regions of the host and guest do not match in this case. The absence of complexation with thioacetic acid **7**, which incorporates a bulkier sulfur atom, indicates that complexation is dependent on the size and shape of the guest. Therefore the existence of inclusion complexes of cycHC and carboxylic acids is proposed. Studies on the exact nature of complexation will be the subject of our further research.

New (*all-S*)- and (*all-R*)-cyclohexylhemicucurbit[6]urils were synthesized: the first enantiometrically pure members of the cucurbituril family. These hemicucurbiturils formed complexes with either HCl or HBr, depending on the acid used for their formation. Complexation of cycHC with carboxylic acids and amines was detected, and their association constants were determined in organic media. Formation of inclusion complexes with carboxylic acids was proposed. CycHC formed diastereomeric complexes with enantiomers of methoxyphenylacetic acids, binding affinities of which were distinguishable. Detailed studies on the complexation and on the synthesis of homologues are currently underway in our group.

**Acknowledgment.** The authors would like to thank Dr. Franz Werner for very useful discussions while he was working at Tallinn University of Technology, Estonia. This research was supported by the Estonian Science Foundation through Grant No. 8698 and the Ministry of Education and Research through Grants No. SF0140060s12 and SF0690021s09, and by the Academy of Finland (KR Grants No. 122350, 140718, 265328 and 263256) and the National Doctoral Programme in Nanoscience, Finland (FT, Ph.D. fellowship).

**Supporting Information Available.** Experimental procedures, characterization of cycHC and its complexes, and crystal data (CIF). These materials are available free of charge via the Internet at <http://pubs.acs.org>.

The authors declare no competing financial interest.

## Publication II

M. Öeren, **E. Shmatova**, T. Tamm, R. Aav "Computational and ion mobility MS study of (*all-S*)-cyclohexylhemicucurbit[6]uril structure and complexes" *Physical Chemistry Chemical Physics*, **2014**, *16*, 19198–19205.

Reprinted with permission from Royal Society of Chemistry.



# Computational and ion mobility MS study of (*all-S*)-cyclohexylhemicucurbit[6]uril structure and complexes†

Cite this: *Phys. Chem. Chem. Phys.*, 2014, **16**, 19198

Mario Öeren, Elena Shmatova, Toomas Tamm and Riina Aav\*

A computational study of (*all-S*)-cyclohexylhemicucurbit[6]uril and its complexes with anions (Cl<sup>-</sup>, Br<sup>-</sup>, I<sup>-</sup> and HCOO<sup>-</sup>), the proton (H<sup>+</sup>) and non-dissociated acid (HCl, HBr, HI and HCOOH) guests was performed. The geometries of guest–host complexes were optimized *via* density functional theory using the BP86 functional, SV(P) basis set and Stuttgart pseudopotentials for iodide. Binding affinities and their trends were evaluated at the BP86/TZVPD level of theory. In addition, the quantum theory of atoms in molecules was used to gain insight into guest–host interactions. A computational study in the gas phase and ion-mobility mass-spectrometry analysis revealed that the studied macrocycle formed inclusion complexes with anions. Protonation of the macrocycle is preferred at the nitrogen atom pointing inside of the cavity. In the studied conditions, non-dissociated acids formed complexes at the oxygen atom pointing outside of the macrocycle.

Received 20th May 2014,  
Accepted 8th July 2014

DOI: 10.1039/c4cp02202e

www.rsc.org/pccp

## 1. Introduction

Although the first cucurbituril (CB) was synthesized more than 100 years ago,<sup>1</sup> and characterized over 30 years ago,<sup>2</sup> this macrocyclic compound has gained wider attention only in recent decades. Applications of CBs<sup>3</sup> are based on their ability to bind guest molecules, mainly alkylammonium cations. CBs are widely used as catalysts,<sup>4</sup> nanomaterials and as drug delivery vehicles.<sup>5</sup> Hemicucurbiturils (HCs) are a relatively new branch in the diverse CB family.<sup>3</sup> The first HCs (HC[*n*] with *n* = 6, 12) were synthesized by Miyahara *et al.*<sup>6</sup> in 2004 and since then only a few new HCs have been reported.<sup>7–9</sup> Amongst new HCs, the first enantiomerically pure member of the cucurbituril family, (*all-S*)- and (*all-R*)-cyclohexylhemicucurbit[6]uril (cycHC[6]), has been synthesized in our group.<sup>10</sup> Unsubstituted HCs have been reported to catalyse organic reactions,<sup>11–13</sup> although their mode of action is still unknown. In contrast to CBs, in which the urea units are aligned, HCs adopt a ‘zig-zag’ orientation, causing a substantial difference in the electronic structure of the macrocycle and thereby allowing for the binding of anions.<sup>6,14</sup> The anion binding properties of structurally close relatives of hemicucurbiturils, namely bambus[*n*]urils<sup>15</sup> (BU[*n*], *n* = 4–6) have also been reported.<sup>16–18</sup>

Since the pioneering computational study of Kim and co-workers in 2001,<sup>19</sup> there has been a steady increase in the

number and quality of computational treatments of cucurbiturils and related systems. In many cases, complexation with various guest molecules has been among the goals of the studies. The size of the system, which is further increased by inclusion of a guest, initially necessitated the use of relatively simple models (Hartree–Fock) and small basis sets (STO-3G, 3-21G).<sup>19–21</sup> Recent advances in computer technology have made treatments with more sophisticated models (DFT with hybrid functionals, up to triple-zeta basis sets) feasible.<sup>22–32</sup> Use of the density fitting (also known as resolution of identity) approximation is routinely used, especially because the associated loss in accuracy is negligible.

Several researchers have paid close attention to the frontier molecular orbitals – the highest occupied MO (HOMO) and lowest unoccupied MO (LUMO) – of the macrocyclic systems,<sup>24,25,33</sup> as well as the electrostatic potential generated by the molecule.<sup>26–32</sup> These properties lead to the prediction of binding sites and modes of guests, and HOMO–LUMO energy gaps can be used as indicators of relative reactivities. The map of electrostatic potential (MESP) outlines electron-rich and electron-poor regions of a macrocycle, which are indicators of locations of possible electrostatic interactions between the host and the guest.

Binding modes and binding energies of various guest molecules have also received research attention.<sup>19,21,25,34–36</sup> Such models can also provide insight into the probable location of the binding site, including whether binding inside or outside of the macrocycle is preferred. Additional information about the nature of chemical bonds between the host and guests has been obtained from the quantum theory of atoms in molecules (QTAIM).<sup>23,31</sup> This model also provides an estimate of the strength of host–guest interactions.

Department of Chemistry, Tallinn University of Technology, Ehitajate tee 5, 19086 Tallinn Estonia. E-mail: riina@chemet.ee

† Electronic supplementary information (ESI) available: Computational and IM-MS CCS details, including optimized geometries. See DOI: 10.1039/c4cp02202e

It has been reported that the HC binds anions<sup>9,23,37</sup> and a few cations.<sup>38,39</sup> In addition, Cong *et al.* have suggested that the binding of a proton inside of HC occurs during catalysis with HC.<sup>12</sup> The chiral hemicucurbituril (*all-S*)-cycHC[6] was isolated as a hydrogen halide complex. Additionally, based on the results of a diffusion NMR study of (*all-S*)-cycHC[6] complexes, it was proposed that substituted hemicucurbituril forms inclusion complexes with carboxylic acids.<sup>10</sup> So far, there is no crystal structure of (*all-S*)-cycHC[6] complexes and it is not known whether the acids are bound as dissociated anions or as non-dissociated neutral species. A computational study of the structure and mode of complexation of cycHC[6] would increase our knowledge in this field.

In this paper, we report the geometry and electronic structure of cycHC[6] and its complexes with the anions  $\text{Cl}^-$ ,  $\text{Br}^-$ ,  $\text{I}^-$  and  $\text{HCOO}^-$  and the proton and non-dissociated ( $\text{HCl}$ ,  $\text{HBr}$ ,  $\text{HI}$  and  $\text{HCOOH}$ ) guests. Different binding sites were evaluated and selected complexes were studied using QTAIM analysis. Additionally, a study of ion mobility mass-spectrometric analysis of cycHC[6] complexes was performed.

## 2. Experimental section

### 2.1 Computational details

**2.1.1 Description of the opening and the cavity of cycHC[6].** Four parameters were chosen to describe the geometric changes of the macrocycle upon complexation with guests. The distances from the carbon  $\text{C}_2$  and oxygen  $\text{O}$  to the centre of the cavity  $\text{X}$  ( $r(\text{C}_2\text{-X})$  and  $r(\text{O-X})$ ) describe the changes of the geometry at the equator of the macrocycle. The distances from the  $\text{C}_{4a}$  and  $\text{C}_7$  to the centre of the cavity ( $r(\text{C}_{4a}\text{-X})$  and  $r(\text{C}_7\text{-X})$ ) describe the opening or closing movement of the cyclohexyl groups. The shortest distance of  $\text{C}_5$  from the axis ( $\text{Z}$ ) ( $r(\text{C}_5\text{-Z})$ ) describes the openings of the macrocycle. The listed distances are graphically depicted in Fig. 1. The cavity size of the optimized structures was studied using the program Swiss-PdbViewer.<sup>40</sup>

**2.1.2 Electronic structure calculations.** All molecular structures in this work were built using the program Avogadro<sup>41</sup> and pre-optimized therein using the MMFF94 molecular-mechanical model. Further geometry optimizations were conducted with

density functional theory (DFT), using the BP86 functional<sup>42–46</sup> along with the def2-SV(P)<sup>47</sup> basis set. The interactions between guest and host were expected to be prevalently electrostatic; hence, in the interest of computational speed, the choice of the lightweight, thus fast functional without dispersion correction was justified. To speed up the geometry optimization, the resolution of identity (RI) approximation was used.<sup>48–51</sup> Vibrational frequency calculations were performed to ensure that all chosen geometries were at minima, and to estimate the zero-point vibrational energies (ZPE). The energies of local minima were refined by single-point calculations with the def2-TZVPD<sup>47</sup> basis set. The iodine atoms were described with the inclusion of the appropriate Stuttgart pseudopotential.<sup>52,53</sup> In addition, counterpoise correction calculations were performed to obtain basis set superposition error (BSSE) corrected energies for host-guest complexes.<sup>54</sup> The transition states were verified using dynamic reaction coordinate calculations. All calculations were performed in the gas phase. Solvation effects were omitted because cycHC[6] complexation was previously studied in hydrophobic solvent ( $\text{CDCl}_3$ )<sup>10</sup> and to model that one should include the first shell explicitly and use a continuum model to describe the bulk solvent. Currently, little information is available about the structure of the first explicit solvation shell of chloroform for the calculated species. Also, in this work complexes were experimentally studied in the gas phase by mass-spectrometric analysis. The density functional theory calculations were performed using the Turbomole 6.4 program package.<sup>55–58</sup>

**2.1.3 Search for binding sites.** The search for binding sites for guests was done systematically, where outside of the macrocycle five latitudes (with  $36^\circ$  increments) and five longitudes (with  $10^\circ$  increments) were combined (Fig. 2).

The crossing points of the meridians and parallels were used as initial locations for the guests in the geometry optimizations. For each guest type, a few locations were added manually as well. The centre of the macrocycle was added to the set for anions and locations on the HOMO were added for the proton. The combinations of anion and proton locations were added for the non-dissociated guest.

**2.1.4 Binding energy of the guest.** The binding energy (BE) was calculated by subtracting the sum of the total energies of

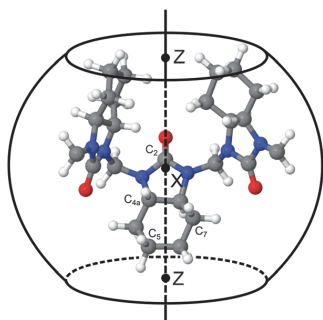


Fig. 1 Atom numbers, centre of the cavity and axis of cycHC[6].

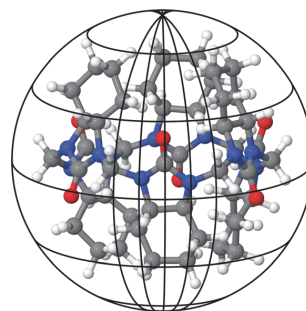


Fig. 2 Latitudes and longitudes used in a systematic search for binding sites.

the reagents from the sum of the total energies of the products. The total energies for each geometry were calculated as sums of DFT energies (DE) and basis set superposition error (BSSE) corrections from def2-TZVPD calculations and the zero-point energy (ZPE) correction from def2-SV(P) calculations. The binding energy of anions and non-dissociated guests with the host were calculated according to eqn (1).

$$BE = (DE_{GH} + ZPE_{GH} + BSSE_{GH}) - (DE_G + ZPE_G + DE_H + ZPE_H), \quad (1)$$

where the equation components with the subscripts GH, G and H denote the aforementioned energies of the guest–host complex, guest and host, respectively.

The calculation of the binding energy of a proton to the macrocycle is shown in eqn (2), and it was found *via* the reaction of an oxonium ion with a host molecule, producing water as the secondary product.

$$BE = (DE_{GH} + ZE_{GH} + DE_{H_2O} + ZE_{H_2O}) - (DE_{H_3O^+} + ZE_{H_3O^+} + DE_H + ZE_H), \quad (2)$$

where the equation components with the subscripts GH, H<sub>2</sub>O, H<sub>3</sub>O<sup>+</sup> and H denote the aforementioned energies of the guest–host complex, water, oxonium ion and host, respectively.

**2.1.5 Post-processing of the results.** For visualization of the map of electrostatic potential (MESP), single-point calculations were repeated at the def2-SV(P) level of theory using Gaussian 09<sup>59</sup> software. Visualizations of geometries, frontier orbitals and MESP were generated from the output files with Jmol<sup>60</sup> and Molekel.<sup>61</sup> The binding properties of the macrocycle were studied *via* QTAIM,<sup>62</sup> using the program Multiwfn<sup>63</sup> with def2-SV(P) density. The required .wfx file for iodine with ECP information was generated with Gaussian 09. Interactions between the host and the guest were investigated *via* locating the bond critical points (BCPs) as defined in the QTAIM model. The interaction energies (*E*) were calculated using the potential energy density (*V*) at the corresponding BCP, as in this case  $E = V/2$ .<sup>64</sup>

## 2.2 Ion-mobility mass-spectrometric analysis

Hemicucurbituril cycHC[6] HCl and HBr adducts were synthesized as previously described.<sup>10</sup> 40 μM solutions of cycHC[6] + HCl and cycHC[6] + HBr in a solvent mixture of H<sub>2</sub>O (47.5%), MeOH (47.5%) and HCOOH (5%) were prepared and analyzed by electrospray ionization ion mobility mass spectrometry (ESI-IM-MS). All of the MS experiments were performed using a Waters Synapt G2 HDMS quadrupole travelling wave ion mobility orthogonal acceleration time-of-flight mass spectrometer (Waters, Manchester, UK), equipped with a normal Z-spray ESI source in both positive and negative ion modes. A source temperature of 100 °C, capillary voltage of 2 kV, desolvation temperature of 150 °C, and cone voltage of 20 V were set as the ESI parameters. All experiments were performed under conditions of 280 m s<sup>-1</sup> wave velocity and 18 V wave height by traveling wave ion-mobility mass spectrometry (TWIM-MS). The experimental collision cross-sections ( $\Omega_D$ ) of cycHC[6] complexes were calculated by the calibration method of Thalassinou *et al.*,<sup>65</sup> with

polyalanine as a calibrant. The published  $\Omega_D$  values of the polyalanine were obtained from the database of the Clemmer group.<sup>66</sup> The theoretical  $\Omega_D$  values were calculated by the projection approximation method, using the radius of each atom<sup>67</sup> from the hard sphere mode.<sup>68</sup>

## 3. Results and discussion

### 3.1 Geometry and electronic structure of cyclohexylhemicucurbit[6]uril

The calculated structure of cycHC[6] had monomers in 'zig-zag' orientation and exhibited *D*<sub>3</sub> point group symmetry. Validation of the computed structure was done *via* comparison of the shortest distances between the centre of the cavity, axis and selected atoms –  $r(C_5-Z)$ ,  $r(C_7-X)$ ,  $r(C_{4a-X})$ ,  $r(C_2-X)$  and  $r(O-X)$  – of the calculated and crystallographic structure<sup>10</sup> (Table 1).

As can be seen from Table 1, the distances  $r(C_2-X)$  and  $r(O-X)$  of the computed structure were very close to the experimental ones, while the difference increased for the atoms that were located closer to the opening from  $r(C_{4a-X})$  to  $r(C_5-Z)$ . The differences between the computed and experimental structure were probably caused by the flexibility of cyclohexyl groups, which were influenced by the packing forces in the crystal structure. The volume of the internal cavity was 22 Å<sup>3</sup> for the calculated structure and 18 Å<sup>3</sup> for the experimental structure.

The highest occupied molecular orbital (HOMO) was mostly distributed over the polar cyclic urea functional groups, and its bulkiest lobes were on the nitrogen atoms (Fig. 3a). Nitrogen atoms were not planar, adopting quasi-sp<sup>2</sup>/quasi-sp<sup>3</sup> geometry, and therefore the HOMO lobes on nitrogen atoms were present both inside and outside of the macrocycle. The HOMO was also located on the cyclohexyl moiety and this orbital only slightly covered the oxygen atoms. The location of the binding site for cations was not uniquely determined by the orbital structure. The binding of a cation could take place inside or outside of the macrocycle, where the HOMO of the latter was delocalized. The lowest unoccupied molecular orbital (LUMO), on the other hand, was concentrated mostly inside the macrocycle (Fig. 3b).

This positioning of the LUMO in the centre of the cavity creates a potential binding site for anions. Therefore, we could expect interaction between the HOMO of the anionic guests and the LUMO of macrocycle, which would result in encapsulation of the anionic guest molecule. The HOMO–LUMO gap was

**Table 1** Distances between the centre of the cavity and axis and selected atoms of computed and experimental cycHC[6] in Å

	Computed parameters	Experimental parameters <sup>a</sup>
$r(C_5-Z)$	3.1	2.7 ± 0.2
$r(C_7-X)$	4.2	3.8 ± 0.1
$r(C_{4a-X})$	4.2	4.1 ± 0.1
$r(C_2-X)$	4.4	4.4 ± 0.2
$r(O-X)$	5.0	5.0 ± 0.1

<sup>a</sup> Radii were the mean values for six atoms of each monomer given with maximum absolute deviation.

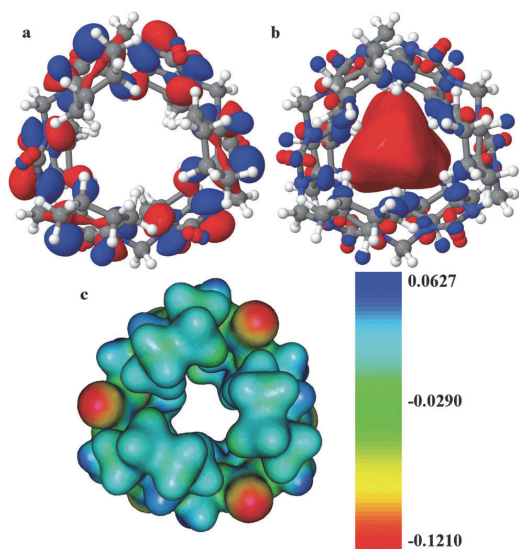


Fig. 3 Electronic structure of cycHC[6]: (a) HOMO; (b) LUMO; (c) MESP.

4.93 eV (SV(P)), making it the lowest amongst analogous macrocycles (6.04–6.58 eV).<sup>2,3</sup>

The map of electrostatic potential (MESP) of cycHC[6] is shown in Fig. 3c. The most electron-rich regions (red area) were on oxygen atoms, while the most electron-deficient areas (blue areas) were found on the methylene bridges and the centres of cyclohexyl groups. Besides oxygen atoms, nitrogen atoms were found to be electron-rich as well (yellow area) and, due to the chirality of the monomer, one electron-rich nitrogen was pointing outside of the macrocycle and the other one inside. The MESP on nitrogen atoms agreed with the HOMO being located on the nitrogen atoms. The openings of the macrocycle were rather electron-poor. The listed characteristics of cycHC[6] electronic structure and frontier orbitals made it possible to visualize possible binding sites of guest molecules. However the complexation of both an anion and a proton inside the cavity of macrocycle is feasible. Further computations of the interaction strengths and binding energies of non-dissociated and dissociated acids with cycHC[6] were carried out.

### 3.2 Structure of cycHC[6]–anion complexes

In the search for the binding sites for anions, geometry optimization of all generated initial structures led to multiple distinct local minima for all anions. In all cases, anions strongly preferred the binding site inside the macrocycle. The energy difference between the lowest-energy minimum, having an anion inside, and the second-lowest one, having an anion outside, was always over 25 kJ mol<sup>-1</sup> and reached 100 kJ mol<sup>-1</sup> for some higher-lying minima. Based on these results, we propose that all anions prefer to reside inside the macrocycle. The lowest energy complexes are shown in Fig. 4. All possible molecular geometries of different binding sites and their energies can be found in the ESI.†

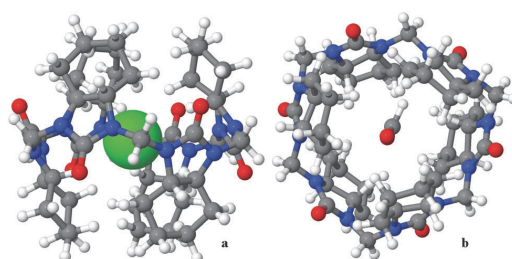


Fig. 4 Lowest energy complexes of cycHC[6] with anions Cl<sup>-</sup> (a) and HCOO<sup>-</sup> (b).

Table 2 Distances between the centre of the cavity, axis and selected atoms of non-complexed and complexed cycHC[6] with anions in Å. Cavity volumes are given without a guest in Å<sup>3</sup>

	Non-complexed cycHC[6]	cycHC[6] complexed with			
		Cl <sup>-</sup>	Br <sup>-</sup>	I <sup>-</sup>	HCOO <sup>-</sup>
$r(\text{H5}_{\text{ax}}-\text{Z})$	2.4	2.2	2.3	2.4	2.3–2.4 <sup>a</sup>
$r(\text{H7}_{\text{ax}}-\text{X})$	3.2	3.0	3.1	3.2	3.0–3.1
$r(\text{H4a}_{\text{ax}}-\text{X})$	3.2	3.0	3.0	3.1	3.0–3.2
$r(\text{C}_2-\text{X})$	4.4	4.5	4.5	4.5	4.4–4.5
Cavity volume	22	21	21	22	21

<sup>a</sup> Minimum and maximum distances are given due to the asymmetrical geometry of the complexes with this anion.

The shortest distances between inside-pointing axial hydrogens (H5<sub>ax</sub>, H7<sub>ax</sub>, H4a<sub>ax</sub>), carbonyl carbon (C<sub>2</sub>) and the centre of the cavity (X) and axis (Z) were measured to compare the geometries of anion complexed macrocycles and non-complexed macrocycles. The relevant distances  $r(\text{H5}_{\text{ax}}-\text{Z})$ ,  $r(\text{H7}_{\text{ax}}-\text{X})$ ,  $r(\text{H4a}_{\text{ax}}-\text{X})$  and  $r(\text{C}_2-\text{X})$  are given in Table 2.

All spherical halogen anions caused symmetrical changes in the geometry of cycHC[6], while the non-spherical formic acid anion led to deformation of the macrocycle. Upon adopting the anions inside the cavity of the macrocycle, the distance  $r(\text{C}_2-\text{X})$  increased, showing that the equator of the cycHC[6] had expanded slightly. At the same time, the distances between the inside-pointing hydrogens of the cyclohexyl rings and axis, as well as the centre of the cavity ( $r(\text{H5}_{\text{ax}}-\text{Z})$ ,  $r(\text{H7}_{\text{ax}}-\text{X})$ ,  $r(\text{H4a}_{\text{ax}}-\text{X})$ ) decreased, indicating that flexible cyclohexyl rings covered the anions, causing a slight shrinkage of the opening. The biggest changes in cavity size took place in the case of the chloride and the smallest with the iodine complex.

According to QTAIM analysis, halogen anions had 12 bonding interactions with the macrocycle. All halogen anions interacted with the same hydrogens (H4a<sub>ax</sub> and H7<sub>ax</sub>) of each monomer of the macrocycle. The calculated interaction energies were close to 5 kJ mol<sup>-1</sup> for both interacting hydrogens and similar for each halogen anion. The HCOO<sup>-</sup> ion interacted with the same hydrogen atoms, although the interaction energies showed large variability (3.0–14 kJ mol<sup>-1</sup>). Additionally, the HCOO<sup>-</sup> formed two extra bonding interactions between the formate hydrogen atom and two nitrogen atoms of different monomers of the macrocycle (H–N interactions (a) and (b) in Table 3).

**Table 3** Interaction and binding energies (kJ mol<sup>-1</sup>) of anions with cycHC[6]

	Cl <sup>-</sup>	Br <sup>-</sup>	I <sup>-</sup>	HCOO <sup>-</sup>
Average interaction energies	4.7	4.9	4.8	9.7 <sup>a</sup>
H-N (a)	—	—	—	7.3
H-N (b)	—	—	—	4.5
Sum of interaction energies	56.7	59.1	58.0	127.8
Binding energy	-102	-87	-65	-83

<sup>a</sup> The average interaction energy for HCOO<sup>-</sup> does not contain H-N energies.

The binding energies of the four anions with the host molecule were computed according to the reaction of cycHC[6] with anion X<sup>-</sup>, as shown below. The binding and interaction energies of anion complexes are listed in Table 3.



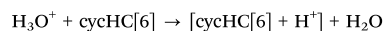
Despite the fact that formate had the highest interaction energy with cycHC[6] (127.8 kJ mol<sup>-1</sup>), the binding energy showed the strongest interaction with chloride (-102 kJ mol<sup>-1</sup>), in the gas phase, as chlorides fit best into the macrocycle. Distortion of the macrocycle geometry by the HCOO<sup>-</sup> ion partially cancelled the effect of the strong interactions by increasing tension in the macrocycle. In the case of halides, the interaction energies decreased with the increase in the size of the halide, which could have been caused by the repulsive force between the anion and heavy atoms of the macrocycle. These computational results agree well with the LUMO localization inside of the

non-complexed macrocycle and confirm that cycHC[6] forms inclusion complexes with halogen and formate anions.

In addition to binding energy, the transition states of ion insertion were studied as well. While Cl<sup>-</sup> and Br<sup>-</sup> insertion is spontaneous, the transition state energies for I<sup>-</sup> and HCOO<sup>-</sup> insertion are 22 kJ mol<sup>-1</sup> and 12 kJ mol<sup>-1</sup> respectively (Fig. 5). At the start of the ion insertion both anions were bound at the opening of the macrocycle. Energies of the corresponding local minima at the opening were higher than the global minima by 11 kJ mol<sup>-1</sup> for I<sup>-</sup> and 20 kJ mol<sup>-1</sup> for HCOO<sup>-</sup>, respectively. During the transition, anions moved along the Z axis, the cyclohexyl groups opened up: the  $r(\text{H5}_{\text{ax}}\text{-Z})$  increased from the value of 2.4 Å up to 3.6 Å. This indicates that the studied anions have low or no insertion barriers, which means that the formation of the inclusion complexes is favored.

### 3.3 Structure of cycHC[6] with a proton

The search for possible binding sites yielded six local minima for the proton. The lowest energy geometries with covalently bound protons are shown in Fig. 6. Energetically, the binding of the proton to the macrocycle was favoured for all local minima, as shown in Table 4. The binding energy of the proton with the cycHC[6] was computed according to the reaction of cycHC[6] with oxonium as shown below:



The results show that, in reaction with an oxonium ion, cycHC[6] is preferably protonated at the nitrogen N<sub>1</sub> atom

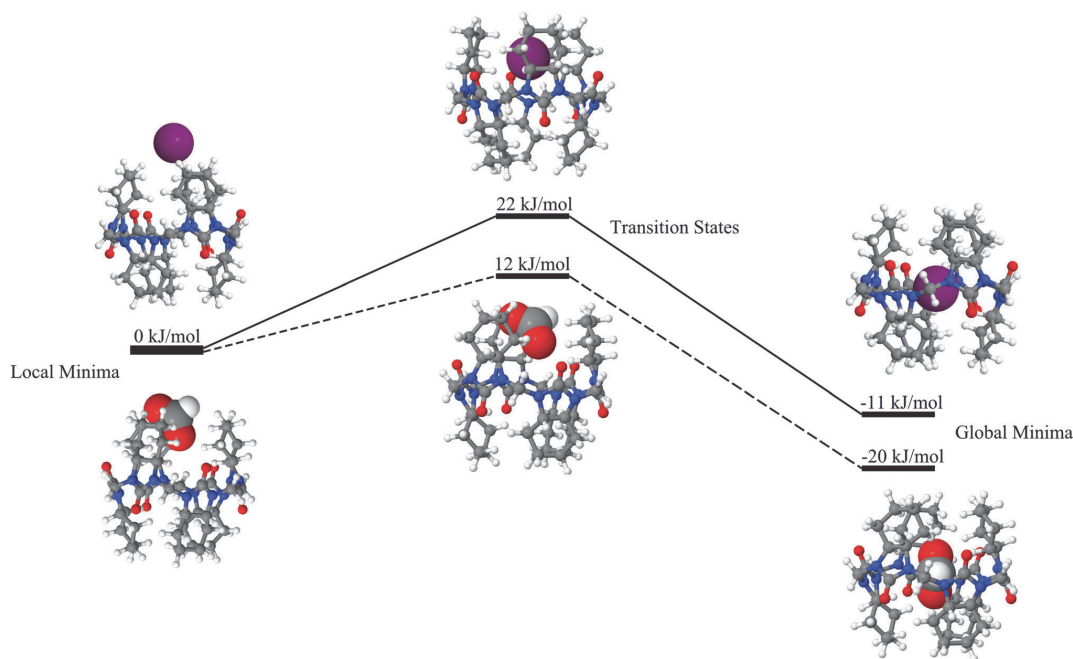


Fig. 5 Reaction coordinates of I<sup>-</sup> (solid line) and HCOO<sup>-</sup> (dashed line) forming inclusion complexes with cycHC[6].

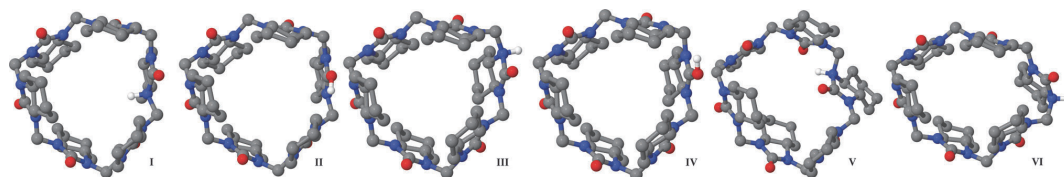


Fig. 6 Structures of protonated cycHC[6]. Hydrogen atoms (except the added proton) were removed.

positioned inside of the macrocycle. According to the Boltzmann distribution, the population of protonated geometry I will be over 90%. Favourable protonation sites were in good agreement with the analysis of the electronic structure of cycHC[6]. However, it should be noted that the binding of bulkier cations inside the cavity of the macrocycle is much less probable, due to the position and size of non-complexed cycHC[6] LUMO.

### 3.4 Structure of cycHC[6] with HCl, HBr, HI or HCOOH

The non-dissociated guests can bind both inside and outside of the macrocycle. Energetically, the outside binding sites were favoured for all guests. The inclusion complexes were at least  $14 \text{ kJ mol}^{-1}$  higher in energy. The representative energetically favored geometries of the complex with hydrogen chloride are shown in Fig. 7; the complexes with HBr, HI and HCOOH were similar. In contrast to the favourable binding site of the proton at the nitrogen of cycHC[6], there was binding of electron-poor hydrogens of non-dissociated acids at the oxygen atom of the macrocycle outside the cavity. This change in the preferred interaction site is most probably caused by steric factors. The binding energies of these complexes confirm that complexation with non-dissociated acids was energetically favourable in the studied conditions (Table 5). The binding energies

Table 4 Energies ( $\text{kJ mol}^{-1}$ ) of the protonation of cycHC[6]

Geometry nr	Protonation site of cycHC[6]	Energy difference from minima	Binding energy
I	At $N_1$ inside	0	-244
II	O	7	-238
III	At $N_3$ outside	9	-236
IV	O	11	-233
V	At $N_3$ inside	13	-232
VI	At $N_1$ outside	34	-211

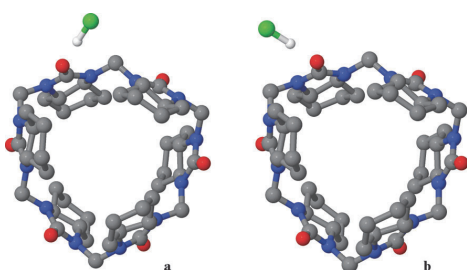
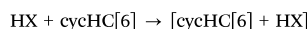


Fig. 7 Lowest energy geometries of cycHC[6] and HCl complexes.

Table 5 Binding energy ( $\text{kJ mol}^{-1}$ ) of the non-dissociated guests with cycHC[6]

Non-dissociated guest	Geometry	Energy difference from minima	Binding energy
HCl	a	0	-67
	b	2	-65
HBr	a	0	-26
	b	1	-25
HI	a	0	-31
	b	1	-30
HCOOH	a	5	-16
	b	0	-21

of the non-dissociated guests with cycHC[6] were computed according to the reaction shown below, where HX denotes the non-dissociated acid:



The results indicate that the cycHC[6] was able to bind the studied non-dissociated guests in the gas phase, although inclusion complexes were not formed.

### 3.5 Ion-mobility mass-spectrometric analysis of cycHC[6] ion complexes

The computationally obtained structures were verified *via* TWIM-MS spectroscopy. The collision cross-section (CCS) values measured by ion-mobility mass spectrometry and calculated from minimum energy conformers of  $\text{Cl}^-$ ,  $\text{Br}^-$  and  $\text{HCOO}^-$  anion complexes were found to agree with each other well (Table 6). The deviation of the calculated CCS from the experimental data was 2%, confirming that anions formed inclusion complexes with cycHC[6]. The lowest-energy protonated cycHC[6] theoretical CCS value also coincided with the experimental data. It should be noted that the CCS of the  $[\text{cycHC}[6] + \text{Na}]^+$  complex was significantly larger than all other ion CCS values, showing that sodium is positioned outside of the macrocycle.

Table 6 Collision cross section value of each *trans*-cycHC[6] complex

Complex	Experimental CCS ( $\text{\AA}^2$ )	Theoretical CCS ( $\text{\AA}^2$ )
$[\text{cycHC}[6] + \text{Cl}]^-$	182	185
$[\text{cycHC}[6] + \text{Br}]^-$	183	186
$[\text{cycHC}[6] + \text{HCOO}]^-$	183	187
$[\text{cycHC}[6] + \text{H}]^+$	194	197 <sup>a</sup>
$[\text{cycHC}[6] + \text{Na}]^+$	225	—

<sup>a</sup> For geometry I in Fig. 6.

## 4. Conclusions

The electronic structure of *trans*-cyclohexylhemicucurbit[6]uril and its complexes with ionic ( $\text{H}^+$ ,  $\text{Cl}^-$ ,  $\text{Br}^-$ ,  $\text{I}^-$  and  $\text{HCOO}^-$ ) and non-dissociated ( $\text{HCl}$ ,  $\text{HBr}$ ,  $\text{HI}$ ,  $\text{HCOOH}$ ) guests was studied. It was shown that cyclohexylhemicucurbituril had numerous possible binding sites for all guests. The conclusions based on our study *in vacuo* are as follows:

(i) Non-complexed cyclohexylhemicucurbituril exhibited  $D_3$  symmetry, and the computed geometry was in good agreement with the crystal structure. Calculations showed electron-rich areas on the oxygen atoms of each of the cyclohexylurea units, while the HOMO was located at the equator of the macrocycle. The largest lobes of the HOMO were on nitrogen atoms, pointing inside and outside the macrocycle. Electron-deficient areas were located on methylene bridges and the centres of cyclohexyl groups. The LUMO was concentrated inside the macrocycle, filling the cavity.

(ii) All of the studied anions favoured binding inside the macrocycle. QTAIM analysis showed that twelve bonding interactions existed between the macrocycle and halogen anions, and fourteen such interactions were found between the macrocycle and  $\text{HCOO}^-$ . The order of the binding preference of the studied anions was  $\text{Cl}^- > \text{Br}^- > \text{HCOO}^- > \text{I}^-$ . The formation of the inclusion complex of anions with cycHC[6] was also confirmed by ion-mobility mass-spectrometry.

(iii) The systematic search for a binding site for a proton resulted in six possible locations. In the lowest-energy geometry, the proton was attached inside of the macrocycle to the nitrogen atom. Proton binding in the reaction of cycHC[6] with oxonium cation was favourable by  $-244 \text{ kJ mol}^{-1}$ .

(iv) Non-dissociated acids preferred binding outside of the macrocycle through electron-poor hydrogens of the acids at the oxygen of cycHC[6]. There were two energetically close and structurally similar binding sites for all of the studied non-dissociated acids. According to the binding energy,  $-65 \text{ kJ mol}^{-1}$ , the strongest complex was formed with hydrogen chloride.

## Acknowledgements

This research was supported by the Estonian Science Foundation through Grant Nos 8255 and 8698 and the Tallinn University of Technology basic financing grant No. B25. The Estonian Ministry of Education and Research through Grants IUT19-32 and the EU European Regional Development Fund (3.2.0101.08-0017) also provided financial support. Computations were performed on the HPC cluster at Tallinn University of Technology, which is part of the ETAIS project. The authors thank Prof. Hugh I. Kim and Ms Hyun Hee Lee L. Lee at the Pohang University of Science and Technology, Korea, for IM-MS data and helpful discussions. The authors would also like to thank Dr Merle Uudsemaa at the Tallinn University of Technology for helpful discussions.

## Notes and references

- 1 R. Behrend, E. Meyer and F. Rusche, *Justus Liebigs Ann. Chem.*, 1905, **339**, 1–37.

- 2 W. A. Freeman, W. L. Mock and N.-Y. Shih, *J. Am. Chem. Soc.*, 1981, **103**, 7367–7368.
- 3 E. Masson, X. Ling, R. Joseph, L. Kyeremeh-Mensah and X. Lu, *RSC Adv.*, 2012, **2**, 1213–1247.
- 4 B. C. Pemberton, R. Raghunathan, S. Volla and J. Sivaguru, *Chemistry*, 2012, **18**, 12178–12190.
- 5 S. Walker, R. Oun, F. J. McInnes and N. J. Wheate, *Isr. J. Chem.*, 2011, **51**, 616–624.
- 6 Y. Miyahara, K. Goto, M. Oka and T. Inazu, *Angew. Chem., Int. Ed.*, 2004, **43**, 5019–5022.
- 7 Y. Li, L. Li, Y. Zhu, X. Meng and A. Wu, *Cryst. Growth Des.*, 2009, **9**, 4255–4257.
- 8 T. Fiala and V. Sindelar, *Synlett*, 2013, 2443–2445.
- 9 M. Lisbjerg, B. M. Jessen, B. Rasmussen, B. Nielsen, A. Ø. Madsen and M. Pittelkow, *Chem. Sci.*, 2014, **5**, 2591–2908.
- 10 R. Aav, E. Shmatova, I. Reile, M. Borissova, F. Topić and K. Rissanen, *Org. Lett.*, 2013, **15**, 3786–3789.
- 11 H. Cong, T. Yamato, X. Feng and Z. Tao, *J. Mol. Catal. A: Chem.*, 2012, **365**, 181–185.
- 12 H. Cong, T. Yamato and Z. Tao, *J. Mol. Catal. A: Chem.*, 2013, **379**, 287–293.
- 13 H. Cong, T. Yamato and Z. Tao, *New J. Chem.*, 2013, **37**, 3778–3783.
- 14 H.-J. Buschmann, E. Cleve and E. Schollmeyer, *Inorg. Chem. Commun.*, 2005, **8**, 125–127.
- 15 J. Svec, M. Necas and V. Sindelar, *Angew. Chem., Int. Ed.*, 2010, **49**, 2378–2381.
- 16 V. Havel, J. Svec, M. Wimmerova, M. Dusek, M. Pojarova and V. Sindelar, *Org. Lett.*, 2011, **13**, 4000–4003.
- 17 A. Révész, D. Schröder, J. Svec, M. Wimmerová and V. Sindelar, *J. Phys. Chem. A*, 2011, **115**, 11378–11386.
- 18 V. Havel, V. Sindelar, M. Necas and A. E. Kaifer, *Chem. Commun.*, 2014, **50**, 1372–1374.
- 19 K. S. Oh, J. Yoon and K. S. Kim, *J. Phys. Chem. B*, 2001, **105**, 9726–9731.
- 20 H. Cong, Q.-J. Zhu, H.-B. Hou, S.-F. Xue and Z. Tao, *Supramol. Chem.*, 2006, **18**, 523–528.
- 21 H. Cong, L.-L. Tao, Y.-H. Yu, Z. Tao, F. Yang, Y.-J. Zhao, S.-F. Xue, G. a. Lawrance and G. Wei, *J. Phys. Chem. A*, 2007, **111**, 2715–2721.
- 22 F. Pichierri, *Dalton Trans.*, 2013, **42**, 6083–6091.
- 23 M. Sundararajan, R. V. Solomon, S. K. Ghosh and P. Venuvanalingam, *RSC Adv.*, 2011, **1**, 1333–1341.
- 24 M. Sundararajan, V. Sinha, T. Bandyopadhyay and S. K. Ghosh, *J. Phys. Chem. A*, 2012, **116**, 4388–4395.
- 25 S. Pan, S. Mondal and P. K. Chattaraj, *New J. Chem.*, 2013, **37**, 2492–2499.
- 26 R. V. Pinjari and S. P. Gejji, *J. Phys. Chem. A*, 2008, **112**, 12679–12686.
- 27 R. V. Pinjari and S. P. Gejji, *J. Phys. Chem. A*, 2009, **113**, 1368–1376.
- 28 P. H. Dixit, R. V. Pinjari and S. P. Gejji, *J. Phys. Chem. A*, 2010, **114**, 10906–10916.
- 29 V. V. Gobre, R. V. Pinjari and S. P. Gejji, *J. Phys. Chem. A*, 2010, **114**, 4464–4470.

- 30 V. V. Gobre, P. H. Dixit, J. K. Khedkar and S. P. Gejji, *Comput. Theor. Chem.*, 2011, **976**, 76–82.
- 31 S. R. Peerannawar, V. V. Gobre and S. P. Gejji, *Comput. Theor. Chem.*, 2012, **983**, 16–24.
- 32 S. R. Peerannawar and S. P. Gejji, *J. Mol. Model.*, 2013, **19**, 5113–5127.
- 33 H. Cong, Y.-J. Zhao, S.-F. Xue, Z. Tao and Q.-J. Zhu, *J. Mol. Model.*, 2007, **13**, 1221–1226.
- 34 J. W. Lee, S. Samal, N. Selvapalam, H.-J. Kim and K. Kim, *Acc. Chem. Res.*, 2003, **36**, 621–630.
- 35 T. S. Choi, J. Y. Ko, S. W. Heo, Y. H. Ko, K. Kim and H. I. Kim, *J. Am. Soc. Mass Spectrom.*, 2012, **23**, 1786–1793.
- 36 D. H. Noh, S. J. C. Lee, J. W. Lee and H. I. Kim, *J. Am. Soc. Mass Spectrom.*, 2014, **25**, 410–421.
- 37 H.-J. Buschmann and A. Zielesny, *Comput. Theor. Chem.*, 2013, **1022**, 14–22.
- 38 H.-J. Buschmann, A. Zielesny and E. Schollmeyer, *J. Inclusion Phenom. Macrocyclic Chem.*, 2006, **54**, 181–185.
- 39 D.-D. Xiang, Q.-X. Geng, H. Cong, Z. Tao and T. Yamato, *Supramol. Chem.*, 2014, 1–8.
- 40 N. Guex and M. C. Peitsch, *Electrophoresis*, 1997, **18**, 2714–2723.
- 41 M. D. Hanwell, D. E. Curtis, D. C. Lonie, T. Vandermeersch, E. Zurek and G. R. Hutchison, *J. Cheminf.*, 2012, **4**, 1–17.
- 42 P. A. M. Dirac, *Proc. R. Soc. A*, 1929, **123**, 714–733.
- 43 J. C. Slater, *Phys. Rev.*, 1951, **81**, 385–390.
- 44 S. H. Vosko, L. Wilk and M. Nusair, *Can. J. Phys.*, 1980, **58**, 1200–1211.
- 45 A. D. Becke, *Phys. Rev. A: At., Mol., Opt. Phys.*, 1988, **38**, 3098–3100.
- 46 J. P. Perdew, *Phys. Rev. B: Condens. Matter Mater. Phys.*, 1986, **33**, 8822–8824.
- 47 F. Weigend and R. Ahlrichs, *Phys. Chem. Chem. Phys.*, 2005, **7**, 3297–3305.
- 48 P. Deglmann, K. May, F. Furche and R. Ahlrichs, *Chem. Phys. Lett.*, 2004, **384**, 103–107.
- 49 M. Sierka, A. Hogekamp and R. Ahlrichs, *J. Chem. Phys.*, 2003, **118**, 9136–9148.
- 50 K. Eichkorn, O. Treutler, H. Öhm, M. Häser and R. Ahlrichs, *Chem. Phys. Lett.*, 1995, **240**, 283–290.
- 51 K. Eichkorn, F. Weigend, O. Treutler and R. Ahlrichs, *Theor. Chem. Acc.*, 1997, **97**, 119–124.
- 52 K. A. Peterson, D. Figgen, E. Goll, H. Stoll and M. Dolg, *J. Chem. Phys.*, 2003, **119**, 11113–11123.
- 53 K. A. Peterson, B. C. Shepler, D. Figgen and H. Stoll, *J. Phys. Chem. A*, 2006, **110**, 13877–13883.
- 54 P. Taylor, S. F. Boys and F. Bernardi, *Mol. Phys.*, 1970, **19**, 553–566.
- 55 O. Treutler and R. Ahlrichs, *J. Chem. Phys.*, 1995, **102**, 346–354.
- 56 M. Von Arnim and R. Ahlrichs, *J. Comput. Chem.*, 1998, **19**, 1746–1757.
- 57 R. Ahlrichs, M. Bär, M. Häser, H. Horn and C. Kölmel, *Chem. Phys. Lett.*, 1989, **162**, 165–169.
- 58 K. Eichkorn, F. Weigend, O. Treutler and R. Ahlrichs, *Theor. Chem. Acc.*, 1997, **97**, 119–124.
- 59 M. J. Frisch, G. W. Trucks, H. B. Schlegel, G. E. Scuseria, M. A. Robb, J. C. Cheeseman, J. R. Montgomery, Jr., J. A. Vreven, T. Kudin, K. N. Burant, J. M. Millam, S. S. Iyengar, J. Tomasi, V. Barone, B. Mennucci, M. Cossi, G. Scalmani, N. Rega, G. A. Petersson, H. Nakatsuji, M. Hada, M. Ehara, K. Toyota, R. Fukuda, J. Hasegawa, M. Ishida, T. Nakajima, Y. Honda, O. Kitao, H. Nakai, M. Klene, X. Li, J. E. Knox, H. P. Hratchian, J. B. Cross, V. Bakken, C. Adamo, J. Jaramillo, R. Gomperts, R. E. Stratmann, O. Yazyev, A. J. Austin, R. Cammi, C. Pomelli, J. W. Ochterski, P. Y. Ayala, K. Morokuma, G. A. Voth, P. Salvador, V. G. Dannenberg, J. J. Zakrzewski, S. Dapprich, A. D. Daniels, M. C. Strain, O. Farkas, D. K. Malick, J. B. Rabuck, A. D. Raghavachari, K. Foresman, J. V. Ortiz, Q. Cui, A. G. Baboul, S. Clifford, J. Cioslowski, B. B. Stefanov, G. Liu, A. Liashenko, P. Piskorz, I. Komaromi, R. L. Martin, D. J. Fox, T. Keith, M. A. Al-Laham, C. Y. Peng, M. Nanayakkara, A. Challacombe, P. M. W. Gill, B. Johnson, W. Chen, M. W. Wong, C. Gonzalez and J. A. Pople, *Gaussian 09, Revision C.01*, Gaussian, Inc., Wallingford, CT, USA, 2004.
- 60 *Jmol: an open-source Java viewer for chemical structures in 3D*, <http://www.jmol.org/>, accessed February 2014.
- 61 U. Varetto, *Molekel version 5.4.0.8*, Swiss National Supercomputing Centre, Lugano, Switzerland, 2006.
- 62 R. F. W. Bader, *Atoms in Molecules: A Quantum Theory*, Oxford University Press, Oxford, United Kingdom, 1990.
- 63 T. Lu, *Multwfn version 3.2.1*, University of Science and Technology Beijing, Beijing, China, 2009.
- 64 E. Espinosa, E. Molins and C. Lecomte, *Chem. Phys. Lett.*, 1998, **285**, 170–173.
- 65 K. Thalassinou, M. Grabenauer, S. E. Slade, G. R. Hilton, M. T. Bowers and J. H. Scrivens, *Anal. Chem.*, 2009, **81**, 248–254.
- 66 [www.indiana.edu/~clemmer](http://www.indiana.edu/~clemmer), accessed December 2013.
- 67 R. S. Rowland and R. Taylor, *J. Phys. Chem.*, 1996, **100**, 7384–7391.
- 68 T. Wyttenbach, G. Von Helden, J. J. Batka and M. T. Bowers, *J. Am. Soc. Mass Spectrom.*, 1997, **8**, 275–282.

### Publication III

M. Fomitšenko, **E. Shmatova**, M. Öeren, I. Järving, R. Aav "New homologues of chiral cyclohexylhemicucurbit[*n*]urils" *Supramolecular Chemistry*, **2014**, *26*, 698–703.

Reprinted with permission from Taylor & Francis.



## New homologues of chiral cyclohexylhemicucurbit[*n*] jurils

Maria Fomitšenko, Elena Shmatova, Mario Öeren, Ivar Järving and Riina Aav\*

Department of Chemistry, Tallinn University of Technology, Akadeemia tee 15, 12618 Tallinn, Estonia

(Received 21 February 2014; accepted 16 May 2014)

The existence of new 7-, 8-, 9- and 10-membered homologues of chiral cyclohexylhemicucurbituril is reported. The barrel-shaped (*all-R*)-cyclohexylhemicucurbit[8]juril ((*all-R*)-cycHC[8]) was isolated and its complexes with anions were detected in negative ion mode MS. Here, 7-, 9- and 10-membered homologues were detected by HPLC–HRMS. Geometries of all reported macrocycles were calculated using quantum chemical methods, which showed that even-numbered homologues were barrel-shaped and odd-numbered homologues were asymmetrical barrel-shaped with unequal dimensions of the openings. The size of the ((*all-R*)-cycHC[8]) cavity was comparable to CB[8] and it probably can serve as a chiral host.

**Keywords:** hemicucurbiturils; cucurbiturils; chiral macrocycles; NMR; host–guest complex

### Introduction

Hemicucurbiturils are members of the cucurbituril (1) family, which has grown enormously in this century (2, 3). There are several homologues (4–6) of normal cucurbiturils and a wide variety of analogues (7–13). In general, glycoluril monomers in these macrocyclic compounds are joined together by two methylene bridges and form strong host–guest pairs with cationic ammonium compounds (3, 14, 15). In hemicucurbiturils, on the other hand, monomers are linked together via one bridge, causing a zigzag orientation of the urea functionalities (16–18). This structural change, compared with the normal cucurbiturils, drastically influences the electronic structure of macrocycles and allows complexation of anions inside the cavity (19, 20). The zigzag orientation of the single-bridged glycoluril monomers in bambusurils (21) exhibits similar anion binding properties (22–24). Presently, the ring sizes of cucurbituril family macrocycles range from 4-membered bambusurils (25) to 14-membered twisted normal cucurbituril (26). The most widely applied normal cucurbituril homologues have six to eight monomers joined together and the inner dimensions of these macrocycles allow for selective complexation of a large number of useful small molecules (2, 3, 14). Until now, only 6- and 12-membered hemicucurbiturils have been isolated. Ten years ago, Miyahara et al. (16) reported that, in strongly acidic conditions, ethyleneurea, in the presence of formalin, can selectively produce two homologues of unsubstituted hemicucurbiturils in very high yields. Hemicucurbit[6]juril (HC[6]) is formed in concentrated HCl at lower temperatures and hemicucurbit[12]juril (HC[12]) in diluted acid at higher temperatures (Figure 1). It has been shown that unsubstituted hemicucurbituril can catalyse organic

reactions (27–29). The structure of the first substituted hemicucurbituril – achiral *meso*-cyclohexylhemicucurbit[6]juril (*meso*-cycHC[6]) – was reported by Li et al. (17) and, due to introduced rigidity in the formed macrocycle, it required much harsher conditions than HC[6] for high-yielding synthesis. In the same conditions, its more rigid analogue, norbornahemicucurbit[6]juril (norHC[6]), was formed in significantly lower yield (30). Together with norHC[6], traces of 4-, 5-, 7- and 8-membered norbornahemicucurbiturils were detected by mass-spectrometric analysis (30). The only presently known chiral analogue of substituted hemicucurbiturils, (*all-S*) or (*all-R*)-cyclohexylhemicucurbit[6]juril (*chiral*-cycHC[6]) (18), has cyclohexyl and urea cycles joined in *trans*-fashion. High-yielding synthesis of the latter required a much longer (24 h) reaction time at the same temperature, compared with other substituted hemicucurbiturils (Figure 1).

In this paper, we report the isolation of a new chiral homologue of substituted hemicucurbituril, enantiomerically pure (*all-R*)-cyclohexylhemicucurbit[8]juril ((*all-R*)-cycHC[8]) and analytical evidence of the existence of its 7-, 9- and 10-membered homologues ((*all-R*)-cycHC[7], (*all-R*)-cycHC[9] and (*all-R*)-cycHC[10]). The calculated geometries of all reported macrocycles are also presented.

### Results and discussion

The formation of hemicucurbiturils occurs as a result of a polymerisation reaction; therefore, in addition to the most favourable 6-membered macrocycles, the existence of homologues was expected. A reaction mixture of previously reported (*all-R*)-cycHC[6] was carefully examined by reverse-phase (RP)-HPLC–MS analysis, and 7-, 8-,

\*Corresponding author. Email: [riina@chemnet.ee](mailto:riina@chemnet.ee)

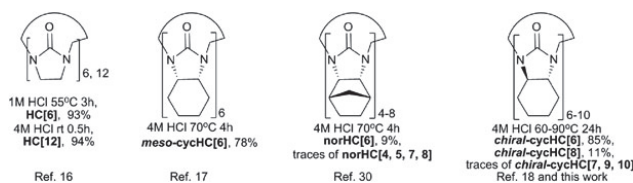


Figure 1. Hemicucurbit[*n*]urils structures and reaction conditions for their synthesis from Refs (16–18, 30) and this work.

9- and 10-membered homologues of (*all-R*)-cycHC[6] were found. A chromatogram of cycHC[6–10] is shown in Figure 2, in which peaks were detected by ultraviolet (UV) light and positive ion mode high-resolution mass spectrometry. The order of homologue elution in RP column was cycHC[9], cycHC[8] and cycHC[7] as one cluster, followed by cycHC[6] and cycHC[10] further apart from each other. The elution order shows that 10- and 6-membered homologues were less polar than their 7-, 8- and 9-membered homologues.

Preliminary attempts were made to increase the degree of formation of higher homologues, by varying the reaction temperature of cyclisation between 60 and 90°C. According to the <sup>1</sup>H NMR analysis, cycHC[6] still remained the main product in all reactions performed in 4 M HCl solution and the reaction temperature did not influence significantly the content of crude product. Additional study is necessary to find out conditions that could drive macrocyclisation towards formation of higher homologues. Nevertheless, the purification of crude product by RP flash chromatography afforded (*all-R*)-cycHC[8] in 11% yield. NMR spectra of (*all-R*)-cycHC[8] showed high symmetry; therefore, signals belonging to all monomers of the macrocycle were identical, adopting the same averaged conformation as in the case of *chiral*-cycHC[6] (18). The chemical shifts of relevant atoms of *chiral*-cycHC[6] and (*all-R*)-cycHC[8] were distinguishable and their assignment is presented in Figure 3.

NMR observations are in good agreement with the calculated geometry of (*all-R*)-cycHC[8] (Figure 4).

The equatorial belt of the macrocycle adopted a square-like shape, having methylene bridges with carbon number C9 on the corners of the macrocycle. Carbon C9 is situated between the stereogenic carbons C2, in which protons H(in) point inside the cavity. According to the optimised structure, all cyclohexyl rings were in chair conformation, which was also supported by the high value of <sup>3</sup>*J*<sub>(HH)</sub>-coupling constants (> 11 Hz) between the cyclohexyl axial protons. Monomers were in zigzag orientation and cyclohexyl rings leaned slightly over the opening, as in the case of cycHC[6]. The diameter of (*all-R*)-cycHC[8] opening was 4.6 Å, which is within the corresponding values of normal cucurbiturils (31) CB[6] (3.9 Å) and CB[7] (5.4 Å). The cavity diameter at the equator of cycHC[8] macrocycle was 8.5 Å, which is comparable to the 8.8 Å of the CB[8] cavity size. (*all-R*)-cycHC[8] had a barrel shape as do normal cucurbiturils, and its cavity dimensions were comparable to the most widely applied normal cucurbiturils. In the negative ion mode of MS analysis, complexes of (*all-R*)-cycHC[8] with chloride and formate anions were detected, confirming that the new substituted hemicucurbituril can bind anions as do other zigzag-oriented cucurbituril family members.

To get a better understanding of the structures of other existing chiral cyclohexylhemicucurbiturils, geometries of

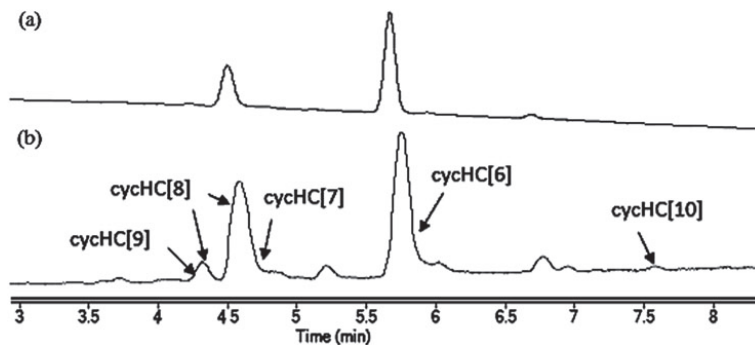


Figure 2. RP-HPLC–MS chromatograms of (*all-R*)-cycHC[9], (*all-R*)-cycHC[8], (*all-R*)-cycHC[7], (*all-R*)-cycHC[6] and (*all-R*)-cycHC[10] (a) detected by UV at 210 nm and (b) detected by (+)ESI-MS.

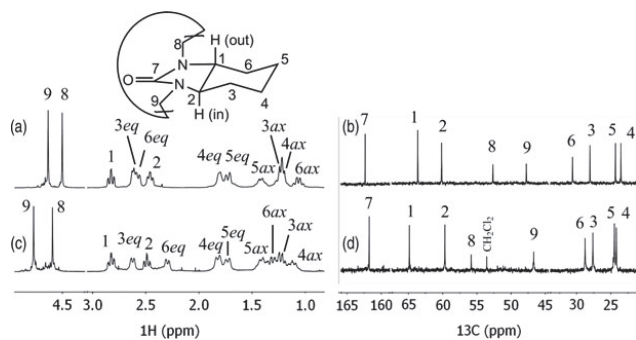


Figure 3. Assigned  $^1\text{H}$  and  $^{13}\text{C}$  NMR spectra of (a), (b) *chiral*-cycHC[6] and (c), (d) (*all-R*)-cycHC[8], respectively.

7-, 9- and 10-membered homologues were also calculated (Figure 5).

Macrocycles with odd numbers of monomers (cycHC[7], cycHC[9]) still formed almost barrel-like shapes. Cyclohexyl rings of zigzag-oriented monomers leaned over the openings, but two aligned urea cycles distorted the symmetry of the macrocycle, leading to two different sized openings (Table 1). The 10-membered homologue was a symmetrical five-cornered barrel. In 7-, 9- and 10-membered macrocycles, the cyclohexyl rings adopted both twisted and chair conformations. The dimensions describing the sizes of the cavities of the chiral hemicucurbiturils are outlined in Table 1.

## Conclusions

As a result of RP liquid chromatography of the crude product of previously known *chiral*-cycHC[6], new 7-, 8-, 9- and 10-membered homologues of chiral cyclohexylhemicucurbituril were found. The barrel-shaped (*all-R*)-cyclohexylhemicucurbit[8]uril was isolated and

its complexes with anions were detected in negative ion mode MS. Here, 7-, 9- and 10-membered homologues were detected by HPLC–HRMS. The geometries of all reported macrocycles were calculated using the density functional theory, which showed that even-numbered homologues were barrel-shaped and odd-numbered homologues were asymmetrical barrel-shaped with unequal dimensions of the openings. The isolated (*all-R*)-cycHC[8] was more polar than its 6-membered homologue. The cavity of (*all-R*)-cycHC[8] was comparable with CB[7] and CB[8]; therefore, it probably will serve as a chiral host for anions of small molecules.

## Experimental section

### General

All used instruments are located at Tallinn University of Technology, Department of Chemistry. RP-HPLC-MS was performed on an Agilent 6540 UHD Accurate-Mass Q-TOF LC/MS spectrometer (Agilent Technologies, Santa Clara, CA, USA) with AJ-ESI ionisation and a Zorbax

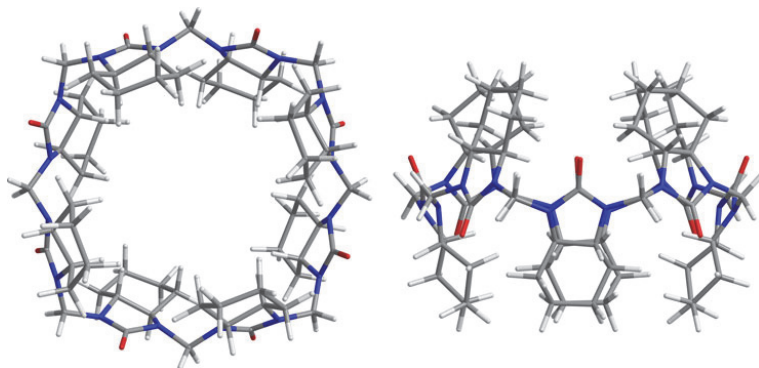


Figure 4. (Colour online) Calculated structures of (*all-R*)-cycHC[8].

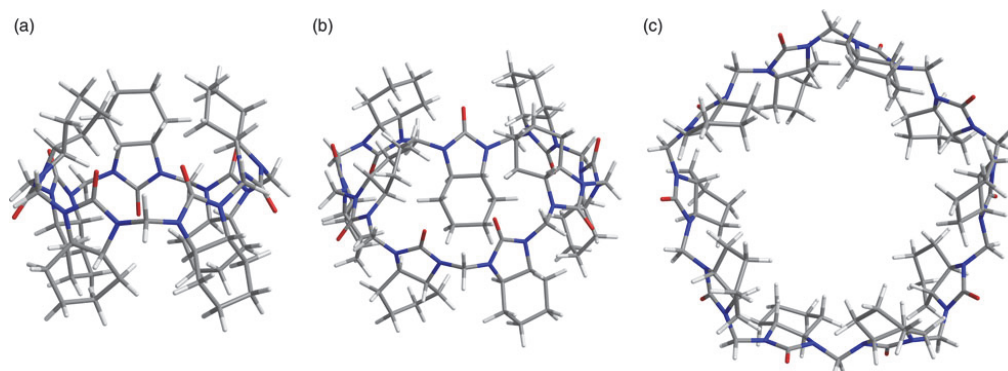


Figure 5. (Colour online) Calculated structures of (a) (*all-R*)-cycHC[7], (b) (*all-R*)-cycHC[9] and (c) (*all-R*)-cycHC[10].

Eclipse Plus C18 column (2.1 mm × 150 mm, 1.8 μm) and is reported as *m/z* ratios. RP flash column chromatography was performed on a Biotage Isolera™ Prime purification system using a Biotage SNAP KP-C18-HS Cartridge (60 g, 50 μm) (Biotage®, Uppsala, Sweden). NMR spectra were recorded using a Bruker Avance III 400 MHz spectrometer (Bruker BioSpin GmbH, Rheinstetten, Germany), and chemical shifts are referenced in carbon spectrum by CDCl<sub>3</sub> at 77.16 ppm and proton spectrum by CDCl<sub>3</sub> at 7.26 ppm. Infrared (IR) spectra were obtained on a Bruker Tensor 27 FT-IR spectrometer (Bruker Optik GmbH, Ettlingen, Germany) and are reported in wave numbers. The intensities of the peaks are reported using the following abbreviations: s: strong, m: medium and w: weak. Optical rotation was measured using an Anton Paar MCP 500 polarimeter (Anton Paar GmbH, Graz, Austria). The melting point was detected using a Nagema melting point microscope.

### Experimental procedures

Synthesis of (*all-R*)-cyclohexylhemicurbiturils was performed as described in an earlier publication (18), except for varying the temperature between 60 and 90°C.

An RP-HPLC-MS analysis of 1 mg/mL crude sample in 0.1% formic acid in acetonitrile was performed using a 10-min gradient from 70% to 100% of eluent A, which was acetonitrile, and eluent B was a 0.1% formic acid aqueous solution. The flow rate was set at 0.4 mL/min and the UV detection at 210 nm. Mass-to-charge ratios were measured using ESI-Q-TOF MS.

RP flash chromatography was performed with 200 mg of crude product (18), which was dissolved in 1 ml of formic acid before loading it into the column. The sample was purified using gradient from 50% to 100% of eluent A with the same eluents as described in the HPLC conditions. The flow rate was adjusted to 40 ml/min, and the sample detection was measured at 210 nm. Here, 22 mg of cycHC[8] was obtained in 11% yield.

### Characterisation data

Compound (*all-R*)-cycHC[8]: It is a white solid (22 mg, 0.018 mmol, yield 11%). Mp = 245–250°C (dec). IR (KBr, cm<sup>-1</sup>) 3502 w, 2936 m, 2858 m, 1711 s, 1435 m, 1359 s, 1332 m, 1232 s, 1134 w, 1058 w, 1014 w, 988 w, 919 w, 830 w, 774 m, 667 w, 628 w, 532 w, 516 w, 476 w. <sup>1</sup>H NMR (400 MHz, CDCl<sub>3</sub>) δ = 1.18–1.05 (m, H<sub>4ax</sub>, 1H), 1.23 (qd, H<sub>3ax</sub>, *J* = 11.0, 2.9, 1H), 1.29 (qd, H<sub>6ax</sub>,

Table 1. Dimensions<sup>a</sup> of (*all-R*)-cyclohexylhemicurbit[6–10]urils in Å.

	cycHC[6] <sup>b</sup>	cycHC[7] <sup>c</sup>	cycHC[8] <sup>c</sup>	cycHC[9] <sup>c</sup>	cycHC[10] <sup>c</sup>
Diameter at the opening	2.2	2.3 4.2	4.6	4.9 7.3	6.6
Diameter at the equator of the cavity	5.3	6.8	8.5	9.8	11.5
Height	12.1	12.8	12.5	12.7	12.4

<sup>a</sup>Taking van der Waals radii into account.

<sup>b</sup>From Ref. (18).

<sup>c</sup>From calculated structures.

$J = 11.3, 3.3, 1\text{H}$ ), 1.47–1.35 (m, **H5ax**, 1H), 1.73 (bd, **H5eq**,  $J = 12.7, 1\text{H}$ ), 1.82 (bd, **H4eq**,  $J = 12.5, 1\text{H}$ ), 2.30 (dd,  $J = 11.5, 2.7$ , **H6eq**, 1H), 2.49 (td,  $J = 11.0, 2.9$ , **H2** (in), 1H), 2.62 (dd,  $J = 11.6, 2.7$ , **H3eq**, 1H), 2.83 (td,  $J = 11.1, 3.1$ , **H1**(out), 1H), 4.59 (s, **H8**, 8H), 4.77 (s, **H9**, 8H).  $^{13}\text{C}$  NMR (101 MHz,  $\text{CDCl}_3$ )  $\delta = 161.77$  (C7), 64.86 (C1), 59.68 (C2), 55.83 (C8), 46.69 (C9), 28.76 (C6), 27.63 (C3), 24.48 (C5), 24.19 (C4). HRMS (ESI +): calculated for  $(\text{C}_{64}\text{H}_{97}\text{N}_{16}\text{O}_8)^+$   $[\text{M} + \text{H}]^+$  1217.7670, found 1217.7670. HRMS (ESI -): calculated for  $(\text{C}_{65}\text{H}_{97}\text{N}_{16}\text{O}_{10})$   $[\text{M} + \text{HCOO}]$  1261.7579, found 1261.7607. HRMS: calculated for  $\text{C}_{64}\text{H}_{96}\text{N}_{16}\text{O}_8\text{Cl}$   $[\text{M} + \text{Cl}]$  1251.7291, found 1251.7283.  $[\alpha]_{\text{D}}^{25} = 60^\circ$  (c 0.62,  $\text{CDCl}_3/\text{CHCl}_3$ ).

Compound (*all-R*)-cycHC[7]: HRMS (ESI +): calculated for  $(\text{C}_{56}\text{H}_{85}\text{N}_{14}\text{O}_7)^+$   $[\text{M} + \text{H}]^+$  1065.6720, found 1065.6720. HRMS (ESI -): calculated for  $(\text{C}_{57}\text{H}_{85}\text{N}_{14}\text{O}_9)$   $[\text{M} + \text{HCOO}]$  1109.6341, found 1109.6621.

Compound (*all-R*)-cycHC[9]: HRMS (ESI +): calculated for  $(\text{C}_{72}\text{H}_{109}\text{N}_{18}\text{O}_9)^+$   $[\text{M} + \text{H}]^+$  1369.8619, found 1369.8621. HRMS (ESI -): calculated for  $(\text{C}_{73}\text{H}_{109}\text{N}_{18}\text{O}_{11})$   $[\text{M} + \text{HCOO}]$  1413.8529, found 1413.8490.

Compound (*all-R*)-cycHC[10]: HRMS (ESI +): calculated for  $(\text{C}_{80}\text{H}_{121}\text{N}_{20}\text{O}_{10})^+$   $[\text{M} + \text{H}]^+$  1521.9569, found 1521.9551.

### Calculation studies

All structures were built and optimised on an MMFF94 (32) level of theory, using the programme Avogadro (33). Further geometry optimisations were conducted using density functional theory, combining BP86 (34–38) functional with a def2-SV(P) (39) basis set. Density functional theory calculations were performed with the program package Turbomole 6.4 (40).

The dimensions of (*all-R*)-cyclohexylhemicucurbiturils were measured using the lengths from the chosen atoms to the centre of the opening or to the centre of the cavity. For the opening, a hydrogen atom closest to the centre was chosen from each monomer. For the cavity, the carbonyl carbon of each monomer was chosen. Next, the average radius for both atom sets was found. For both dimensions, the Van der Waals radius was subtracted from the average radius and the diameter was obtained by multiplying the radius by two. The centre points were arithmetic averages of the Cartesian coordinates of chosen atom sets. Heights are distances between opening centres, positioned closest to the edge with two added Van der Waals radii of the hydrogens.

### Funding

This work was supported by Estonian Science Foundation [grant number 8698], Tallinn University of Technology base financing

[grant number B25], the Ministry of Education and Research [grant numbers IUT19-32, IUT19-9] and the EU European Regional Development Fund [grant number 3.2.0101.08-0017].

### Supplementary data

Supplementary data for this article can be accessed at <http://dx.doi.org/10.1080/10610278.2014.926362>.

### References

- Freeman, W.A.; Mock, W.L.; Shih, N.-Y. *J. Am. Chem. Soc.* **1981**, *103*, 7367–7368.
- Isaacs, L. *Chem. Commun.* **2009**, *6*, 619–629.
- Lagona, J.; Mukhopadhyay, P.; Chakrabarti, S.; Isaacs, L. *Angew. Chem. Int. Ed.* **2005**, *44*, 4844–4870.
- Day, A.; Arnold, A.P.; Blanch, R.J.; Snushall, B. *J. Org. Chem.* **2001**, *66*, 8094–8100.
- Kim, J.; Jung, I.-S.; Kim, S.-Y.; Lee, E.; Kang, J.-K.; Sakamoto, S.; Yamaguchi, K.; Kim, K. *J. Am. Chem. Soc.* **2000**, *122*, 540–541.
- Day, A.I.; Blanch, R.J.; Arnold, A.P.; Lorenzo, S.; Lewis, G.R.; Dance, I. *Angew. Chem. Int. Ed.* **2002**, *41*, 275–277.
- Lagona, J.; Fettingler, J.C.; Isaacs, L. *Org. Lett.* **2003**, *5*, 3745–3747.
- Flinn, A.; Hough, G.C.; Stoddart, J.F.; Williams, D. *J. Angew. Chem.* **1992**, *31*, 1475–1477.
- Isobe, H.; Sato, S.; Nakamura, E. *Org. Lett.* **2002**, *4*, 1287–1289.
- Zhao, Y.J.; Xue, S.F.; Zhu, Q.J.; Tao, Z.; Zhang, J.X.; Wei, Z.B.; Long, L.S.; Hu, M.L.; Xiao, H.P.; Day, A.I. *Chin. Sci. Bull.* **2004**, *49*, 1111–1116.
- Zhao, J.; Kim, H.-J.; Oh, J.; Kim, S.-Y.; Lee, J.W.; Sakamoto, S.; Yamaguchi, K.; Kim, K. *Angew. Chem. Int. Ed.* **2001**, *40*, 4233–4235.
- Lucas, D.; Minami, T.; Iannuzzi, G.; Cao, L.; Wittenberg, J. B.; Anzenbacher, Jr, P.; Isaacs, L. *J. Am. Chem. Soc.* **2011**, *133*, 17966–17976.
- Ma, D.; Zavalij, P.Y.; Isaacs, L. *J. Org. Chem.* **2010**, *75*, 4786–4795.
- Masson, E.; Ling, X.; Joseph, R.; Kyeremeh-Mensah, L.; Lu, X. *RSC Adv.* **2012**, *2*, 1213–1247.
- Chernikova, E.Yu.; Fedorov, Yu.V.; Fedorova, O.A. *Russ. Chem. Bull. Int. Ed.* **2012**, *61*, 1363–1390.
- Miyahara, Y.; Goto, K.; Oka, M.; Inazu, T. *Angew. Chem. Int. Ed.* **2004**, *43*, 5019–5022.
- Li, Y.; Lin, L.; Zhu, Y.; Meng, X.; Wu, A. *Cryst. Growth Des.* **2009**, *9*, 4255–4257.
- Aav, R.; Shmatova, E.; Reile, I.; Borissova, M.; Topic, F.; Rissanen, K. *Org. Lett.* **2013**, *15*, 3786–3789.
- Buschmann, H.-J.; Cleva, E.; Schollmeyer, E. *Inorg. Chem. Commun.* **2005**, *8*, 125–127.
- Buschmann, H.-J.; Zielesny, A.; Schollmeyer, E. *J. Incl. Phenom. Macrocyc. Chem.* **2006**, *54*, 181–185.
- Svec, J.; Necas, M.; Sindelar, V. *Angew. Chem. Int. Ed.* **2010**, *49*, 2378–2381.
- Svec, J.; Dusek, M.; Fejfarova, K.; Stacko, P.; Klán, P.; Kaifer, A.E.; Li, W.; Hudeckova, E.; Sindelar, V. *Chem. Eur. J.* **2011**, *17*, 5605–5612.
- Havel, V.; Sindelar, V.; Necas, M.; Kaifer, A.E. *Chem. Commun.* **2014**, *50*, 1372–1374.
- Révész, Á.; Schröder, D.; Svec, J.; Wimmerov, M.; Sindelar, V. *J. Phys. Chem. A* **2011**, *115*, 11378–11386.
- Havel, V.; Svec, J.; Wimmerova, M.; Dusek, M.; Pojarova, M.; Sindelar, V. *Org. Lett.* **2011**, *13*, 4000–4003.

- (26) Cheng, X.-J.; Liang, L.-L.; Chen, K.; Ji, N.-N.; Xiao, X.; Zhang, J.-X.; Zhang, Y.-Q.; Xue, S.-F.; Zhu, Q.-J.; Ni, X.-L.; et al. *Angew. Chem. Int. Ed.* **2013**, *52*, 7252–7255.
- (27) Cong, H.; Yamato, T.; Feng, X. *J. Mol. Catal. A Chem.* **2012**, 181–185.
- (28) Cong, H.; Yamato, T.; Zhu Tao *J. Mol. Catal. A Chem.* **2013**, 287–293.
- (29) Cong, H.; Yamato, T.; Zhu Tao *New J. Chem.* **2013**, *37*, 3778–3783.
- (30) Fiala, T.; Sindelar, V. *Synlett* **2013**, *24*, 2443–2445.
- (31) Lee, J.W.; Samal, S.; Selvapalam, N.; Kim, H.-J.; Kim, K. *Acc. Chem. Res.* **2003**, *36*, 621–630.
- (32) Halgren, T.A. *J. Comput. Chem.* **1998**, *17*, 490–519.
- (33) Hanwell, M.D.; Curtis, D.E.; Lonie, D.C.; Vandermeersch, T.; Zurek, E.; Hutchison, G.R. *J. Cheminform.* **2012**, *4* (1), 17–33.
- (34) Dirac, P.A.M. *Proc. Roy. Soc. (Lond.) A* **1929**, *123*, 714–733.
- (35) Slater, J.C. *Phys. Rev.* **1951**, *81*, 385–390.
- (36) Vosko, S.H.; Wilk, L.; Nusair, M.; *Can J. Phys.* **1980**, *58*, 1200–1211.
- (37) Becke, A.D. *Phys. Rev. A* **1988**, *38*, 3098–3100.
- (38) Perdew, J.P. *Phys. Rev. B* **1986**, *33*, 8822–8824.
- (39) Weigend, F.; Ahlrichs, R. *Phys. Chem. Chem. Phys.* **2005**, *7*, 3297–3305.
- (40) Ahlrichs, R.; Bär, M.; Häser, M.; Horn, H.; Kölmel, C. *Chem. Phys. Lett.* **1989**, *162*, 165–169.

#### Publication IV

**E. Prigorchenko**, M. Öeren, S. Kaabel, M. Fomitšenko, I. Reile, I Järving, T. Tamm, F. Topić, K. Rissanen, R. Aav "Template-controlled synthesis of chiral cyclohexylhemicucurbit[8]uril" *Chemical Communications*, **2016**, 51, 10921–10924.

Reprinted with permission from Royal Society of Chemistry.



Cite this: *Chem. Commun.*, 2015, 51, 10921Received 18th May 2015,  
Accepted 3rd June 2015

DOI: 10.1039/c5cc04101e

www.rsc.org/chemcomm

## Template-controlled synthesis of chiral cyclohexylhemicucurbit[8]uril†

E. Prigorchenko,<sup>a</sup> M. Öeren,<sup>a</sup> S. Kaabel,<sup>a</sup> M. Fomitšenko,<sup>a</sup> I. Reile,<sup>b</sup> I. Järving,<sup>a</sup> T. Tamm,<sup>a</sup> F. Topić,<sup>c</sup> K. Rissanen<sup>c</sup> and R. Aav\*<sup>a</sup>

Enantiomerically pure cyclohexylhemicucurbit[8]uril (cycHC[8]), possessing a barrel-shaped cavity, has been prepared in high yield on a gram scale from either (*R,R,N,N'*)-cyclohex-1,2-diyurea and formaldehyde or cycHC[6]. In either case, a dynamic covalent library is first generated from which the desired cycHC can be amplified using a suitable anion template.

Research on new and selective host–guest systems and their applications is currently progressing very quickly.<sup>1</sup> Along with the search for new selective host–guest pairs, new and more efficient synthesis methods for hosts are being developed. Based on the recent success in the field of reversible non-covalent interactions in supramolecular chemistry,<sup>2</sup> the concept of dynamic covalent chemistry (DCC) has been established.<sup>3</sup> Controlling covalent bond formation by non-covalent interactions can serve as an excellent tool for developing efficient adaptive systems, where the formation of the host molecule is based on the structure of the guest.

Cucurbit[*n*]urils<sup>4</sup> (CB) are non-toxic host molecules<sup>5</sup> with a wide range of applications.<sup>1a,d,6</sup> Mechanistic studies have shown that the formation of oligomers and larger CBs proceeds reversibly, indicating that the principles of DCC are applicable in CB chemistry.<sup>7</sup> Hemicucurbiturils<sup>8</sup> (HC) are a sub-group of the cucurbituril family (Fig. 1). HCs are known to form complexes with anions<sup>9</sup> and unsubstituted HCs have been applied as catalysts in organic reactions.<sup>10</sup> It has been shown that biotin[6]uril esters can be applied as transmembrane anion carriers.<sup>9c</sup> Miyahara *et al.*<sup>9a</sup> were the first to describe an efficient synthesis of HC[6] and HC[12].

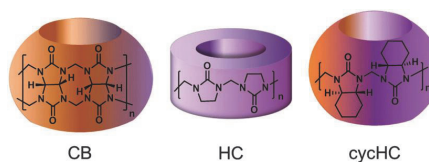


Fig. 1 Generalized shapes of normal CB, HC and chiral cycHC.

High selectivity towards the HC[6] was explained by the template effect of the chloride anion, which was recently confirmed in a biotin[6]uril synthesis.<sup>9f</sup> The halogen anion is also the necessary template in the synthesis of bambus[6]urils (BU),<sup>11</sup> which can be classified as substituted HCs. Presently, besides HC[12], only 6-membered HCs<sup>8</sup> and 4- and 6-membered BUs<sup>11</sup> have been isolated as main products. Until now, there has not been an efficient synthetic method available for the synthesis of 8-membered HCs. The existence of norbornahemicucurbit[8]uril<sup>8d</sup> has been detected only by mass-spectrometry and (all-*R*)-cyclohexylhemicucurbit[8]uril (cycHC[8]) has only been isolated as a by-product in low yield.<sup>8c</sup>

Herein we report an efficient synthesis of enantiomerically pure cycHC[8], starting either from its homologue cycHC[6] or (*R,R,N,N'*)-cyclohex-1,2-diyurea **1a** and paraformaldehyde. A mechanism of the transformation of cycHC[6] to cycHC[8] is proposed and proof of complexation with carboxylic acids is presented.

CycHC[6] was synthesized earlier in our group.<sup>8c</sup> Subsequently, a small amount of its homologue cycHC[8]<sup>8c</sup> was isolated from the crude product of cycHC[6]. Moreover, we noticed that in the chromatographic sample of cycHC[6] containing formic acid the amount of cycHC[8] gradually increased over time. The screening of reaction conditions for this conversion showed that cycHC[6] was transformed to cycHC[8] in the presence of sulphuric, formic and trifluoroacetic acid, but not acetic acid (S4, ESI†). The conversion of cycHC[6] to cycHC[8] by trifluoroacetic acid catalysis is approximately ten times faster than by formic acid (Table 1, entries 1 and 2). Nevertheless, the isolated yield of cycHC[8] was in both cases 71% in gram scale.

<sup>a</sup> Department of Chemistry, Tallinn University of Technology, Akadeemia tee 15, 12618 Tallinn, Estonia. E-mail: riina.aav@ttu.ee

<sup>b</sup> National Institute of Chemical Physics and Biophysics, Akadeemia tee 23, 12618 Tallinn, Estonia

<sup>c</sup> University of Jyväskylä, Department of Chemistry, Nanoscience Center, P.O. Box 3, FI-40014 Jyväskylä, Finland

† Electronic supplementary information (ESI) available: A detailed description of synthesis, MS, NMR, crystallographic and computational details. CCDC 1053111. For ESI and crystallographic data in CIF or other electronic format see DOI: 10.1039/c5cc04101e

Table 1 Selected reaction conditions and the list of templates for cycHC synthesis

No.	Starting comp.	(Additive)/acid/solvent <sup>a</sup>	Template	Time (h), T	Ratio <sup>b</sup> of cycHC[8] to cycHC[6]	Product	Isolated yield of product (%)
1	cycHC[6]	HCOOH/CH <sub>3</sub> CN	HCO <sub>2</sub> <sup>-</sup>	24, rt	92:8	cycHC[8]	71
2	cycHC[6]	CF <sub>3</sub> COOH/CH <sub>3</sub> CN	CF <sub>3</sub> CO <sub>2</sub> <sup>-</sup>	1.5, rt	95:5	cycHC[8]	71
3	cycHC[6]	NaPF <sub>6</sub> (50 eq.)/CH <sub>3</sub> COOH/CH <sub>3</sub> CN	PF <sub>6</sub> <sup>-</sup>	24, rt	99:1	cycHC[8]	90
4	1a	HCOOH/CH <sub>3</sub> CN	HCO <sub>2</sub> <sup>-</sup>	24, rt	92:8	cycHC[8]	7
5	1a	NaPF <sub>6</sub> (50 eq.)/CH <sub>3</sub> COOH/CH <sub>3</sub> CN	PF <sub>6</sub> <sup>-</sup>	24, rt	95:5	cycHC[8]	55
6	1a	CF <sub>3</sub> COOH/CH <sub>3</sub> CN	CF <sub>3</sub> CO <sub>2</sub> <sup>-</sup>	2, rt	96:4	cycHC[8]	73
7 <sup>c</sup>	1a	HCl/H <sub>2</sub> O	Cl <sup>-</sup>	24, 70 °C	0:100	cycHC[6] + HCl	85
8	cycHC[8]	HCl/H <sub>2</sub> O	Cl <sup>-</sup>	24, 70 °C	5:95	cycHC[6] + HCl	71
9	cycHC[8]	NaCl (50 eq.)/CH <sub>3</sub> COOH	Cl <sup>-</sup>	24, 70 °C	40:60	cycHC[6] + HCl	21

<sup>a</sup> Generally 300 eq. of organic acid or 4 M HCl were used. <sup>b</sup> Determined by HPLC. <sup>c</sup> Described previously in ref. 8c.

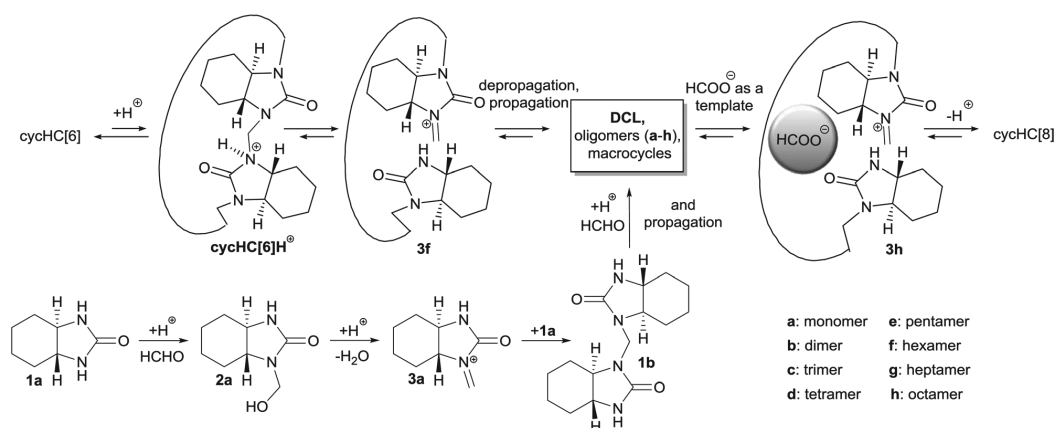
The kinetic data for the conversion of cycHC[6] to cycHC[8] revealed that the overall reaction was pseudo first-order, with a plateau. The fact, that the transformation of cycHC[6] to cycHC[8] proceeds faster in stronger acids (Table 1, compare entries 1 and 2) in combination with the results from DFT computational study of model structures (S29, ESI<sup>†</sup>) allows us to state, that the rate-limiting step of this process is protonation of the macrocycle. Occurrence of side reactions was minimal and no intermediates were detected by NMR (S16, ESI<sup>†</sup>).

Pittelkow *et al.* have shown that dimers are the main intermediates in the formation of biotin[6]uril.<sup>8f</sup> Also, since cycHC[6] and cycHC[8] differ from each other by a dimer unit, we wanted to examine whether the cycHC[8] formation proceeds *via* dimer addition. We thus introduced <sup>13</sup>C labels to methylene bridges of cycHC[6]<sup>8c</sup> and subsequently used a 1:1 mixture of <sup>13</sup>C-labelled and non-labelled cycHC[6] in cycHC[8] synthesis. The number of <sup>13</sup>C-labelled methylene groups in isolated cycHC[8] varied from 0 to 8, following a normal distribution, thus confirming that beside dimers, other oligomers or monomers are involved in the reaction (S7, ESI<sup>†</sup>).

HRMS analysis of the reaction mixture showed the presence of cycHC[6–10]<sup>12</sup> and various oligomers (up to an octamer, S14, ESI<sup>†</sup>). The large number of observed intermediates pointed to the presence of a dynamic combinatorial library (DCL).<sup>3b</sup>

According to DFT-calculated Gibbs' energies of cycHCs it is not the cycle strain, but the inclusion complex with formate anions that induces a preference towards the formation of cycHC[8] (S27, ESI<sup>†</sup>). Based on the experimental observations described above and the energy calculations on a model system (S29, ESI<sup>†</sup>), we propose that the transformation of cycHC[6] to cycHC[8] proceeds through the key steps outlined in Scheme 1. First, a reaction rate-limiting protonation of cycHC[6] occurs, then breakage of the first methylene bridge of cycHC[6]H<sup>+</sup> takes place, forming the iminium 3f. The DCL, whose members have been observed by HRMS, is generated through depropagation and propagation reactions. A formate acts as an anionic template and shifts the thermodynamic equilibrium between DCL members towards the formation of cycHC[8].

To verify that an anionic template is necessary to drive the reaction towards the formation of cycHC, we selected an anion that possessed the size and shape suitable for the cavity of cycHC[8], the hexafluorophosphate, in combination with acetic acid. Acetic acid alone was shown not to facilitate the formation of cycHC[8] (S4, ESI<sup>†</sup>). As expected, in the presence of NaPF<sub>6</sub> in acetic acid/acetonitrile, cycHC[6] was efficiently converted to cycHC[8] (Table 1, entry 3). This observation confirmed that even though reaction rate depends on the acid strength, the macrocycle formation is controlled by the anion, acting as a template.



Scheme 1 Proposed reaction mechanism of the cycHC[8] formation catalysed by formic acid.

And with catalysis of formic and trifluoroacetic acid, their conjugate anions act as templates (Table 1, entries 1 and 2).

Next, based on the proposed mechanism, we envisioned that the DCL members could be generated starting from monomers **1a**. Indeed, using either formic acid, trifluoroacetic acid, or NaPF<sub>6</sub>/acetic acid as catalysts afforded cycHC[8] (Table 1, entries 4–6). The lower rate of formation of cycHC[8] from **1a** than from cycHC[6], was due to the additional acid-promoted reactions necessary for building methylene bridges. The best yield and selectivity were achieved with trifluoroacetic acid, giving the cycHC[8] from **1a** on a gram scale in 73% yield. This synthetic method allowed for the preparation of enantiopure chiral macrocycle cycHC[8] very efficiently, in only two steps, starting from commercially available 1,2-cyclohexanediamine.<sup>13</sup>

According to the proposed mechanism, the conversion of cycHC[8] to cycHC[6] in the presence of a halide template, should also be possible. Indeed, using the classic conditions of CB formation (Table 1, entry 8), cycHC[8] was efficiently converted to cycHC[6] with the aid of the chloride anion. Similarly, using NaCl as a templating additive in acetic acid at elevated temperature, cycHC[8] was also converted to cycHC[6] (Table 1, entry 9), again highlighting the role of the templating anion in the reaction.

The crystal structure confirmed the barrel-like shape of cycHC[8] (Fig. 2). According to the crystal structure, the cavity of cycHC[8], similar in size to that of CB[6], is of sufficient size for the encapsulation of a number of organic and inorganic guests (Table 2).

Complexation studies of the cycHC[8] with carboxylic acids were performed by diffusion NMR in CDCl<sub>3</sub>. The comparative results of the complexation of cycHC[6] and cycHC[8] are presented in Table 3. The association constants of simple carboxylic acids – acetic, formic and trifluoroacetic acids – follow the order of their acidity (Table 3, entries 1–3) for both hosts.

Analogously to small carboxylic acids, complexation with the more acidic  $\alpha$ -methoxy- $\alpha$ -trifluoromethylphenylacetic acid (MTPA) was stronger than with  $\alpha$ -methoxyphenylacetic acid (MPA) (Table 3, entries 5 and 6). The opposite preference of complexation of *R*-handed cycHC[6] and cycHC[8] toward MPA enantiomers may suggest different geometries of complexes in these cases. Nevertheless *R*-handed cycHC[8] showed nearly double affinity for *S*-MPA, compared to the *R*-MPA. This result confirms that cycHC[8] forms complexes enantioselectively.

In conclusion, we have presented the first highly efficient synthesis of an 8-membered representative of the cucurbituril family, the (all-*R*)-cyclohexylhemicucurbit[8]uril. We have shown that the reversibility of

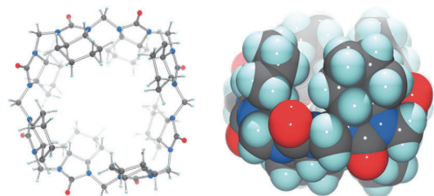


Fig. 2 Crystal structure of cycHC[8]: top view in ball and stick (left) and side view in CPK (right) representations (colour code: C grey, N blue, O red, H turquoise).

Table 2 Dimensions of cycHC[6,8] and CB[6,8]

Parameters <sup>a</sup>	CycHC[6] <sup>b</sup>	CycHC[8]	CB[6] <sup>c</sup>	CB[8] <sup>c</sup>
Opening diameter (Å)	2.2	4.6	3.9	6.9
Cavity diameter (Å)	5.3	8.5	5.8	8.8
Height (Å)	12.1	12.5	9.1	9.1
Cavity volume (Å <sup>3</sup> )	35 <sup>d</sup>	123 <sup>d</sup>	119 ± 21	356 ± 16

<sup>a</sup> Dimensions account for the van der Waals radii of the various atoms.

<sup>b</sup> Opening, cavity and height values are from ref. 14a and cavity volume from ref. 14b.

<sup>c</sup> Opening, cavity and height values are from ref. 8c and cavity volume from ref. 14b.

<sup>d</sup> Cavity volume of cycHC[6] from ref. 8c and cycHC[8] calculated by analysing the solvent accessible voids in the respective crystal structures using PLATON<sup>15</sup> with a probe radius of 1.2 Å<sup>3</sup> and grid steps of 0.2 Å.

Table 3 Association constants  $K_a$  (M<sup>-1</sup>) of carboxylic acids with cycHC[6] and cycHC[8] in 1:1 mixtures in CDCl<sub>3</sub>

No.	Guest	CycHC[6] $K_a$	CycHC[8] $K_a$
1	CH <sub>3</sub> COOH	8.0 ± 0.5 <sup>a</sup>	17 ± 2
2	HCOOH	97 ± 1	72.6 ± 0.5
3	CF <sub>3</sub> COOH	21(±3) × 10 <sup>3</sup>	29(±1) × 10 <sup>3</sup>
4	<i>R</i> -MPA	27.2 ± 0.8 <sup>a</sup>	27.0 ± 0.5
5	<i>S</i> -MPA	20.1 ± 0.2 <sup>a</sup>	53 ± 3
6	<i>R</i> -MTPA	n.d.	3.3(±0.1) × 10 <sup>2</sup>
7	<i>S</i> -MTPA	n.d.	3.0(±0.1) × 10 <sup>2</sup>

<sup>a</sup> Association constants from ref. 8c; n.d. - not determined.

the methylene bridge formation allows the size of the cycHC macrocycles to be controlled by the anionic templates, with halides driving the equilibrium towards the formation of cycHC[6], while carboxylates and PF<sub>6</sub><sup>-</sup> promoted the formation of cycHC[8].

Chiral cycHC[8] and cycHC[6] were obtained very efficiently in one step, starting from enantiomerically pure (*R,R,N,N'*)-cyclohex-1,2-diyurea **1a** or either homologue. (all-*R*)-cycHC[8] enantioselectively formed complexes with chiral carboxylic acids, demonstrating chiral discrimination ability. CycHC[8] shows potential for application in host-guest chemistry.<sup>9g,10,16</sup>

In the present study, DCL members were formed from identical monomeric units. It can be envisioned that by utilizing a mixture of different monomeric ureas and suitable templates, a very efficient yet diverse library of useful hemicucurbituril hosts could become accessible *via* dynamic covalent chemistry.

The authors would like to thank Tiina Aid, Marina Kudrjašova and Jasper Adamson for experimental assistance and Aivar Lõökene, Mart Reimund and Omar Parve for help with the manuscript. This research was supported by the Academy of Finland (KR, grants 263256 and 265328), the Estonian Ministry of Education and Research through Grants IUT19-32, IUT19-9, IUT23-7 and PUT692, TUT grant no. B25, the ESF DoRa, and the EU European Regional Development Fund (3.2.0101.08-0017). Computations were performed on the HPC cluster at TUT, which is part of the ETAIS. FT acknowledges support from NGS-NANO through a PhD fellowship.

## Notes and references

- (a) X. Ma and Y. Zhao, *Chem. Rev.*, 2015, DOI: 10.1021/cr500392w;
- (b) Special Issue: Responsive Host-Guest Systems, *Acc. Chem. Res.*, 2014, 47, 1923; (c) G. Ghale and W. M. Nau, *Acc. Chem. Res.*, 2014, 47, 2150; (d) J. Hu and S. Liu, *Acc. Chem. Res.*, 2014, 47, 2084.

- 2 (a) C. J. Pedersen, *Angew. Chem., Int. Ed. Engl.*, 1988, 27, 1021; (b) J.-M. Lehn, *Angew. Chem., Int. Ed. Engl.*, 1988, 27, 89; (c) D. J. Cram, *Angew. Chem., Int. Ed. Engl.*, 1988, 27, 1009; (d) J.-M. Lehn, *Angew. Chem., Int. Ed.*, 2013, 52, 2836.
- 3 (a) J.-M. Lehn, *Chem. – Eur. J.*, 1999, 5, 2455; (b) S. J. Rowan, S. J. Cantrill, G. R. L. Cousins, J. K. M. Sanders and J. F. Stoddart, *Angew. Chem., Int. Ed.*, 2002, 41, 898; (c) P. T. Corbett, J. Leclaire, L. Vial, K. R. West, J. L. Wietor, J. K. M. Sanders and S. Otto, *Chem. Rev.*, 2006, 106, 3652; (d) Y. Jin, C. Yu, R. J. Denman and W. Zhang, *Chem. Soc. Rev.*, 2013, 42, 6634; (e) Y. Jin, Q. Wang, P. Taynton and W. Zhang, *Acc. Chem. Res.*, 2014, 47, 1575; (f) A. Herrmann, *Chem. Soc. Rev.*, 2014, 43, 1899; (g) M. Matache, E. Bogdan and N. D. Hádade, *Chem. – Eur. J.*, 2014, 20, 2106.
- 4 (a) E. Masson, X. Ling, R. Joseph, L. Kyeremeh-Mensah and X. Lu, *RSC Adv.*, 2012, 2, 1213; (b) K. I. Assaf and W. M. Nau, *Chem. Soc. Rev.*, 2015, 44, 394.
- 5 (a) R. Oun, R. S. Floriano, L. Isaacs, E. G. Rowan and N. J. Wheate, *Toxicol. Res.*, 2014, 3, 447; (b) U. Hoffmann, M. Grosse-Sundrup, K. Eikermann-Haerter, S. Zaremba, C. Ayata, B. Zhang, D. Ma, L. Isaacs and M. Eikermann, *Anesthesiology*, 2013, 119, 317; (c) V. D. Uzunova, C. Cullinane, K. Brix, W. M. Nau and A. I. Day, *Org. Biomol. Chem.*, 2010, 8, 2037.
- 6 (a) S. Walker, R. Oun, F. J. McInnes and N. J. Wheate, *Isr. J. Chem.*, 2011, 51, 616; (b) A. I. Day and J. G. Collins, Cucurbituril receptors and drug delivery, in *Supramolecular Chemistry: From Molecules to Nanomaterials*, ed. J. W. Steed and P. A. Gale, John Wiley & Sons, Ltd, 2012, vol. 3, p. 983; (c) L. Peng, A. Feng, M. Huo and J. Yuan, *Chem. Commun.*, 2014, 50, 13005; (d) V. Mandadapu, A. I. Day and A. Ghanem, *Chirality*, 2014, 26, 712; (e) A. A. Elbashir and H. Y. Aboul-Enein, *Crit. Rev. Anal. Chem.*, 2015, 45, 52; (f) S. Gürbüz, M. Idrisa and D. Tuncel, *Org. Biomol. Chem.*, 2015, 13, 330.
- 7 (a) A. Day, A. P. Arnold, R. J. Blanch and B. Snusball, *J. Org. Chem.*, 2001, 66, 8094; (b) A. Chakraborty, A. Wu, D. Witt, J. Lagona, J. C. Fettinger and L. Isaacs, *J. Am. Chem. Soc.*, 2002, 124, 8297; (c) W.-H. Huang, P. Y. Zavalij and L. Isaacs, *J. Am. Chem. Soc.*, 2008, 130, 8446; (d) L. Isaacs, *Chem. Commun.*, 2009, 619; (e) L. Isaacs, *Isr. J. Chem.*, 2011, 51, 578; (f) D. Lucas, T. Minami, G. Iannuzzi, L. Cao, J. B. Wittenberg, P. Anzenbacher Jr. and L. Isaacs, *J. Am. Chem. Soc.*, 2011, 133, 17966.
- 8 (a) Y. Miyahara, K. Goto, M. Oka and T. Inazu, *Angew. Chem., Int. Ed.*, 2004, 43, 5019; (b) Y. Li, L. Li, Y. Zhu, X. Meng and A. Wu, *Cryst. Growth Des.*, 2009, 9, 4255; (c) R. Aav, E. Shmatova, I. Reile, M. Borissova, F. Topić and K. Rissanen, *Org. Lett.*, 2013, 15, 3786; (d) T. Fiala and V. Sindelar, *Synlett*, 2013, 2443; (e) M. Fomitsenko, E. Shmatova, M. Ören, I. Järving and R. Aav, *Supramol. Chem.*, 2014, 26, 698; (f) M. Lisbjerg, B. M. Jessen, B. Rasmussen, B. Nielsen, A. U. Madsen and M. Pittelkow, *Chem. Sci.*, 2014, 5, 2647.
- 9 (a) For anion binding of hemicucurbiturils see ref. 8 and H.-J. Buschmann, E. Cleva and E. Schollmeyer, *Inorg. Chem. Commun.*, 2005, 8, 125; (b) H.-J. Buschmann, A. Zielesny and E. Schollmeyer, *J. Inclusion Phenom. Macrocyclic Chem.*, 2006, 54, 181; (c) M. Sundararajan, R. V. Solomon, S. K. Ghosh and P. Venunalingam, *RSC Adv.*, 2011, 1, 1333; (d) H.-J. Buschmann and A. Zielesny, *Comput. Theor. Chem.*, 2013, 1022, 14; (e) M. Ören, E. Shmatova, T. Tamm and R. Aav, *Phys. Chem. Chem. Phys.*, 2014, 16, 19198; (f) A. M. Lisbjerg, B. E. Nielsen, B. O. Milhøj, S. P. A. Sauer and M. Pittelkow, *Org. Biomol. Chem.*, 2015, 13, 369; (g) M. Lisbjerg, H. Valkenier, B. M. Jessen, H. Al-Kerdi, A. P. Davis and M. Pittelkow, *J. Am. Chem. Soc.*, 2015, 137, 4948.
- 10 (a) H. Cong, T. Yamato and X. Feng, *J. Mol. Catal. A: Chem.*, 2012, 181; (b) H. Cong, T. Yamato and Z. Tao, *J. Mol. Catal. A: Chem.*, 2013, 287; (c) H. Cong, T. Yamato and Z. Tao, *New J. Chem.*, 2013, 37, 3778.
- 11 (a) J. Svec, M. Necas and V. Sindelar, *Angew. Chem., Int. Ed.*, 2010, 49, 2378; (b) V. Havel, J. Svec, M. Wimmerova, M. Dusek, M. Pojarova and V. Sindelar, *Org. Lett.*, 2011, 13, 4000; (c) J. Rivollier, P. Thuéry and M.-P. Heck, *Org. Lett.*, 2013, 15, 480; (d) M. A. Yawer, V. Havel and V. Sindelar, *Angew. Chem., Int. Ed.*, 2015, 54, 276; (e) M. Singh, E. Solel, E. Keinan and O. Reany, *Chem. – Eur. J.*, 2015, 21, 536.
- 12 ref. 8e and ESI† for detailed MS data.
- 13 (a) Enantiopure 1,2-cyclohexanediamine can also be isolated from racemic mixture: J. F. Larrow, E. N. Jacobsen, Y. Gao, Y. Hong, X. Nie and C. M. Zepp, *J. Org. Chem.*, 1994, 59, 1939; (b) J. F. Larrow and E. N. Jacobsen, *Org. Syn., Coll.*, 2004, 10, 96.
- 14 (a) J. Kim, I.-S. Jung, S.-Y. Kim, E. Lee, J.-K. Kang, S. Sakamoto, K. Yamaguchi and K. Kim, *J. Am. Chem. Soc.*, 2000, 122, 540; (b) W. M. Nau, M. Florea and K. I. Assaf, *Isr. J. Chem.*, 2011, 51, 559.
- 15 A. L. Spek, *Acta Crystallogr.*, 2009, D65, 148.
- 16 (a) P. A. Gale, *Acc. Chem. Res.*, 2011, 44, 216; (b) J. Lacour and D. Moraleda, *Chem. Commun.*, 2009, 7073; (c) R. J. Phipps, G. L. Hamilton and F. D. Toste, *Nat. Chem.*, 2012, 4, 603; (d) K. Wichmann, B. Antonioli, T. Söhnel, M. Wenzel, K. Gloe, K. Gloe, J. R. Price, L. F. Lindoy, A. J. Blake and M. Schröder, *Coord. Chem. Rev.*, 2006, 250, 2987; (e) T. J. Wenzel, *J. Inclusion Phenom. Macrocyclic Chem.*, 2014, 78, 1.

## Publication V

**E. Prigorchenko**, S. Kaabel, T. Narva, A. Baškir, M. Fomitšenko, J. Adamson, I. Järving, K. Rissanen, T. Tamm, R. Aav "Formation and trapping of the thermodynamically unfavoured *inverted*-hemicucurbit[6]uril" 2019, *manuscript available from ChemRxiv doi: 10.26434/chemrxiv.7977566.v1*.



# Formation and Trapping of the Thermodynamically Unfavoured *inverted*-hemicucurbit[6]uril

Elena Prigorchenko<sup>†</sup>, Sandra Kaabelt<sup>†</sup>, Triin Narva<sup>†</sup>, Anastassia Baškirt<sup>†</sup>, Maria Fomitšenko<sup>†</sup>, Jasper Adamson<sup>‡</sup>, Ivar Järving<sup>†</sup>, Kari Rissanen<sup>§</sup>, Toomas Tamm<sup>†</sup>, Riina Aav<sup>\*†</sup>.

<sup>†</sup>Department of Chemistry and Biotechnology, Tallinn University of Technology, Akadeemia tee 15, 12618 Tallinn, Estonia; <sup>‡</sup>National Institute of Chemical Physics and Biophysics, Akadeemia tee 23, 12618 Tallinn, Estonia; <sup>§</sup>Department of Chemistry, University of Jyväskylä, P.O. Box 35, 40014 Jyväskylä, Finland  
Electronic Supplementary Information (ESI) available: Synthetic procedures, characterization of compounds, single crystal structure, computational details and NMR titration data are given in supporting information

## Abstract

Amplification of a thermodynamically unfavoured macrocyclic product through the directed shift of the equilibrium between dynamic covalent chemistry library members is difficult to achieve. We show for the first time that during condensation of formaldehyde and *cis*-*N,N'*-cyclohexa-1,2-diylurea formation of *inverted*-*cis*-cyclohexanohemicucurbit[6]uril (*i-cis*-cycHC[6]) can be induced at the expense of thermodynamically favoured *cis*-cyclohexanohemicucurbit[6]uril (*cis*-cycHC[6]). The formation of *i-cis*-cycHC[6] is enhanced in low concentration of the templating chloride anion and suppressed in excess of this template. We found that reaction selectivity is governed by the solution-based template-aided dynamic combinatorial chemistry and continuous removal of the formed cycHC[6] macrocycles from the equilibrating solution by precipitation. Notably, the *i-cis*-cycHC[6] was isolated with 33% yield. Different binding affinities of three diastereomeric *i-cis*-, *cis*-cycHC[6] and their chiral isomer (*R,R*)-cycHC[6] for trifluoroacetic acid demonstrate the influence of macrocycle geometry on complex formation.

## Introduction

Reactions forming multiple chemical bonds simultaneously are challenging. Efforts to develop such reactions can, however, be rewarded by leading to complex target compounds in a single step. Many examples of single-step synthesis of oligomeric macrocycles have been described, yet achieving product selectivity often remains an obstacle<sup>1–15</sup>. Templates can offer control over product formation through preorganization of a corresponding linear precursor, or through altered thermodynamic equilibrium of the reaction. For example, we recently demonstrated that macrocyclic chiral hemicucurbiturils (HC) can selectively be obtained both in solution<sup>16,17</sup> and in the solid state<sup>18</sup>, with the product determined by the choice of the anionic template in the reaction media. The parent compounds, double-bridged cucurbiturils (CBs),<sup>7,19–22</sup> are also synthesized in a single step, but the product distribution is not as efficiently influenced by the addition of templates<sup>23</sup>. Currently, four-<sup>24–29</sup>, six-, eight-<sup>30</sup> and twelve<sup>16</sup>-membered HCs are known, with the largest variation in substituents achieved for the six-membered<sup>16,24–29,31–35</sup> HCs. The cavity shape and electronic structure of HCs vary, leading to distinct applications in host–guest systems<sup>36–48</sup>. To date, no reports on the formation of stereoisomeric HCs from the same monomer units have been presented. Herein, we report for the first time the amplification of formation of a thermodynamically unfavoured *inverted*-*cis*-cyclohexanohemicucurbit[6]uril **1** (Figure 1) through dynamic covalent chemistry. Such a single monomer modification and formation of diastereomeric macrocycles lead to the enrichment of the pool of hosts, which is important for the development of highly selective host–guests interactions.

## Results and discussion

In the course of our investigation on the synthesis and binding properties of chiral cyclohexanohemicucurbiturils<sup>30,34,36,44,49,50</sup> (cycHCs), we repeated the synthesis of the previously known achiral *cis*-cycHC<sup>33</sup> **2** (Figure 1).

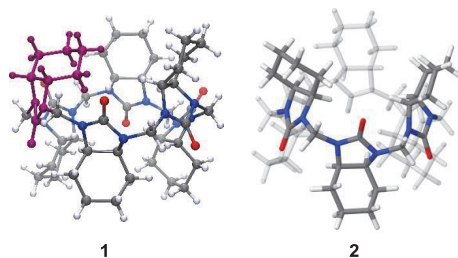


**Figure 1.** Crystal structure of **1** CCDC 1569570 showing the inverted monomer in purple. Positional disorder of the inverted monomer (Figure S8, A) is omitted for clarity. The DFT model of **2** (see details in SI and co-ordinates in S23).

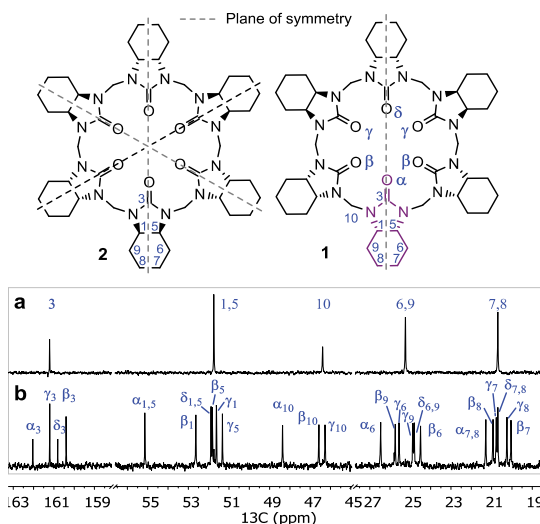


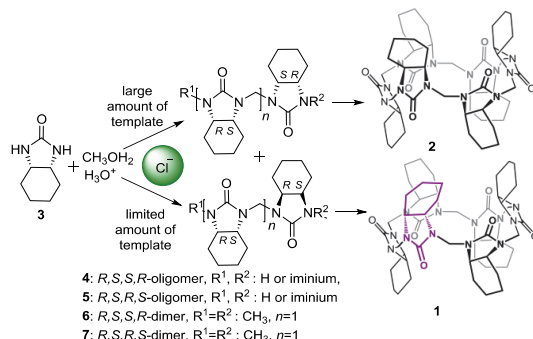
**Figure 2.** Structures of **2** and **1** with atom numbers shown on **1** and fragments of <sup>13</sup>C-NMR spectra of **2** (a) and **1** (b). (For assignment details see SI)

To our surprise, heating *cis*-*N,N'*-cyclohexa-1,2-diylurea **3** and paraformaldehyde in 4 M HCl gave a new six-membered cycHC **1** (Figure 1) along with the expected **2** in nearly equal quantities (Figure 2, Scheme 1).

Thorough NMR and single-crystal XRD analysis revealed that the new cycHC[6] had one monomer in an inverted configuration. Consequently, the new macrocycle was named *inverted-cis*-cyclohexanohemicucurbit[6]uril **1**. Similarly to **2**, its diastereoisomer **1** is achiral, however, the latter contains only a single symmetry element—a plane of symmetry (Figure 2). Therefore, compared with the highly symmetric HC **2**, in which the <sup>13</sup>C NMR signals of all six monomers overlap (Figure 2a), the carbon spectrum of **1** reflects the differences of the urea monomers in the macrocycle (Figure 2b). The uneven distribution of electron density in **1** is demonstrated by large variations in the <sup>13</sup>C-NMR chemical shifts.

Single crystals of compound **1** (Figure 1) were obtained from deuterated chloroform. The location of the inverted monomer appears as disordered between four positions in hexameric **1**. Two disorder components (sum of 0.5) corresponding to the inverted monomer were located in the asymmetric unit, which consists of half of the **1** molecule. The remaining two components are generated by symmetry. Inversion of the monomer does not affect the direction of hydrogen bonding between *i-cis*-cycHC[6] **1** and the solvent (SI, Figure S8 B), nor does it significantly change the shape of the molecule, which results in the extensive disorder observed in the crystal structure and apparent isostructurality to *cis*-cycHC[6] **2**.

The first inverted HC **1** can be obtained in up to 33% isolated yield (Table 1). This contrasts the synthesis of analogous *inverted* double bridged CBs, the *i*-CB[6] and *i*-CB[7], which were isolated in 2.0% and 0.4% yield, respectively.<sup>51</sup>



**Scheme 1.** Formation of **2** and **1** through diastereomeric intermediates **4** and **5**.

Formation of diastereomeric macrocycles from achiral *cis*-(*R,S*)-monomers proceeds through desymmetrisation of the monomer, resulting in either *R,S,S,R*- or *R,S,R,S*- ordered oligomers **4** and **5** (Scheme 1). Such desymmetrisation can in principle occur with all HCs, where the monomers are not C<sub>2</sub>-symmetric. Trapping of an inverted isomer hence suggests also novel opportunities for the synthesis of non-centrosymmetric HCs, from achiral monomers.

In the described synthesis conditions, Wu *et al.*<sup>30</sup> isolated **2** in 78% yield, however in our hands the same conditions led to the formation of **2** and **1** in nearly equal amounts. The macrocycles were isolated in an overall 55–77% yield, with the ratio of **2** to **1** varying from batch-to-batch in the range of 1.4:1 to 1:1.4 (Table 1, line 1). We have previously shown that the formation of chiral cycHCs occurs through the dynamic covalent chemistry and macrocyclic products are thermodynamically stabilized by suitably shaped and sized anionic templates.<sup>18,30</sup>

The potential ability of isomer **1** or **2** to rearrange into a more thermodynamically stable diastereomer was checked by subjecting both **2** and **1** independently to analogous reaction conditions (Table 1, lines 5 and 6). A very small portion of **2** was observed to react in 4 M HCl, whereas nearly two-thirds of **1** was converted to the more symmetric **2**. This clearly indicated that *cis*-cycHC[6] **2** is the thermodynamically more stable diastereomer of the two, with *i-cis*-cycHC[6] **1** undergoing reversible conversion in the presence of aqueous hydrochloric acid. The analogous *i*-CBs were shown to be kinetic intermediates, that can be converted to thermodynamically more stable CBs.<sup>51</sup> However, increasing the temperature, from 70 °C to 80 °C under microwave (MW) or to 110 °C in an oil-bath, which should accelerate the reaction and lead to faster accumulation of the thermodynamically more stable product **2**, appeared not to affect the ratio of the formed cycHC diastereomers (Table 1, lines 2 and 3). This ratio remained constant even if the reaction time was increased from 4 to 17 hours (see SI, Table S1). The amount of **2** was, however, clearly increased by increasing the concentration of HCl from 4 M to 8 M (Table 1, line 4), indicating that **2** is preferably formed in higher template Cl<sup>-</sup> and acid concentrations.

**Table 1.** Screened reaction conditions, the ratio of formed macrocycles and their total isolated yield.

No	Starting compound	aq. HCl (M)	Temp., Time	Ratio of <b>1:2</b> <sup>a</sup>	Yield <b>1+2</b> (%)
1	<b>3</b> <sup>c</sup>	4	70 °C, 4 h	1.4 : 1 to 1:1.4 <sup>b</sup>	55–77
2	<b>3</b>	4	MW (80 °C), 2h	1:1.2	74
3	<b>3</b>	4	110 °C, 4h	1:1.1	78
4	<b>3</b>	8	70 °C, 4h	1:3.3	84
5	<b>2</b>	4	100 °C, 3h	1:19	n.d.
6	<b>1</b>	4	100 °C, 3h	1:1.3	n.d.

<sup>a</sup> Determined through UV-HPLC calibration curves, the maximum standard deviation of determined ratios was 11%; <sup>b</sup> Reaction was repeated five times, from 100 mg to 1 g scale of starting compound **3** (see SI for details). <sup>c</sup> Representative synthesis procedure: suspension of 1.43 mmol of comp. **3** and 1.43 mmol paraformaldehyde was heated at 70 °C in 5.7 mL of aqueous 4 M HCl. Products formed in the heterogeneous reaction were filtered, washed with water and dried. Crude product purified by flash chromatography. Total isolated yield of macrocycles was 77%, including 33% of **1**, 31% of **2** and their mixture 13%. Characterization of products is given in SI.

To gain a better understanding of the stability of the involved oligomers and macrocycles, that lead to the trapping of **1**, computational studies were performed. A DFT study at the BP86/def-TZVP level<sup>52–55</sup> (see SI) of model structures of *R,S,S,R*- and *R,S,R,S*-ordered dimers **6** and **7** (Scheme 1; SI, Figure S9), showed **7** to be 3 kJ/mol higher in energy. The gap between energies of the C-shaped and S-shaped dimers **6** and **7**, respectively, was even further increased to 14 kJ/mol by complexation with the chloride anion (Figure 3). To distinguish between geometric and electronic influences, the chloride was deleted from the optimized geometry and a single-point calculation was performed. Without the chloride, the unoptimized S-shaped dimer was 6 kJ/mol lower than the C-shaped one. This confirms that the C-shaped form is stabilized by the interactions with the chloride ion.

These results reflect that the chloride anion is templating the formation of C-shaped oligomers, and therefore in **2** and **1** the *R,S,S,R*-ordered configuration prevails. Higher stability of C-shaped oligomers is similar to findings from core cucurbituril C- and S-shaped dimers<sup>56</sup> which showed that C-shaped dimers are thermodynamically favoured.

A computational study on the diastereomeric cycHC[6] macrocycles indicated that compound **1** has 17 kJ/mol higher energy than **2** and upon encapsulation of the chloride anion, the energy difference increased to 30 kJ/mol (see the structure of Cl<sup>-</sup>@**1** in Figure 4A).

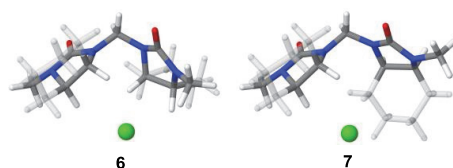


**Figure 3.** DFT models of dimers **6** (C-shaped and *R,S,S,R*-ordered) and **7** (S-shaped and *R,S,R,S*-ordered) complexes with chloride anion.

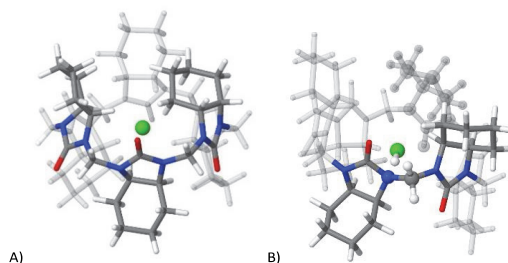


Figure 4. DFT models A) Cl<sup>-</sup>@1 complex and B) lowest energy geometry HCl@1 formed during geometry optimisation of iminium chloride intermediate.

This demonstrates that the formation of the inverted diastereomer is thermodynamically unfavourable and its formation is especially hampered if the Cl<sup>-</sup>@2 complex is formed. This result is consistent with the experimental outcome, as the proportion of **2** depends principally on the concentration of hydrochloric acid; however, it does not explain the equimolar formation of the unfavourable inverted isomer **1** in 4 M HCl.

Modelling of the formation of **1** and **2** from six-membered iminium intermediates unexpectedly showed, that all the studied hexameric iminium chloride geometries formed HCl@cycHC[6] inclusion complexes upon energy minimization (see SI for details). Therefore, we can state that the final macrocyclisation step proceeds without a transition state. Even more significantly, the resulting inclusion complexes of the diastereomeric macrocycles with hydrochloric acid were energetically very similar. The lowest-energy geometry of the HCl inclusion complex of **1**, which is depicted in Figure 4B, was even 1.5 kJ/mol lower than that of **2**.

This outcome indicates that in the final macrocyclisation step, the formation of inverted diastereomer **1** is as favourable as the formation of **2**. The fact that the reactions end in a heterogeneous mixture suggests that the kinetic product **1** is trapped by precipitation. Low solubility of the macrocyclic products **1** and **2** does not allow for the equilibration of **1** to the thermodynamically more favourable macrocycle **2**.

To probe the influence of geometry of cycHCs on their application as hosts, binding of the three diastereomers **1**, **2** and **8** and their methylated monomers the (*R,S*)- and racemic (*R\*,R\**)-(N,N'-dimethyl)-cyclohexa-1,2-diyureas, **9** and **10** to trifluoroacetic acid (TFA) was compared (Table 2). TFA was selected as a guest because it serves as an efficient template for conversion of (*R,R*)-cycHC[6] **8** to (*R,R*)-cycHC[8]<sup>30</sup>. The stoichiometry of the binding of urea derivatives with TFA was assessed by Job's method, which indicated a 1:2 stoichiometry for cycHCs and 1:1 for mono-ureas **9** and **10** (See SI). Fitting of the cycHCs titration data to a two-step binding isotherm revealed that the second TFA molecule complexes with all macrocycles with positive cooperativity with interaction parameter<sup>57</sup> in the range of 3 to 9.

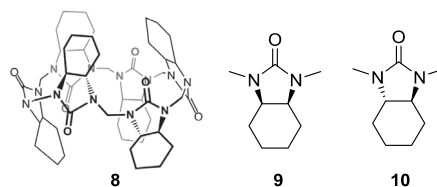


Figure 5. Structures of (*R,R*)-cycHC[6]<sup>34</sup> **8** and diastereomeric monoureas **9** and **10**.

Table 2. Association constants<sup>a</sup> of cycHC[6]s **1**, **2**, **8** and mono-ureas **9** and **10** with TFA, determined by <sup>19</sup>F-NMR titration in CDCl<sub>3</sub>.

No	Urea derivative	$K_{11}$ (M <sup>-1</sup> ) · 10 <sup>2</sup>	$K_{12}$ (M <sup>-1</sup> ) · 10 <sup>2</sup>	$K_{tot}$ (M <sup>-2</sup> ) · 10 <sup>5</sup>
1	<b>1</b>	8.8 ± 0.7	7.6 ± 0.9	6.7 ± 0.9
2	<b>2</b>	7.3 ± 0.7	16 ± 1	12 ± 2
3	<b>8</b> <sup>b</sup>	2.8 ± 0.1	6.3 ± 0.2	1.8 ± 0.1
4	<b>9</b>	43 ± 5	-	-
5	<b>10</b>	21 ± 2	-	-

<sup>a</sup> Titration data were fitted to 1:2 two-step binding isotherm, first formation of cycHC[6]•TFA with  $K_{11}$ , followed by the formation of cycHC[6]•2TFA with  $K_{12}$  and deviation of  $K$  values is the standard deviation of fitting.; <sup>b</sup> In our previous study in ref. 30 1:1 binding was incorrectly assumed for chiral cycHCs association with TFA.

The affinity of the chiral cycHC **8** towards the first TFA molecule ( $K_{11}$ , Table 2, line 3) was significantly lower than with **2** and **1**. The second TFA and the cumulative association was strongest with **2**, which has the largest distance between cyclohexane rings at the portals. (Table 2, line 2, Figure 1). These observations reflect the correlation between the geometry and size of the openings of cycHC[6]s and acid binding (Table 2, lines 1 to 3, Figure 1). Following the protons that point inside and outside of the cavity of

macrocyclic (see SI, Figure S13), confirms that external complexes with fast exchange on the NMR time scale are formed. Previously, 1:1 and 1:2 binding of carboxylic acids and carboxylates have also been studied for other single-bridged cucurbiturils, the bambus[6]urils<sup>40,58,59</sup>.

## Conclusions

Our research shows that the first inverted HC **1** can be isolated with up to 33% yield and the diastereoselectivity of the formation of **2** and **1** can be shifted towards **2** by increasing the concentration of HCl in the reaction mixture. The combined experimental and DFT study of the formation of macrocycles revealed that the ratio of diastereomeric cycHCs **2** and **1** depends on an interplay of three important steps during the synthesis: first, the thermodynamic control over templated oligomerisation and macrocyclisation, second, kinetically favoured and non-selective macrocyclisation step and third, the solubility equilibrium of cycHCs. A correlation between the geometry of diastereomeric cycHCs and affinity towards TFA was demonstrated. This study contributes to an understanding of the formation mechanism and binding capacity of cycHC[6]s that can be utilized in supramolecular and catalytic applications of single-bridged cucurbiturils.

## Acknowledgements

This research was supported by the Academy of Finland (KR: grants 263256, 265328 and 292746), the Estonian MER through Grants IUT19-9, IUT23-7, PUT692, PUT1683, PRG399 and the ERDF through the CoE 3.2.0101.08-0017, CoE 2014-2020.4.01.15-0013 and H2020-FETOPEN, 828779, INITIO. Computations were performed on the HPC cluster at TUT, which is part of the ETAIS. The authors would like to thank Madli Trunin for assisting in the synthesis Marina Kudrjašova for assisting NMR titrations and Filip Topić for fruitful discussions.

## Notes and references

‡ Author Contributions : EP, AB performed synthesis, AB, MF NMR titrations, SK, KR crystallographic analysis, JA NMR analysis of cycHCs, TN, TT computational study, IJ HRMS measurements, RA planning, analysis and supervision.

§ The manuscript was written through contributions of all authors.

- 1 W. J. Ong and T. M. Swager, *Nature Chemistry*, 2018, **10**, 1023.
- 2 D. Komáromy, M. C. A. Stuart, G. Monreal Santiago, M. Tezcan, V. V. Krasnikov and S. Otto, *J. Am. Chem. Soc.*, 2017, **139**, 6234–6241.
- 3 K. Ono, K. Johmoto, N. Yasuda, H. Uekusa, S. Fujii, M. Kiguchi and N. Iwasawa, *J. Am. Chem. Soc.*, 2015, **137**, 7015–7018.
- 4 K. D. Okochi, G. S. Han, I. M. Aldridge, Y. Liu and W. Zhang, *Org. Lett.*, 2013, **15**, 4296–4299.
- 5 R. Cacciapaglia, S. Di Stefano and L. Mandolini, *J. Am. Chem. Soc.*, 2005, **127**, 13666–13671.
- 6 H. Fu, H. Chang, J. Shen, L. Yu, B. Qin, K. Zhang and H. Zeng, *Chem. Commun.*, 2014, **50**, 3582–3584.
- 7 W. A. Freeman, W. L. Mock and N. Y. Shih, *J. Am. Chem. Soc.*, 1981, **103**, 7367–7368.
- 8 K. Łęczycka-Wilk, K. Dąbrowa, P. Cmoch and S. Jarosz, *Org. Lett.*, 2017, **19**, 4596–4599.
- 9 C. D. Gutsche and M. Iqbal, *Organic Syntheses*, 1990, **68**, 234.
- 10 Z. Zhang, Y. Luo, B. Xia, C. Han, Y. Yu, X. Chen and F. Huang, *Chem. Commun.*, 2011, **47**, 2417–2419.
- 11 S. D. Stefano and L. Mandolini, *Phys. Chem. Chem. Phys.*, 2019, **21**, 955–987.
- 12 K. Yamato, M. Kline and B. Gong, *Chem. Commun.*, 2012, **48**, 12142–12158.
- 13 V. Martí-Centelles, M. D. Pandey, M. I. Burguete and S. V. Luis, *Chem. Rev.*, 2015, **115**, 8736–8834.
- 14 L. Yuan, Y. Han, T. Tao, H. Phan and C. Chi, *Angew. Chem. Int. Ed.*, 2018, **57**, 9023–9027.
- 15 P. Hodge, *React. Funct. Polym.*, 2014, **80**, 21–32.
- 16 Y. Miyahara, K. Goto, M. Oka and T. Inazu, *Angew. Chem. Int. Ed.*, 2004, **43**, 5019–5022.
- 17 M. Lisbjerg and M. Pittelkow, in *Comprehensive Supramolecular Chemistry II*, ed. J. L. Atwood, Elsevier, Oxford, 2017, pp. 221–236.
- 18 S. Kaabel, R. S. Stein, M. Fomitšenko, I. Järving, T. Friscic and R. Aav, *Angew. Chem. Int. Ed.*, DOI:10.1002/anie.201813431.
- 19 R. Aav, S. Kaabel and M. Fomitšenko, in *Comprehensive Supramolecular Chemistry II*, ed. J. L. Atwood, Elsevier, Oxford, 2017, pp. 203–220.
- 20 J. A. McCune and O. A. Scherman, in *Comprehensive Supramolecular Chemistry II*, ed. J. L. Atwood, Elsevier, Oxford, 2017, pp. 405–434.
- 21 E. Masson, *Comprehensive Supramolecular Chemistry II*, 2nd Edition., 2017, vol. 5.
- 22 D. H. Macartney, in *Comprehensive Supramolecular Chemistry II*, ed. J. L. Atwood, Elsevier, Oxford, 2017, pp. 479–494.
- 23 S. Kaabel and R. Aav, *Israel Journal of Chemistry*, 2018, **58**, 296–313.
- 24 V. Havel, J. Svec, M. Wimmerova, M. Dusek, M. Pojarova and V. Sindelar, *Org. Lett.*, 2011, **13**, 4000–4003.
- 25 J. Rivollier, P. Thuéry and M.-P. Heck, *Org. Lett.*, 2013, **15**, 480–483.
- 26 V. Havel, T. Sadilová and V. Šindelář, *ACS Omega*, 2018, **3**, 4657–4663.
- 27 D. Azarna, M. Lafosse, J. Rivollier, J. Wang, I. B. Cheikh, M. Meyer, P. Thuéry, J.-P. Dognon, G. Huber and M.-P. Heck, *Chem. Eur. J.*, 2018, **24**, 1–10.
- 28 M. Singh, E. Solel, E. Keinan and O. Reany, *Chem. Eur. J.*, 2015, **21**, 536–540.

- 29 M. Singh, E. Solel, E. Keinan and O. Reany, *Chemistry – A European Journal*, 2016, **22**, 8848–8854.
- 30 E. Prigorchenko, M. Öeren, S. Kaabel, M. Fomitšenko, I. Reile, I. Järving, T. Tamm, F. Topić, K. Rissanen and R. Aav, *Chem. Commun.*, 2015, **51**, 10921–10924.
- 31 J. Svec, M. Necas and V. Sindelar, *Angewandte Chemie International Edition*, **49**, 2257–2257.
- 32 M. A. Yawer, V. Havel and V. Sindelar, *Angew. Chem. Int. Ed.*, 2015, **54**, 276–279.
- 33 Y. Li, L. Li, Y. Zhu, X. Meng and A. Wu, *Cryst. Growth Des.*, 2009, **9**, 4255–4257.
- 34 R. Aav, E. Shmatova, I. Reile, M. Borissova, F. Topić and K. Rissanen, *Org. Lett.*, 2013, **15**, 3786–3789.
- 35 M. Lisbjerg, B. M. Jessen, B. Rasmussen, B. E. Nielsen, A. Ø. Madsen and M. Pittelkow, *Chem. Sci.*, 2014, **5**, 2647–2650.
- 36 S. Kaabel, J. Adamson, F. Topić, A. Kiesilä, E. Kalenius, M. Öeren, M. Reimund, E. Prigorchenko, A. Löökene, H. J. Reich, K. Rissanen and R. Aav, *Chem. Sci.*, 2017, **8**, 2184–2190.
- 37 C. Lang, A. Mohite, X. Deng, F. Yang, Z. Dong, J. Xu, J. Liu, E. Keinan and O. Reany, *Chem. Commun.*, 2017, **53**, 7557–7560.
- 38 T. Fiala, L. Ludvíková, D. Heger, J. Švec, T. Slanina, L. Vetráková, M. Babiak, M. Nečas, P. Kulhánek, P. Klán and V. Sindelar, *J. Am. Chem. Soc.*, 2017, **139**, 2597–2603.
- 39 A. Šlampová, V. Šindelář and P. Kubáň, *Anal. Chim. Acta*, 2017, **950**, 49–56.
- 40 V. Havel and V. Sindelar, *ChemPlusChem*, 2015, **80**, 1601–1606.
- 41 V. Havel, M. A. Yawer and V. Sindelar, *Chem. Commun.*, 2015, **51**, 4666–4669.
- 42 M. Lisbjerg, H. Valkenier, B. M. Jessen, H. Al-Kerdi, A. P. Davis and M. Pittelkow, *J. Am. Chem. Soc.*, 2015, **137**, 4948–4951.
- 43 M. Lisbjerg, B. E. Nielsen, B. O. Milhøj, S. P. A. Sauer and M. Pittelkow, *Organic & Biomolecular Chemistry*, 2015, **13**, 369–373.
- 44 M. Öeren, E. Shmatova, T. Tamm and R. Aav, *Phys. Chem. Chem. Phys.*, 2014, **16**, 19198–19205.
- 45 H. Cong, T. Yamato and Z. Tao, *Journal of Molecular Catalysis A: Chemical*, 2013, **379**, 287–293.
- 46 H. Cong, T. Yamato and Z. Tao, *New J. Chem.*, 2013, **37**, 3778–3783.
- 47 H. Cong, T. Yamato, X. Feng and Z. Tao, *Journal of Molecular Catalysis A: Chemical*, 2012, **365**, 181–185.
- 48 J. Svec, M. Dusek, K. Fejfarova, P. Stacko, P. Klán, A. E. Kaifer, W. Li, E. Hudeckova and V. Sindelar, *Chem. Eur. J.*, **17**, 5605–5612.
- 49 M. Fomitšenko, E. Shmatova, M. Öeren, I. Järving and R. Aav, *Supramol. Chem.*, 2014, **26**, 698–703.
- 50 M. Fomitšenko, A. Peterson, I. Reile, H. Cong, S. Kaabel, E. Prigorchenko, I. Järving and R. Aav, *New J. Chem.*, 2017, **41**, 2490–2497.
- 51 L. Isaacs, S.-K. Park, S. Liu, Y. H. Ko, N. Selvapalam, Y. Kim, H. Kim, P. Y. Zavalij, G.-H. Kim, H.-S. Lee and K. Kim, *J. Am. Chem. Soc.*, 2005, **127**, 18000–18001.
- 52 A. D. Becke, *Phys. Rev. A*, 1988, **38**, 3098–3100.
- 53 J. P. Perdew and A. Zunger, *Phys. Rev. B*, 1981, **23**, 5048–5079.
- 54 J. P. Perdew, *Phys. Rev. B*, 1986, **33**, 8822–8824.
- 55 K. Eichkorn, O. Treutler, H. Öhm, M. Häser and R. Ahlrichs, *Chemical Physics Letters*, 1995, **242**, 652–660.
- 56 A. Chakraborty, A. Wu, D. Witt, J. Lagona, J. C. Fettingler and L. Isaacs, *J. Am. Chem. Soc.*, 2002, **124**, 8297–8306.
- 57 P. Thordarson, *Chem. Soc. Rev.*, 2011, **40**, 1305–1323.
- 58 V. Havel, V. Sindelar, M. Necas and A. E. Kaifer, *Chem. Commun.*, 2014, **50**, 1372–1374.
- 59 J. Sokolov and V. Šindelář, *Chem. Eur. J.* 2018, **24**, 15482–15485.

# Curriculum vitae

## Personal data

Name: Elena Prigorchenko (Shmatova)

Date of birth: 10.07.1989

Place of birth: Tallinn, Estonia

Citizenship: Russian

## Contact data

E-mail: elena.prigorchenko@gmail.com

## Education

2013 – 2019 Tallinn University of Technology – PhD

2011 – 2013 Tallinn University of Technology – MSc (*cum laude*)

2008 – 2011 Tallinn University of Technology – BSc (*cum laude*)

2005 – 2008 Tallinna Tõnismäe Reaalkool – High school (gold medal)

## Language competence

Russian Native

English Fluent

Estonian Fluent

French Intermediate

## Professional employment

2012 Member of the organisation committee for the conference Balticum Organicum Syntheticum 2012, Tallinn

2013 – 2019 Tallinn University of Technology, Department of Chemistry and Biotechnology, PhD Student and Early Stage Researcher

## Professional associations

2013 – 2019 The Estonian Chemical Society

## Honours and awards

- 1st place at Tallinn University of Technology in 2011 with BSc thesis 'New Chiral Hemicucurbit[6]uril'
- JCI Tallinn ja Balti Kella AS scientific thesis contest finalist in 2011 with BSc thesis „New Chiral Hemicucurbit[6]uril“
- Tiina Mõisa Scholarship, Tallinn University of Technology, 2015

## Supervised Theses

Madli Trunin, **MSc**, 2016

'The Synthesis of Substituted Hemicucurbit[6]urils', Tallinn University of Technology, Department of Chemistry (co-supervised with Prof. Riina Aav)

Madli Kruusamägi, **BSc**, 2014

'The Synthesis of Chiral and Achiral Cyclohexylhemicucurbit[6]urils', Tallinn University of Technology, Department of Chemistry (co-supervised with Prof. Riina Aav)

## Teaching experience

Autumn 2014, Tutorials for Organic Chemistry I

Spring 2015, Tutorials for of Organic Chemistry II

# Elulookirjeldus

## Isikuandmed

Nimi: Elena Prigorchenko (Shmatova)

Sünniaeg: 10.07.1989

Sünnikoht: Tallinn, Estonia

Kodakondsus: Vene

## Kontaktandmed

E-post: elena.prigorchenko@gmail.com

## Hariduskäik

2013 – 2019 Tallinna Tehnikaülikool – PhD

2011 – 2013 Tallinna Tehnikaülikool – MSc (*cum laude*)

2008 – 2011 Tallinna Tehnikaülikool – BSc (*cum laude*)

2005 – 2008 Tallinna Tõnismäe Reaalkool – Keskhariidus (kuldmedal)

## Keelteoskus

Vene keel – emakeel

Inglise keel – Kõrgtase

Eesti keel – Kõrgtase

Prantsuse keel – Kesktase

## Teenistuskäik

2012 Balticum Organicum Syntheticum 2012 konverentsi kohaliku korraldamiskomitee liige, Tallinn

2013 – 2019 Tallinna Tehnikaülikool, Keemia ja Biotehnoloogia instituut, doktorant-nooremteadur

## Kuuluvus erialaühingutesse

2013 – 2019 Eesti Keemiaselts

## Teaduspreemiad ja tunnustused

- I. koht Tallinna Tehnikaülikooli tudengite teadustööde konkursil 2011 bakalaureuse tööga 'Uus Kiraalne Poolkukurbit[6]uril'
- JCI Tallinn ja Balti Kella AS teadustööde konkursi finalist 2011 bakalaureuse tööga 'Uus Kiraalne Poolkukurbit[6]uril'
- Tiina Mõisa Stipendium, Tallinna Tehnikaülikool, 2015

## Juhendatud väitekirjad

Madli Trunin, **MSc**, 2016

'Asendatud Poolkukurbit[6]uriilide Süntees', Tallinna Tehnikaülikool, Keemiainstituut (kaasjuhendaja dotsent Riina Aav)

Madli Kruusamägi, **BSc**, 2014

'Kiraalsete ja Akiraalsete Tsükloheksüülpoolkukurbit[6]uriilide Süntees' Tallinna Tehnikaülikool, Keemiainstituut (kaasjuhendaja dotsent Riina Aav)

## Õpetamiskogemus

Sügis 2014, Orgaanilise keemia I harjutustunnid

Kevad 2015, Orgaanilise keemia II harjutustunnid

